

Electronic Thesis and Dissertation Repository

7-31-2017 12:00 AM

Predictive Energy Management of Islanded Microgrids with Photovoltaics and Energy Storage

Dennis G. Michaelson
The University of Western Ontario

Supervisor
Dr. Jin Jiang
The University of Western Ontario

Graduate Program in Electrical and Computer Engineering
A thesis submitted in partial fulfillment of the requirements for the degree in Doctor of Philosophy
© Dennis G. Michaelson 2017

Follow this and additional works at: <https://ir.lib.uwo.ca/etd>



Part of the [Power and Energy Commons](#)

Recommended Citation

Michaelson, Dennis G., "Predictive Energy Management of Islanded Microgrids with Photovoltaics and Energy Storage" (2017). *Electronic Thesis and Dissertation Repository*. 4861.
<https://ir.lib.uwo.ca/etd/4861>

This Dissertation/Thesis is brought to you for free and open access by Scholarship@Western. It has been accepted for inclusion in Electronic Thesis and Dissertation Repository by an authorized administrator of Scholarship@Western. For more information, please contact wlsadmin@uwo.ca.

Abstract

Islanded microgrids powered primarily by photovoltaic (PV) arrays present a challenging control problem due to the intermittent production and the relatively close scale between the sources and the loads. Energy storage in such microgrids plays an important role in balancing supply with demand, and in extending operation during periods when the PV supply is not available or insufficient. The efficient operation of such microgrids requires effective management of all resources. A predictive energy management strategy can potentially avoid or effectively mitigate upcoming outages. This thesis presents an energy management system (EMS) for such microgrids. The EMS uses a predictive approach to set operational schedules in order to (a) prolong the supply to critical system loads and (2) minimize the chances and duration of system-wide outages, specifically through pre-emptive load shedding. Online weather forecast data has been combined with the PV system model to assess potential energy production over a 48 hour period. These predictions, along with load forecasts and a model of the energy storage system, are used to predict the state-of-charge of the storage devices and characterize potential power shortages. Pre-emptive load shedding is subsequently planned and executed to avert outages or minimize the duration of unavoidable outages. A bounding technique has also been proposed to account for uncertainties in estimates of the stored energy. The EMS has been implemented using an event-driven framework with network communication. The approach has been validated through simulations and experiments using recorded real-world solar irradiance data. The results show that the outage durations have been reduced by a factor of 87% to 100% for an example operating scenario, selected to demonstrate the features of the scheme. The impact of uncertainties in the prediction models has also been investigated, specifically for the PV system rating and the battery capacity. A technique has been developed to compensate for such uncertainties by analyzing the data streams from the source and storage units. The technique is applied to the developed EMS strategy, where it is able to shorten the total outage duration by a factor of 12% over a 42-day scenario exhibiting a variety of irradiance conditions.

Keywords: Microgrids, energy storage, photovoltaic systems, energy management.

Co-Authorship Statement

All the work presented in this thesis, including the developed concepts, analysis, architecture, programming, simulation and experimental design, and the figure preparation is the original work of the candidate, Dennis Michaelson. Dr. Hisham Mahmood has provided invaluable assistance by designing the lower-layer real-time controllers for the dc-dc converters and inverters used in the experimental system, and has assisted with the experimental apparatus and procedures. The design and construction of the laboratory microgrid apparatus was performed jointly by Dennis Michaelson, Dr. Hisham Mahmood, and Andrew Moore.

To Laura, Evan, Sarah, and Lillian Michaelson.

Acknowledgements

This work would not have been possible without the ongoing assistance of Dr. Jin Jiang, who has advised, supported, and encouraged me in this research. I would also like to acknowledge Dr. Hisham Mahmood for his friendship and critical help with our collaborative work. Finally, I wish to thank Dr. Xinhong Huang for her encouragement and organizational help, and Andrew Moore for his work on our laboratory facilities.

Funding for this research has been provided in part by the Ontario Research Fund, the Ontario Centres of Excellence, the Natural Sciences and Engineering Research Council of Canada, and the Semiconductor Research Corporation.

Contents

Abstract	ii
Co-Authorship Statement	iii
Dedication	iv
Acknowledgements	v
List of Figures	ix
List of Tables	xi
List of Abbreviations and Nomenclature	xii
1 Introduction	1
1.1 Motivation	1
1.2 Problem Statement	3
1.3 Background	4
1.3.1 Microgrids	4
1.3.2 Microgrid Control	5
1.3.3 Energy Management	7
1.3.4 Energy Management in Microgrids	8
1.3.5 Stored Energy Prediction Uncertainties	12
1.3.6 Model Parameter Uncertainties	13
1.4 Research Objectives and Scope	14
1.5 Contributions	16
1.6 Thesis Organization	17
2 Problem Description	18
2.1 Concept Overview	18
2.1.1 Energy Management in Microgrids	18

2.1.2	Model Parameter Uncertainties	20
2.2	Preliminaries	21
2.2.1	System Description	21
2.2.2	Assumptions	23
2.2.3	Operating States	25
2.2.4	Modeling	26
2.3	Predictive Energy Management in Microgrids	27
2.4	Model Parameter Uncertainties	28
2.5	Summary	29
3	Methodology for Energy Management and Parameter Compensation	30
3.1	Proposed Predictive Energy Management Strategy	30
3.1.1	Overview	30
3.1.2	PV Production Forecasting	31
3.1.3	Prediction of Energy Imbalance	34
3.1.4	Mitigation of Outages	36
3.1.5	Uncertainties in Prediction	38
3.2	Model Parameter Uncertainties	40
3.2.1	Overview	40
3.2.2	Compensation Factor for Uncertainties in the PV System Rating	41
3.2.3	Compensation Factor for Uncertainties in the Battery Capacity	44
3.3	Summary	45
4	Experimental Setup	47
4.1	Apparatus	47
4.1.1	Overview of the Experimental Microgrid	47
4.1.2	Specifications	49
4.1.3	Power Electronic Converters	50
4.1.4	Supporting Apparatus	58
4.2	Software Architecture	60
4.2.1	EMS Software	60
4.2.2	Model Parameter Uncertainties Compensation Features	63
4.2.3	Supporting Software Applications	63
4.3	Summary	65
5	Validation and Discussion	66
5.1	Validation Scenarios	66

5.1.1	Predictive Energy Management	66
5.1.2	Model Parameter Uncertainties Compensation	68
5.2	Predictive Energy Management	70
5.2.1	Analysis of Simulation Results	70
5.2.2	Analysis of Experimental Results	73
5.3	Model Parameter Uncertainties Compensation	77
5.3.1	Improvement in the Accuracy of PV Production Predictions	77
5.3.2	Improvement in the Accuracy of SOC Predictions	79
5.3.3	Effect of Model Parameter Uncertainties Compensation on Outage Du- rations	80
5.4	Summary	83
6	Conclusions and Future Work	84
6.1	Summary	84
6.1.1	Predictive Energy Management System	84
6.1.2	Compensation of Model Parameter Uncertainties	85
6.2	Conclusions	85
6.3	Future Work	86
	Bibliography	88
	Appendix A Supporting Tools	96
A.1	Rooftop Data Acquisition	96
A.2	High-speed Ring Buffer	97
	Appendix B Copyright Release	100
	Curriculum Vitae	101

List of Figures

1.1	Illustrative microgrid structure	5
1.2	Microgrid control hierarchy	6
2.1	Outage caused when the battery is depleted and the PV supply cannot meet the load demand.	19
2.2	Effect of uncertainties in the PV system rating.	20
2.3	Effect of uncertainties in the battery capacity.	21
2.4	System Structure	22
2.5	Microgrid operating states and transitions	25
3.1	Predictive energy management strategy	31
3.2	PV production forecasting.	32
3.3	Solar forecasts	33
3.4	Weather forecast horizons	33
3.5	Lower stored energy limit and energy deficit region.	35
3.6	Pre-scheduling of load shedding action	37
3.7	Scheduling of load shedding endpoint	37
3.8	Lower stored energy limit with the uncertainty bounds.	40
3.9	PV compensation steps	42
3.10	Flowchart of algorithm to remove near-zero datapoints.	43
4.1	Experimental microgrid overview	48
4.2	Experimental microgrid	49
4.3	TMS320F28335 microcontroller board.	50
4.4	Sensor Circuits	53
4.5	Simplified schematic of the PV dc-dc converter.	54
4.6	PV dc-dc converter.	54
4.7	Simplified schematic of the battery dc-dc converter.	55
4.8	Battery dc-dc converter, prior to packaging.	56
4.9	Schematic of the 3-phase inverter.	57

4.10	3-phase 3 kVA Inverter	57
4.11	Serial-to-Ethernet adapter.	60
4.12	Architecture of the EMS.	62
4.13	Developed NHR load controller software user interface.	65
5.1	Chosen four day PV generation and load profiles.	67
5.2	Chosen 42 day PV generation profile.	69
5.3	Simulated results with the predictive EMS disabled.	70
5.4	Simulated results with the predictive EMS enabled	72
5.5	Simulated results with the bounded EMS feature enabled.	74
5.6	Experimental results with the predictive EMS disabled.	75
5.7	Experimental results with the predictive EMS enabled.	76
5.8	Experimental results with the bounded EMS feature enabled.	77
5.9	The original forecast PV prediction, the compensated forecast PV prediction, and the measured PV power for Day 21.	78
5.10	Daily PV actual vs. forecast RMSE, with and without uncertainty compensation.	78
5.11	The predicted SOC with and without compensation for a period of one day.	79
5.12	The RMSE between the actual and predicted SOC with and without compen- sation.	80
5.13	The behavior of the microgrid with the exact model parameters. (Scenario 1)	81
5.14	The behavior of the microgrid with incorrect model parameters. (Scenario 2)	82
5.15	The behavior of the microgrid with the developed uncertainty compensation scheme enabled. (Scenario 3)	82
A.1	Rooftop data acquisition apparatus.	96
A.2	High-speed ring buffer.	98
A.3	Example of data recorded by the high-speed ring buffer.	99

List of Tables

4.1	System Parameters	49
5.1	Performance Improvement using Parameter Uncertainties Compensation	83

List of Abbreviations and Nomenclature

\mathcal{B}	Set of data points from the battery unit.
E_{batt}	Energy stored in the battery (Wh).
$E_{\text{batt}}^{\text{max}}$	Battery capacity (Wh).
$E_{\text{batt-0}}^{\text{max}}$	Uncompensated battery capacity (Wh).
$E_{\text{batt}}^{\text{min}}$	Minimum battery charge level (Wh).
E_{deficit}	Outage energy deficit (Wh).
\mathcal{F}	Set of irradiance forecasts.
G	Forecast irradiance (W/m^2).
i, j, k	Index variables.
k_{endshed}	Index of planned shedding end point.
k_{outage}	Index of start of outage.
k_{recover}	Index of end of outage.
$k_{\text{startshed}}$	Index of planned shedding start point.
\mathcal{L}	Set of load forecasts.
L	Threshold limit for determining a sunny day.
M	Number of elements in the non-zero prediction dataset.
N	Upper limit of the index, representing the end of the stored sequence.
\mathcal{P}	Set data points from the PV unit.
P_{batt}	Power measured at the battery unit (W).
\hat{P}_{batt}	Battery power prediction (W).
$\hat{P}_{\text{batt}}^{>0}$	Battery power supplied prediction (W).
P_{load}	Actual load (W).
\hat{P}_{load}	Load prediction (W).
P_{PV}	Power measured at the PV unit (W).
\hat{P}_{PV}	PV prediction (W).
$P_{\text{PV}}^{\text{max}}$	PV system rating (W).

P_{PV-0}^{\max}	Uncompensated PV system rating (W).
\hat{P}_{PV-0}	PV prediction based on the uncompensated PV system rating (W).
P_{PV-nor}	Normalized PV power values.
\hat{P}_{PV-nor}	Normalized PV power prediction values.
P_{PV-nz}	Non-zero normalized PV power measurements.
\hat{P}_{PV-nz}	Non-zero normalized PV power prediction values.
$P_{PV-peak}$	Daily peak PV power value (W).
$\hat{P}_{PV-peak}$	Daily peak PV power prediction value (W).
P_{shed}	Load available for shedding (W).
$RMSE_{PV}$	Root-mean-square error between the prediction and actual PV datasets.
$RMSE_{PV-nz}$	Root-mean-square error between the non-zero prediction and actual PV datasets.
\mathcal{S}	Shedding schedule.
SOC	Battery state-of-charge (%).
\widehat{SOC}	Predicted state-of-charge (%).
\widehat{SOC}_0	Uncompensated SOC prediction (%).
T_{outage}	Duration of the outage (h).
T_s	Sampling interval (h).
$T_{shedding}$	Duration of scheduled shedding (h).
ΔSOC	Difference between SOC datapoints.
$\Delta \widehat{SOC}$	Difference between SOC prediction datapoints.
δ	Bound magnitude (Wh).
ϵ	Per-timestep bounding parameter (Wh).
η_{batt}	Battery efficiency.
η_{MPP}	PV system efficiency at the MPP.
γ_{PV}	PV system rating compensation factor.
γ_{batt}	Battery capacity compensation factor.

Chapter 1

Introduction

1.1 Motivation

At present approximately 1.2 billion people, or 16% of the global population, have no access to electricity [1]. This energy poverty problem is a critical barrier to economic and social development in a world that has become increasingly dependent on information and communication technologies for commerce and education. In addition, a significant portion of the population that does have access to electricity is under-served, and must contend with rolling blackouts, unreliable service, and poor quality power. This sporadic electricity supply also inhibits economic and social growth, particularly for the poor who are least likely to be able to afford backup power alternatives.

Microgrids have been proposed as a part of the solution to this energy poverty problem, particularly in areas where economic realities make traditional grid extension projects infeasible [2]. In such cases, microgrids can be used to supply electricity in remote areas, or as building blocks for electrification in the developing world [3]. When powered by renewable energy sources, these microgrids can provide a low-carbon path to electrification while avoiding the pollution and climate impacts of traditional approaches [4]. The microgrid approach also allows for easy expansion, resulting in a modular and robust alternative that can comple-

ment traditional centralized generation [5]. Microgrids can also provide enhanced reliability in situations where electricity is supplied over transmission lines that are subject to natural disruptions, such as avalanches or mudslides. As the costs of renewable energy technologies and storage systems decrease, such microgrids become more economically feasible.

In the Canadian context, most parts of the country have ready access to electricity. However, in many remote Indigenous communities electricity is primarily provided by diesel generation [6], and there are approximately 200,000 people living in such off-grid locations. This approach to providing electricity comes with high operational and environmental costs, as the only way to deliver diesel fuel to some of these communities is through very expensive charter flights, or via winter-access ice roads [7,8]. Compounding the issue, climate change is reducing the operating season of some ice roads, further impacting the cost of generation, and increasing the risk of disruption to the electricity supply. Therefore, there is the potential to both reduce the operational cost and improve the environmental impact of electricity generation in these communities by using stand-alone microgrids powered by renewable energy sources.

The operation of islanded microgrids based on renewable energy, however, presents several challenging control problems. Microgrids must perform the operational tasks that are needed in any power system autonomously, such as frequency regulation, power management, and generation scheduling. This is particularly difficult when the main energy sources are wind and solar, due to their intermittent nature. In such systems, energy storage is utilized to maintain the power balance between supply and demand, effectively making up for short-term imbalances by charging or discharging as needed. However, there are practical limitations to the operation of such energy storage systems that must be accommodated, such as finite storage capacity and charge/discharge rate limitations [9].

These constraints lead to issues that are not typically encountered in traditional power generation systems, where a high priority is placed on availability of supply. From a traditional residential customer's perspective, the grid is, 'by definition,' always available. However, in an islanded photovoltaic based microgrid this assumption is not necessarily valid. In the absence

of a larger grid, an islanded microgrid may experience outages that could have been avoided by judicious management of the available energy resources and loads. This energy management task, with the goal of reducing the duration of outages, is the main focus of investigation in this thesis.

In addition, another key enabling feature of microgrid technology is the capacity for self-configuration. One of the early goals of the microgrid concept is that such systems should be modular and easily reconfigurable, which is often referred to as having “plug-and-play” capabilities. Such features result in less situation-specific engineering work, and make it possible for microgrids to automatically accommodate variations in their operating environment. Ideally, a technician would be able to install and upgrade such systems with a minimum of configuration steps, and the system itself would be able to address any issues accordingly. The investigation of such self-configuration features is also a topic of interest, specifically the ability of the microgrid to use operational data to detect and compensate for parameter uncertainties that may be caused by configuration errors or component degradation.

1.2 Problem Statement

This section presents a brief description of the problems under investigation in this thesis. A detailed description of the problem is formulated in Chapter 2.

The main question under investigation is how to design a predictive energy management system (EMS) for islanded photovoltaic microgrids, with an emphasis on automated techniques that can improve the performance of such microgrids with the available energy resources. Specifically, the question of how to perform energy management using pre-emptive load shedding to reduce the duration of outages is considered in this work.

In addition, to improve the self-configuration capability of the microgrid, the question of how to use existing data to compensate for prediction uncertainties that can affect the quality of energy management decisions is also addressed. Specifically, the compensation of uncer-

tainties in the PV system rating and battery capacity parameters has been considered.

1.3 Background

In this section, the key developments in the literature are considered, starting with a brief review of microgrids and microgrid control, and then moving to the microgrid energy management areas under investigation in this thesis. Finally, the existing literature on the effect of uncertainties in both predictions and prediction model parameters is discussed.

1.3.1 Microgrids

The key ideas behind the microgrid concept were introduced by Lasseter [10] in 1998, and grew into a significant field of research in the years that followed [11–13]. The CIGRE definition of a microgrid is: “Microgrids are electricity distribution systems containing loads and distributed energy resources, (such as distributed generators, storage devices, or controllable loads) that can be operated in a controlled, coordinated way either while connected to the main power network or while islanded.” [14]. Control of the microgrid is structured such that the microgrid as a whole appears to the larger grid as a single load (or generator). The original microgrid examples were fossil fuel generator based, and included a thermal network as a key part of the concept [15], but most recent research activities do not include this aspect. An illustrative microgrid configuration is shown in Fig. 1.1.

Microgrids can be used for improving the reliable delivery of power within the existing grid [16], and as an incremental approach to electrification in developing nations [3]. Microgrids can also play a role in integration of renewable energy resources, though the task is much more challenging than an islanded mode of operation [4]. While islanded, the microgrid controllers must maintain the power balance between power supply and load demand, in the presence of intermittent renewable resources, which requires coordination of storage, auxiliary generation, and/or controllable loads.

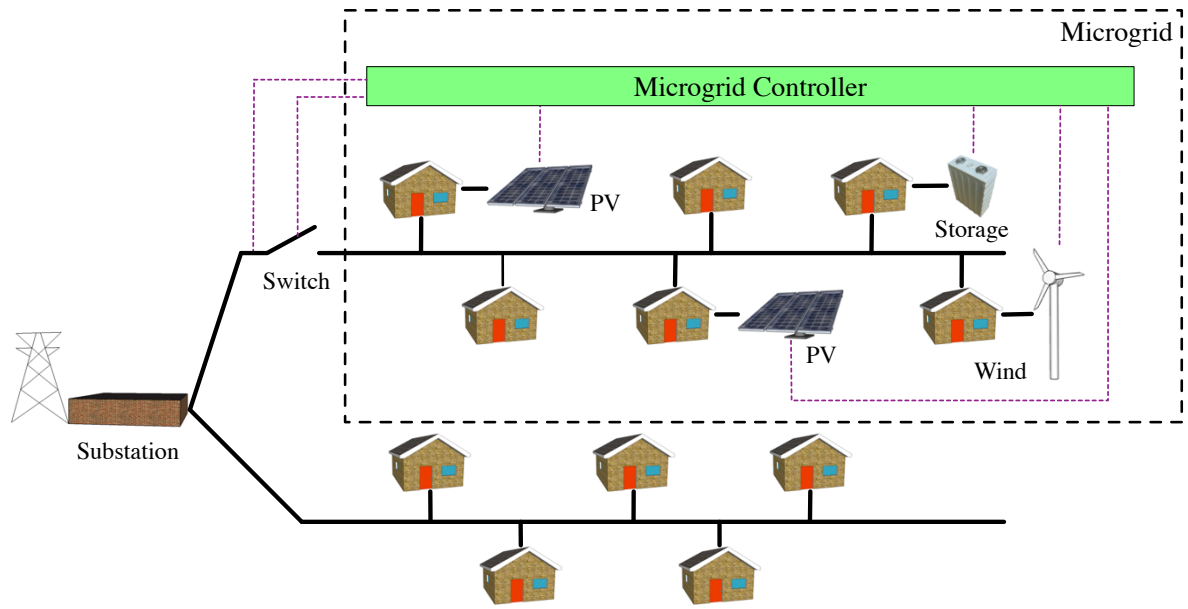


Figure 1.1: Illustrative microgrid structure

Some form of storage is often included in a microgrid in order to perform frequency regulation, maintain power balance, and to enable grid-connected operating strategies, such as peak shaving. Commercial battery systems with the potential for microgrid integration are starting to appear on the market, both as home-scale solutions such as the Panasonic/Tabuchi Eco Intelligent Battery System and the Tesla Powerwall, and as neighbourhood-level systems like the AEP Community Energy Storage offering. Storage is particularly critical for islanded operation when the microgrid is dominated by intermittent renewable generation sources such as solar photovoltaic arrays and wind generators. In this case the energy storage system is usually the only element that can regulate the frequency and maintain the power balance when a renewable energy source supply fluctuates. Therefore, the control of microgrids, including storage, is of critical importance, and is an active topic of research.

1.3.2 Microgrid Control

The control of inverter-based microgrids is typically separated into four layers [17–21], which loosely correspond to the timescale separation that is often used to characterize a larger power

system [22]. The fastest and most fundamental “zero-th” layer includes the low-level real-time control of the power electronic converters. This layer includes inner current loops and, where appropriate, outer voltage control loops that allow the converters to regulate the output to follow a desired setpoint. These layers are illustrated conceptually in Fig. 1.2.

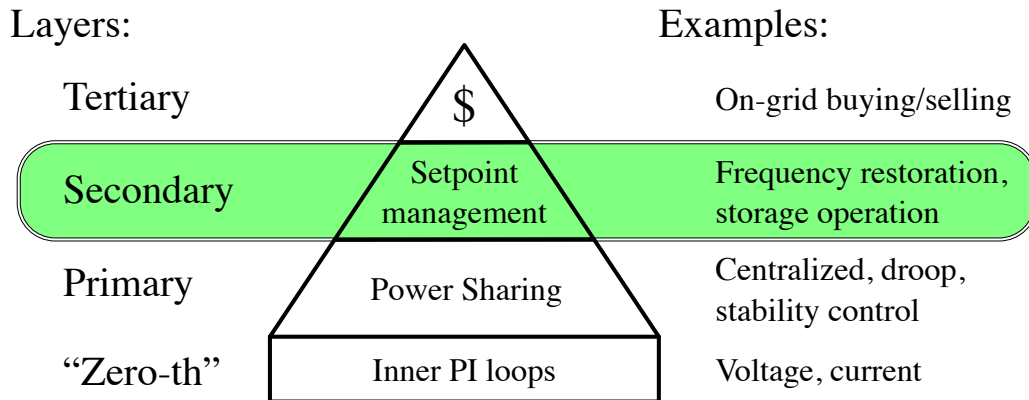


Figure 1.2: Microgrid control hierarchy

The primary control layer is concerned with sharing of power among the converters, including the problem of maintaining the power balance, either by using a single grid-forming unit and current control of renewable sources [23], or by using techniques that integrate multiple voltage-controlled sources. This control of power, or power management, can be achieved through either centralized or distributed control mechanisms [24–26]. Centralized power management requires high-speed communication links to each of the units, and runs the potential risk for catastrophic failure if these communication links are disrupted.

Distributed control of power sharing can be achieved through a droop mechanism [27, 28], which operates entirely based on measurements at the terminals of the unit, and does not require any communication links to maintain the power balance. This technique is related to the droop characteristics that balance power flow and system frequency to maintain synchronization among generators in a larger power grid. One challenge that can arise at this layer is the accommodation of the operating limits of the storage devices. Recently, a real-time technique to smoothly handle the state-of-charge limits of a PV/battery hybrid system by using

an adaptive droop approach without using central communication [29–31] has been presented. The work has also been extended to non-hybrid configurations where the storage system and the PV system are connected to the microgrid through separate voltage source converters, and managed using a multi-segment adaptive droop approach [28]. A generalized approach to cyber-synchronous machines based on synchronverter technology and robust droop control is discussed in [32], where the concepts are extended to include power-electronic interfaced load participation in system stabilization without the need for explicit communication.

The secondary microgrid control layer is concerned with managing setpoints of the units in the microgrid, and includes functions such as frequency restoration, voltage profile regulation in multi-bus microgrids, and management of reactive power sharing [33–36]. The secondary layer is also concerned with managing the use of storage within the microgrid, which is required in order to serve the load demand when the primary sources cannot fully support the demand, and to deal with peak loads [19].

Finally, the tertiary layer is mostly focused on the economic operation of the microgrid in relation to the external grid. At this layer, price-based decisions about buying and selling electricity are made, which may also include agreements relating to provisioning of reserve capacity and operational requirements for participation in the grid under contingency conditions.

1.3.3 Energy Management

In general, energy management is a task of orchestrating various sources, storage, and controllable loads to meet the operational objectives (e.g. economic, environmental, reliability) of the power system. Energy management in a centralized electric power system is separated into two major tasks: unit commitment, and economic dispatch. Unit commitment is performed on a day-ahead to week-ahead basis, and consists of assigning the necessary generation resources to meet the forecast load demand while respecting the various system constraints and specific constraints of the chosen generators. A committed generator is “on” and its full capacity is presumed to be available on demand. Economic dispatch is the related minutes-ahead process

of adjusting the setpoints of the committed generators to meet the load demand at a minimum operational cost.

1.3.4 Energy Management in Microgrids

In microgrids, similar essential energy management tasks must be performed, except at a much smaller scale and without any operator involvement [37]. Microgrid energy management involves the scheduling of generation, loads, and storage to meet operational objectives such as availability, cost, and/or environmental goals [38]. There are two general approaches: real-time immediate techniques that adjust the operating points of the microgrid without considering the future behaviours of the system [39], and predictive techniques which use forecasts and/or historical data to generate predictions of future generation and load demand, and then select setpoints to meet the assigned objectives over time.

Predictive techniques generally follow the approach of obtaining generation and load forecasts, and then creating a prediction of the microgrid behaviour into the future. The predictions can be used to optimize certain performance criteria to meet the chosen operational objectives [40]. When the profiles of the loads and/or generation can be predicted, it is possible to improve the performance of the system by taking advantage of the additional information when making operational decisions. For example, foreknowledge of an expected increase in load can lead to dispatch of additional generation, or shedding of less critical loads in advance. Also, weather forecasts can be used to predict the future availability of renewable power generation, although the accuracy of such forecasts can vary. Typically, the accuracy of such predictions degrades as the prediction horizon extends further into the future, since the uncertainty increases with time [41].

Note that predictive techniques require forecasts of power production and load demand. The forecasting of photovoltaic generation is based on historical data, predictive weather models, or a combination of the two. The two key variables that affect the power generated by a photovoltaic system are the solar insolation on the panel and the local temperature. While

both of these variables show significant random behaviour in the short term, the dominant diurnal and seasonal patterns can be used to generate a forecast if only historical information is available, however this information will be subject to a significant short-term error.

Recent research on photovoltaic forecasting is well described in the IEA report by Pelland, *et al.* [42]. The report reviews techniques including the use of numerical weather prediction (NWP) models, satellite and sky imagery, and local measurements to create predictions of solar production from timescales of a few minutes to several hours. The report also presents a survey of 15 organizations who contributed information on case studies of solar forecasting, which gives an overview of the resolution, time horizons, and, for some cases, uncertainty measures of the forecasting techniques.

In the highly cited paper by Villalva, *et al.* [43], a physics-based model is developed along with the techniques to determine the model parameters. In Mahmoud, *et al.* [44] simplified models for a PV array are developed. In Beltran, *et al.* [45] a cloudiness coefficient is defined and used to modify the projected generation estimates of the chosen model. These improved estimates are then used to better manage the charge/discharge behaviour of the energy storage system discussed in the paper. Furthermore, the technique results in an estimate of a minimum energy storage requirement for the system.

There are several possible approaches to creating the load predictions [46,47], including the use of historical data. Microgrid scale load forecasting has also been investigated using back propagation neural networks [48], a bilevel strategy for a self-optimizing hybrid forecaster [49], and using self-organizing maps [50].

The energy management tasks are performed by the energy management system in the microgrid, which monitors the key measurements and makes decisions to meet the overall operational goals of the microgrid [38]. The architectures of the microgrid EMS can be either centralized or decentralized, and operational scheduling strategies can be optimization-based [51], stochastic [52], or heuristic [53] in nature. Several of these approaches focus on economical operation of the system, and are structured in a model predictive framework [54], with

the optimization formulated as a mixed-integer linear programming problem [55]. The model predictive approach is often used to handle prediction errors in the forecast process without explicitly modeling them, since the approach makes use of the latest state information from the real system in each new prediction.

The work of Kanchev, *et al.* [53] presents a deterministic energy management approach for a microgrid containing so-called photovoltaic active generators. The active generators are hybrid units that combine a photovoltaic array and one or more storage devices with a 3-phase inverter. Each unit is controlled such that it delivers a desired level of real power, constrained by the storage system limits and available PV production. Controllable loads are also defined as part of the microgrid, along with natural gas microturbines. The microgrid EMS in [53] operates at multiple time scales, with the long-term planning problem considering emissions, market pricing, and renewable energy predictions. The shorter term actions manage controllable loads, storage, and local controller setpoints. Predictions are made on a 24-hour horizon with half-hour steps. At each step the requested real power reference is sent to the active generator, which is used along with the SOC to manage storage charging and MPP tracking. The approach is heuristic, with multiple if-then rules presented as flow charts.

The receding horizon approach is used in [41], with emphasis on economic operation. This work notably includes some details on the implementation architecture, and makes use of a lead acid battery model that accounts for SOC-dependent charging rate limitations. A load shifting demand response scheme is chosen, but uncertainties in stored energy have not been considered explicitly and no experimental results are presented, though plans for such studies are mentioned.

In order to reduce the computational complexity of the problem, a knowledge-based expert system is discussed in [56]. However, demand response and load shedding are not considered. The main focus is on the scheduling of storage operation to reduce the use of a dump load.

The design, planning, and management of a laboratory-scale microgrid is presented in the work of Valverde, *et al.* [57]. This system includes a battery, a fuel cell, an electrolyzer, and

metal hydride hydrogen storage. All the sources are integrated through a DC bus, with AC loads fed via a single inverter. Charge and discharge actions are triggered based on the status of the SOC, with hysteresis and a dead band included to reduce state chattering. The focus here is on managing the operation of the hydrogen storage system and demonstrating the approach experimentally.

Another aspect of energy management can be found in more complex multi-bus microgrids, where the distribution network within the microgrid adds additional constraints [58, 59]. For example, it has been demonstrated that the use of a detailed three-phase model within a predictive energy management strategy can improve the control system performance of an islanded microgrid, even with a high degree of imbalance in the loads [60].

The works of Parisio and Glielmo are generally concerned with the operational management of grid-connected microgrids [52, 55, 58, 61, 62]. In [58] the problem is formulated as a mixed-integer linear programming model, which is evaluated with commercial solvers to minimize the operating cost of the microgrid. This model is then used as part of a model-predictive control scheme in [55, 61], which is simulated and also tested experimentally on the CRES microgrid test bed in Greece. Further extensions include a stochastic formulation [52], and a variation that considers multiple operating objectives [62].

While most of the energy management strategies focus on the scheduling of generation, the use of controllable loads can provide additional management options [63]. The increasing availability of smart devices and ubiquitous connectivity make fine-grained control of loads possible [64], though the communication infrastructure requirements can present a challenge [32]. Load management can be performed using market demand response, which encourages voluntary load reduction through economic incentives, or by emergency load shedding [65]. Emergency load shedding is an action for dealing with imminent contingencies in the grid [66]. To facilitate emergency load shedding, the loads in a microgrid can be categorized in terms of their criticalities, with less-critical controllable loads identified, and the mechanisms to turn them on and off are made available to the intelligent load shedding module [67]. Load

shedding in microgrids has also been discussed in [68], specifically during the transition from a grid-connected to an islanded mode, under circumstances when the available generation within the island cannot meet the total load demand. Additionally, some works consider loads such as hot water heaters, refrigeration devices, or water pumps with reservoirs, where the load may be shifted in time in order to optimize the operation of the microgrid [65,69].

The majority of the work discussed above has been focused on economic optimization, and is illustrated with scenarios where the combined energy production and energy storage is able to meet the load demand. When this condition is not met, the islanded microgrid will have to suffer from outages. The use of a predictive approach has the potential to predict and characterize upcoming outages, and to eliminate or minimize the outage duration by using pre-emptive load shedding. This approach forms the central theme in this thesis.

1.3.5 Stored Energy Prediction Uncertainties

Since intermittent renewable sources, such as PV and wind, and the load demand both have a significant degree of variability, there have been several approaches taken to account for these variations in the energy management system. In many cases, no explicit attempt has been made to model such uncertainties. Instead, model-predictive control strategies are used, which base the starting point of their decisions on the most recent information available from the system operating variables. Another approach is to attempt to establish proper bounds on the variations [70,71] and to use these bounds in the decision making process. In addition to deterministic approaches, several investigators have pursued the use of stochastic formulations in this regard [52,72–75].

While these approaches do account for variations in the power production and load demand, none have considered prediction uncertainties in the SOC estimate caused by limitations in the accuracy of the SOC prediction mechanism. Therefore, this aspect is considered within the energy management strategy developed in this thesis.

1.3.6 Model Parameter Uncertainties

The mathematical model of the microgrid plays a critical role in predictive EMS approaches, as it is used to predict the microgrid behaviour, and to plan operational actions. Errors in these models will result in incorrect predictions, leading to poor decisions. A discrete battery model is often used within predictive microgrid EMS formulations, which integrates the power flowing in or out of the battery and accounts for storage losses [53, 76]. This type of model is generally computationally efficient, and can provide an appropriate level of abstraction for energy management purposes, as opposed to detailed equivalent-circuit models [77].

Note that the separate but related SOC estimation problem is typically handled by the real-time controller associated with the battery dc-dc converter [78, 79]. Since the interior state of the battery is not easily determined from measurements taken at the battery terminals, this SOC estimate sometimes contains errors. However, for energy management purposes the SOC estimate provided by the real-time controller is assumed to be accurate, and the the model of concern within the EMS is the simplified model used for prediction.

Since a stand-alone microgrid is meant to work without an operator and with minimum maintenance, parameter errors may go un-noticed, which can lead to less than optimal performance. For example, an incorrect parameter representing the size of the battery may result in an inaccurate estimate of the SOC. Actions planned based on this incorrect information could result in either unnecessary load shedding, or in unexpected outages when the stored energy is depleted earlier than was expected. Such uncertainties in the microgrid prediction models can be caused by incorrect configuration of the EMS during system installation, or by the degradation of the battery itself over time [80].

Note that none of the existing energy management solutions discussed so far in the literature address the problem of uncertainties in the model parameters, though, as previously mentioned, some deal with uncertainties in the predictions [52, 70, 72–74].

While little work has been done on the question of incorrect prediction model parameters in energy management systems for islanded microgrids, the work described in [81] does consider

the problem of the difference between real and predicted photovoltaic production in a grid-connected microgrid. A scaling factor which is based on the ratio of the most recent two real PV power measurements relative to the most recent two forecast predictions has been introduced. The scaling factor is used in a model predictive control scheme that minimizes the energy drawn from the grid. However, this method is sensitive to the significant variations in forecast accuracy that can occur, particularly during low solar irradiance levels.

Given that relatively little work has been done to deal with model parameter uncertainties in microgrids, it is desirable to investigate this problem in depth and to develop methods to compensate for such uncertainties, preferably without requiring additional information beyond what is available to the EMS. This research is also included as a part of this thesis work.

1.4 Research Objectives and Scope

In this section, an overview of the research objectives and the scope is presented.

The system under consideration is a single-bus three-phase microgrid operating in an islanded mode. The microgrid contains a photovoltaic source, its associated dc-dc converter, and an inverter that connects to the microgrid bus. It also contains a battery storage system, consisting of a battery bank, dc-dc converter, and inverter. The loads in the microgrid include both controllable and independent ones, representing sheddable and critical loads, respectively. The elements of the microgrid communicate over an Ethernet network to a central control platform that houses the energy management system.

The objectives of this research are to:

1. Develop a predictive energy management strategy for islanded photovoltaic microgrids that can extend the operational duration of critical loads given limited energy resources.
2. Consider the impact of uncertainties in the estimation of the stored energy within the system, and account for these uncertainties in making energy management decisions.

3. Explore the impact of model parameter uncertainties on the predictions used in energy management, and develop techniques to compensate for these uncertainties.
4. Demonstrate the effectiveness of the developed strategies on both simulated and physical platforms.

The effectiveness of these techniques is assessed using two metrics: the number and duration of outages that affect the critical loads.

Also, in defining the scope of this thesis, the following points have not been considered:

1. Specific load prediction algorithms: An accurate load prediction is presumed to be available.
2. The presence of additional dispatchable generation: The only primary source of energy is the PV array.
3. Reactive power management, phase imbalance, or voltage profiles within the microgrid: The configuration under investigation is a simple single-bus microgrid with balanced resistive loads.
4. Stochastic formulations or techniques: The problem is posed and solved in a deterministic domain.
5. Communication disruptions or delays: The communication links are presumed to be reliable.

1.5 Contributions

The contributions of this research can be summarized as:

1. Development of a deterministic microgrid energy management strategy that uses preemptive load shedding to reduce the number and length of outages. The strategy makes use of online weather forecasts to predict the photovoltaic power production, and then uses that information together with the load profile to predict upcoming outages. The shedding of non-critical loads is then scheduled to eliminate or reduce the duration of the outages [82,83].
2. Consideration of a bounding technique that considers uncertainties in the SOC predictions over time. This bound can be used to adjust the timing and duration of the load shedding actions [83].
3. Investigation of compensation strategies to reduce the effect of uncertainties in the PV system rating and battery capacity parameters that are used in the prediction model.
4. Design of an implementation framework that enables energy management functionality within an experimental laboratory-scale microgrid. This framework allows for both simulation and experimental studies to be performed using previously recorded data from a real system, in order to evaluate the performance of the developed energy management strategies [83].
5. Design and construction of an experimental microgrid facility with data communication features that has also been used to support research into real [28–31] and reactive [35,36] power sharing strategies.¹

¹The author's contribution to these studies was in the design and implementation of the network communication software and hardware, and in the collaborative design and construction of the power electronic converters.

1.6 Thesis Organization

The remainder of the thesis is structured as follows: The energy management and model parameter uncertainty problems are formalized in Chapter 2, including the necessary assumptions, key models, and core problem statements. In Chapter 3, the solutions are presented in detail, starting with the predictive energy management strategy, followed by the techniques for model uncertainties compensation. The experimental apparatus and software architecture are discussed in Chapter 4, along with a description of the validation scenarios. The results of the simulation and experimental studies are presented in Chapter 5. Finally, the conclusions and suggestions for future work are provided in Chapter 6. The appendix provides additional implementation details that may be of interest to practitioners who are performing related investigations.

Chapter 2

Problem Description

In this chapter, the problems under investigation are described and formalized. First, the problems are presented conceptually with illustrated examples of the key issues of concern. Following that, the system structure is described, and the underlying assumptions are laid out. The predictive energy management problem is then formulated, followed by a description of the model parameter uncertainty problem.

2.1 Concept Overview

2.1.1 Energy Management in Microgrids

The energy management problem is fundamentally the supervisory task of ensuring that energy is available for the desired applications at the times when it is needed. This involves managing the startup/shutdown/dispatch of energy resources, the charging/discharging of energy storage devices, and the management of controllable loads. In a modern power system, this energy management task is mostly hidden from end users, although one routinely performs such tasks in other contexts. For example, any automobile driver is familiar with the responsibility of managing when and where to fuel up the vehicle. In addition, managing charging of mobile devices is a daily reality for the 2.3 billion smartphone users worldwide. As electricity market

mechanisms such as time-of-use pricing are adopted, some customers will change their energy utilization habits for financial gains. Within an islanded microgrid, however, the effects of energy management decisions can be much more immediate and consequential. One can therefore benefit from additional automation and decision support tools.

In an islanded photovoltaic powered microgrid, the load can be served when the available PV power meets or exceeds the load demand. Using storage devices, the load can also be served during periods when the PV production is lower than the load demand, when the battery has been adequately charged. However, if the battery is not charged enough, the microgrid can experience an outage at some point in time, as illustrated for a constant load case in Fig. 2.1. The outage starts when the battery state-of-charge (SOC) drops below its lower limit, forcing the microgrid to shut down, and it returns back to service when the available PV production again reaches the level needed to serve the load demand.

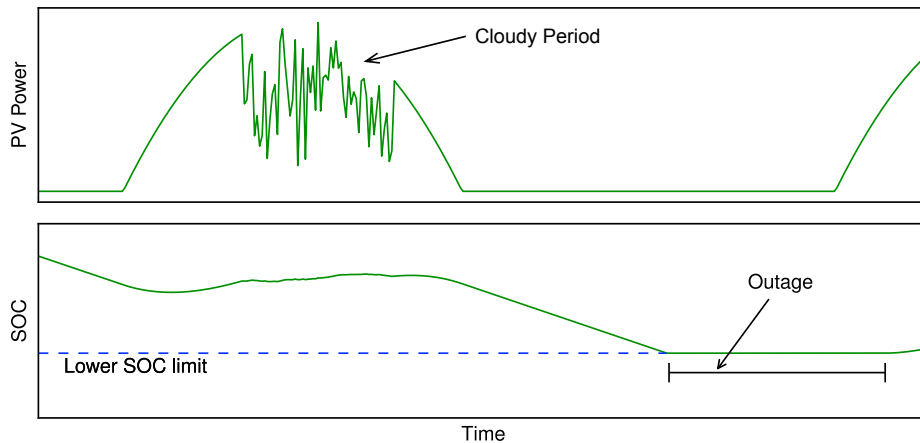


Figure 2.1: Outage caused when the battery is depleted and the PV supply cannot meet the load demand.

In this case, it may be possible to improve the situation by employing an energy management strategy. If the upcoming outage can be predicted, preventative actions can be taken to either dispatch additional generation resources, if they are available, or to reduce the load demand. If non-critical portions of the loads can be shed pre-emptively for a period of time, such a strategy may be able to eliminate the outage, or at least reduce its duration.

2.1.2 Model Parameter Uncertainties

The problem of energy management in microgrids is often treated within a model predictive framework, and as such requires models that represent various elements in the microgrid. These models are used to predict the behaviour of the microgrid up to a prediction horizon. The presence of incorrect parameters within these models can lead to inaccurate predictions, and thus to poor energy management decisions. Therefore, online identification of such model uncertainties and their effective compensation are also within the scope of investigation in this research.

Since the microgrid operates autonomously, the effects of model uncertainties may be masked by feedback actions and not be noticeable immediately. However, over the course of prolonged operation, the accumulated effects can be detrimental to the performance of the overall system. For example, suppose that the capacity of the PV system has been overrated, which could lead to overconfidence in the amount of PV production. This situation can be illustrated by a practical example as shown in Fig. 2.2, where the actual PV production results in an earlier than expected outage.

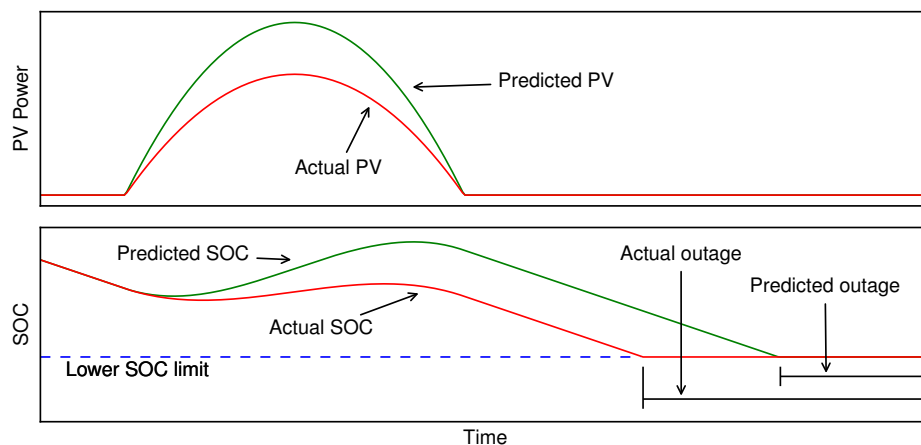


Figure 2.2: Effect of uncertainties in the PV system rating.

A similar situation can also be observed in Fig. 2.3, where an uncertainty in the battery capacity specification parameter used in the prediction model leads to an inaccurate prediction

of the SOC, and therefore the upcoming outage is not detected. This outage could potentially have been averted, or at least reduced in duration, by energy management actions if an accurate prediction had been available. Therefore, the differences in outage durations shown in Fig. 2.2 and Fig. 2.3 represent potential performance improvements that could be gained if the prediction accuracy can be improved by compensating for the model parameter uncertainties properly.

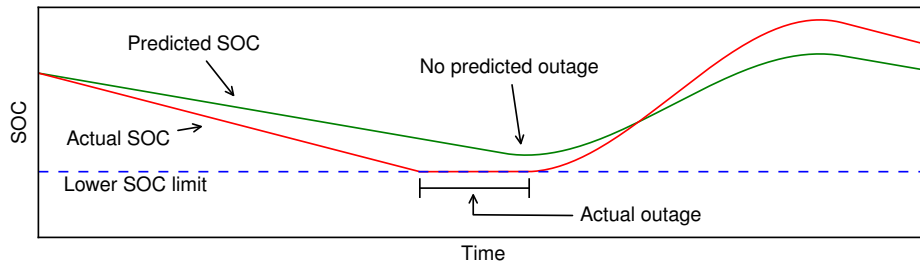


Figure 2.3: Effect of uncertainties in the battery capacity.

2.2 Preliminaries

2.2.1 System Description

The system under investigation is a 3-phase islanded microgrid shown in Fig. 2.4. Note that the developed techniques can be extended to more complex configurations with more energy sources and storage units. The renewable energy source is a PV array connected to the bus through a dc-dc converter and an inverter. The dc-dc converter uses a maximum power-point tracking (MPPT) algorithm and can also be commanded to curtail its output via dc-link voltage signalling. An energy storage unit consisting of a battery bank, a bidirectional dc-dc converter, and an inverter is also connected to the bus. The low-level controllers of the inverters use a droop mechanism, similar to the strategy described in [28], to control the voltage and frequency, and to maintain the power balance within the system. The strategy also includes a mechanism to curtail the surplus PV power production when the battery is fully charged and

the potential PV production exceeds the load demand. The battery converter is also responsible for estimating the SOC using the Coulomb counting technique. The load is separated into a critical part, and a controllable part that can be shed if necessary. An Ethernet network connects the power electronic converters and the sheddable load controller to the central EMS. This network is used to transmit periodic power measurements and SOC estimates from the converters to the EMS, and to deliver load shedding signals from the EMS to the sheddable load.

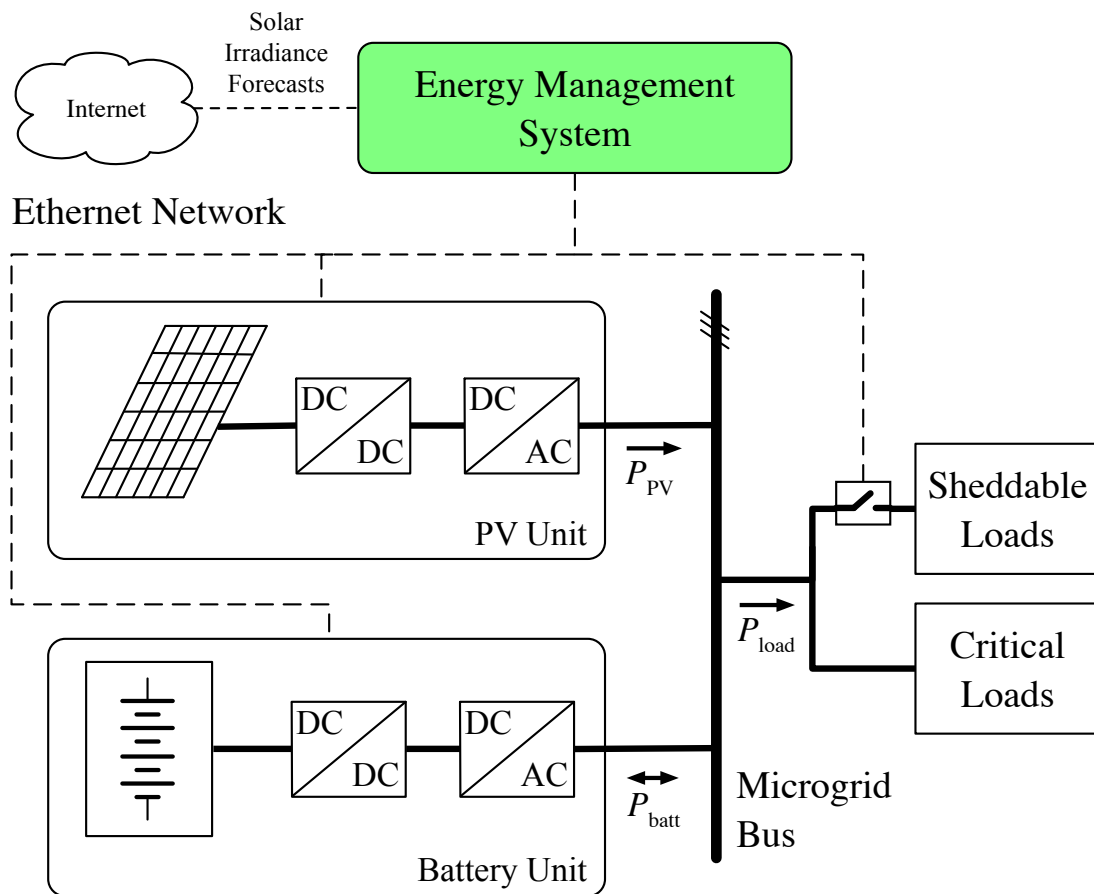


Figure 2.4: System structure of the microgrid used to develop and validate the EMS.

2.2.2 Assumptions

It is assumed that the measurements from the PV and battery units are made available to the EMS in the form of data sequences sampled at a rate of $1/T_s$, where T_s is the sampling interval.

PV Unit

For the PV unit, the power production can be represented by a data sequence \mathcal{P} :

$$\mathcal{P} = \{P_{PV}[k] \mid k = 0, \dots, N\} \quad (2.1)$$

where P_{PV} is the power measurement in W and N is the index of the most recent sample. In the current system, the sampling interval is 2 minutes.

Battery Unit

The power exchanged with the battery unit can be characterized by the dataset \mathcal{B} :

$$\mathcal{B} = \{P_{batt}[k], SOC[k] \mid k = 0, \dots, N\} \quad (2.2)$$

where P_{batt} is the measured power in W flowing into or out of the battery, and SOC is the estimate of the state-of-charge provided by the battery dc-dc converter.

Note that the information on the amount of stored energy is represented in terms of the SOC as a percentage. The relationship between these values can be expressed by

$$SOC[k] = \frac{E_{batt}[k]}{E_{batt}^{\max}} \cdot 100\% \quad (2.3)$$

where E_{batt} is the energy stored in the battery, and E_{batt}^{\max} is the battery capacity in Wh.

Irradiance Forecast

The irradiance up to the horizon can be represented by the set \mathcal{F} :

$$\mathcal{F} = \{G[k] \mid k=0, \dots, N\} \quad (2.4)$$

where G is the forecast irradiance in W/m^2 . This forecast is produced by processing the data provided by a weather forecast service for a chosen location, and the horizon is the duration of the available forecast data.

Load Forecast

A forecast for the load is also assumed to be available, and is represented by the set \mathcal{L} :

$$\mathcal{L} = \{P_{\text{load}}[k] \mid k=0, \dots, N\} \quad (2.5)$$

where P_{load} is the forecast load in W . In this case, an averaged characteristic daily load profile is used, with the emphasis being placed on the PV production predictions.

Sheddable Load

A portion of the load is designated as less critical or sheddable. The proposed shedding schedule, which is an outcome of the EMS strategy, is represented by the set \mathcal{S} :

$$\mathcal{S} = \{P_{\text{shed}}[k] \mid k=0, \dots, N\} \quad (2.6)$$

where $P_{\text{shed}}[k]$ is the amount of load in W to be shed at time step k .

2.2.3 Operating States

Four operating states of the microgrid can be defined as shown in Fig. 2.5. These states are a subset of the operating states commonly used in conventional power systems [22]. The definitions and transitions between the states are as follows:

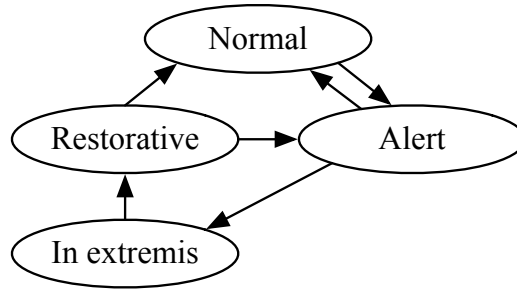


Figure 2.5: Microgrid operating states and transitions

Normal State

In the normal state, the battery system is able to maintain the balance between the energy production and the load, and no energy imbalance will occur.

Alert State

In the alert state, the battery system is still able to maintain the balance between energy production and the load demand, however an energy imbalance has been predicted to occur at some point in the future. This state will initiate the necessary outage mitigation actions.

In extremis State

When the available power from the generators and storage cannot meet the load demand, the microgrid will shut down and stay in this state until the available power becomes sufficient again to restore the system. This state is also referred to as the shutdown or outage state.

Restorative State

In this state, the black start procedures necessary to restart the microgrid will be performed, including bringing up the first inverter to establish the desired voltages at some key points and the frequency, then synchronizing additional inverters, and finally reconnecting the controllable loads back into the system.

2.2.4 Modeling

Modeling of PV Production

The predicted power output from the PV unit can be expressed by using the irradiance forecast as follows [84]

$$\hat{P}_{PV}[k] = \frac{G[k]}{1000} P_{PV}^{\max} \eta_{MPP} \quad (2.7)$$

where η_{MPP} is the efficiency of the unit at the maximum power point. The sequence $\hat{P}_{PV}[k]$ is then used by the EMS algorithm to predict the future behaviour of the microgrid.

Power Balance

Any imbalance between the PV generation and the load consumption must be provided or absorbed by the battery. Hence, the predicted power supplied (i.e. $\hat{P}_{batt} > 0$) or absorbed (i.e. $\hat{P}_{batt} < 0$) by the battery can be expressed as:

$$\hat{P}_{batt}[k] = \hat{P}_{load}[k] - \hat{P}_{PV}[k] \quad (2.8)$$

where \hat{P}_{load} is the forecast load demand.

Modeling of Battery Charging and Discharging Process

The amount of energy stored in the battery can be estimated using the battery model and the actual energy flowing into or out of the battery unit [53]. Therefore, the relationship between the stored energy and the charging/discharging power can be represented as follows:

$$\hat{E}_{\text{batt}}[k] = \hat{E}_{\text{batt}}[k-1] - (\hat{P}_{\text{batt}}[k] + \epsilon_{\text{batt}})T_s\eta_{\text{batt}} \quad (2.9)$$

where $\hat{E}_{\text{batt}}[k]$ (Wh) is the estimated energy stored in the battery at k , and ϵ_{batt} and η_{batt} are parameters that account for losses and the efficiency of the battery charging/discharging systems, respectively.

Furthermore, the battery capacity is limited by the constraint

$$E_{\text{batt}}^{\min} < \hat{E}_{\text{batt}}[k] < E_{\text{batt}}^{\max} \quad (2.10)$$

where E_{batt}^{\max} is the storage capacity of the battery, and E_{batt}^{\min} is the minimum discharge level, below which the battery will stop supplying power.

2.3 Predictive Energy Management in Microgrids

The overall objective of this energy management strategy is to improve the uptime of the critical loads in the microgrid by avoiding or minimizing the duration of any outages. This is achieved by using generation and load predictions to schedule pre-emptive load shedding as needed to ensure that the stored energy is effectively managed to serve the critical load, whenever possible. Predictions of the amount of stored energy are used to identify upcoming outages. Therefore, the key variable of interest is the SOC.

More specifically, the objective of the energy management scheme is to use the measurement data sets \mathcal{P} , \mathcal{B} , and the forecasts \mathcal{F} and \mathcal{L} to predict the SOC up the the horizon. Based on this information, an effective load shedding schedule \mathcal{S} will be developed to eliminate, if

possible, or reduce the duration of any outages.

2.4 Model Parameter Uncertainties

For the microgrid illustrated in Fig. 2.4, the presumed PV array rating is P_{PV-0}^{\max} , and the presumed battery capacity is $E_{\text{batt}-0}^{\max}$. Due to the lack of complete knowledge of the exact conditions of the PV system and battery, there are potential uncertainties in these two parameters. Thus, using them to predict the PV production and stored energy can lead to erroneous results. As these are two relatively constant parameters, it is assumed that the true values of these parameters, P_{PV}^{\max} and E_{batt}^{\max} , are in proportion to the presumed values, P_{PV-0}^{\max} and $E_{\text{batt}-0}^{\max}$:

$$P_{PV}^{\max} = \gamma_{PV} P_{PV-0}^{\max} \quad (2.11)$$

and

$$E_{\text{batt}}^{\max} = \gamma_{\text{batt}} E_{\text{batt}-0}^{\max} \quad (2.12)$$

where γ_{PV} and γ_{batt} are known as the PV and battery compensation factors, respectively.

The objective of this investigation is to use the measurement data sets \mathcal{P} , \mathcal{B} , and the forecast \mathcal{F} , to accurately determine the compensation factors γ_{PV} and γ_{batt} so that the PV production prediction, \hat{P}_{PV} , and the stored energy prediction, $\widehat{\text{SOC}}$, use more accurate values of P_{PV}^{\max} and E_{batt}^{\max} , such that

$$|P_{PV} - \hat{P}_{PV}| < |P_{PV} - \hat{P}_{PV-0}| \quad (2.13)$$

where $|P_{PV} - \hat{P}_{PV}|$ represents the error between the actual PV production and the compensated prediction, and $|P_{PV} - \hat{P}_{PV-0}|$ represents the error between the actual PV production and the

original uncompensated prediction. For the SOC,

$$|\text{SOC} - \widehat{\text{SOC}}| < |\text{SOC} - \widehat{\text{SOC}}_0| \quad (2.14)$$

where $|\text{SOC} - \widehat{\text{SOC}}|$ represents the error between the actual SOC and the compensated prediction, and $|\text{SOC} - \widehat{\text{SOC}}_0|$ represents the error between the actual SOC and the original uncompensated prediction.

The effectiveness of these compensation factors will also be demonstrated by showing the improvement in critical load outage performance that can be achieved when using the technique within a predictive energy management system.

2.5 Summary

This chapter has described the single-bus microgrid under investigation, laid out the key assumptions and definitions, and presented the predictive energy management problem and the model parameter uncertainty problem.

Chapter 3

Methodology for Energy Management and Parameter Uncertainties Compensation

The proposed methodology is presented in two parts: the solution to the energy management problem is presented first, including a bounding technique to deal with modeling uncertainties in the SOC. The second part introduces techniques to compensate for model parameter uncertainties in the PV system rating and the battery capacity specifications.

3.1 Proposed Predictive Energy Management Strategy

3.1.1 Overview

The proposed energy management strategy can be separated into three steps:

1. PV production forecasting
2. Prediction of microgrid behaviour, including characterization of potential outages
3. Scheduling of load shedding actions to avoid or reduce the duration of outages for critical loads

A simplified flowchart of the strategy is shown in Fig. 3.1. A PV prediction is made using information from a weather forecast service, and a load forecast is presumed to be available based on historical data. These forecasts are then applied to a model of the microgrid in order to predict the SOC, starting from the latest SOC value reported by the battery unit controller. If the SOC prediction indicates an upcoming outage, the pre-emptive shedding of some less critical load will be scheduled and carried out.

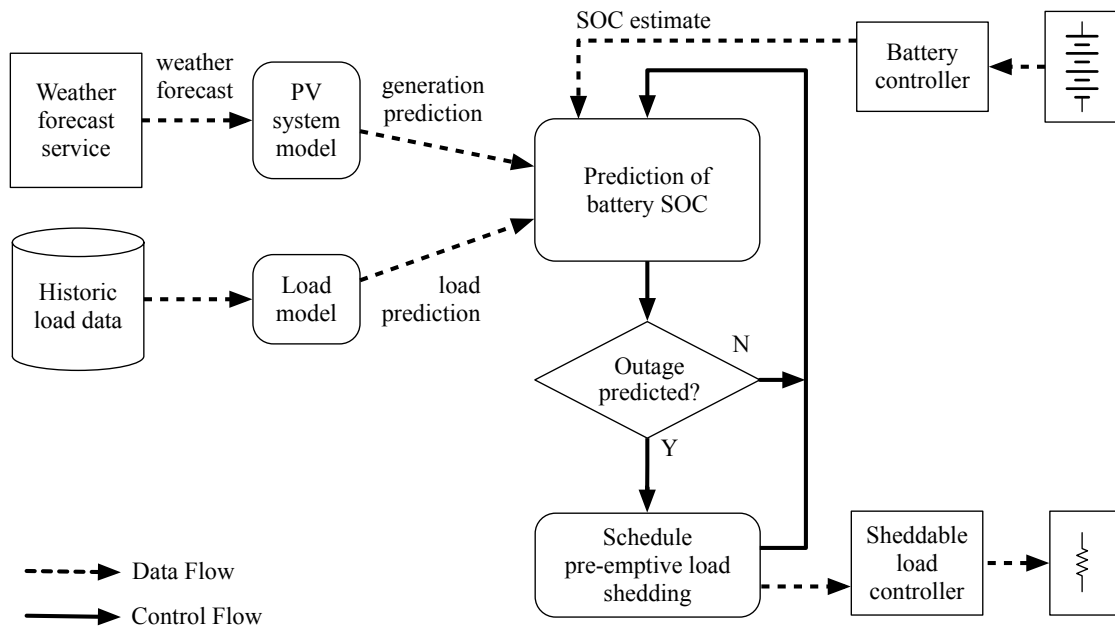


Figure 3.1: Predictive energy management strategy

3.1.2 PV Production Forecasting

PV Prediction Approach

A power production prediction for the PV array is created based on forecasts of accumulated solar flux and temperature provided by an online weather forecast service. These forecasts are calculated by the service on a periodic basis using a numerical weather prediction (NWP) model [42]. Such services are available in many parts of the world, including the Americas, Europe, and Asia, and are typically offered free of charge. While the accuracy of such forecasts

varies significantly based on the nature of the underlying model, the monthly average root mean square error ranged between 4 % and 14 % for the systems evaluated in [42]. Note that while there will be some differences between the forecasts and the actual irradiance incident on the PV array, particularly under cloudy conditions, the forecasts will still result in an overall improvement in the operation of the system over time. The forecast for a given location and time is combined with the specifications of the given solar array to build an effective PV power generation forecast as discussed in [85].

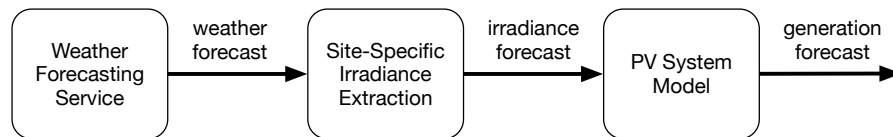


Figure 3.2: PV production forecasting.

An overview of the process used to create the PV production forecast is shown in Fig. 3.2. The weather forecasts are from the Environment Canada Global Environmental Multiscale NWP model, which is a free service provided by the Government of Canada. The specific service selected is the experimental High Resolution Deterministic Prediction System dataset, which provides a 48 hour forecast for points on a 2.5 km grid covering most of Canada and the northern United States [86]. The forecasts have a 1-hour time resolution, so they have to be interpolated to match the EMS update rate and then processed through the PV system model to create a PV production forecast as shown in Fig. 3.3.

The weather forecast is only updated four times a day at six hour intervals, and there is also a processing interval of up to eight hours between the start time of the forecasting process and the time when the full weather forecast is available for download. The resulting forecast horizon will therefore vary from 40 hours (for a fresh forecast) to just over 34 hours (for a forecast that is about to be replaced with a new one). This rolling set of forecasts is shown in Fig. 3.4, with an example illustrating the changing forecast horizon.

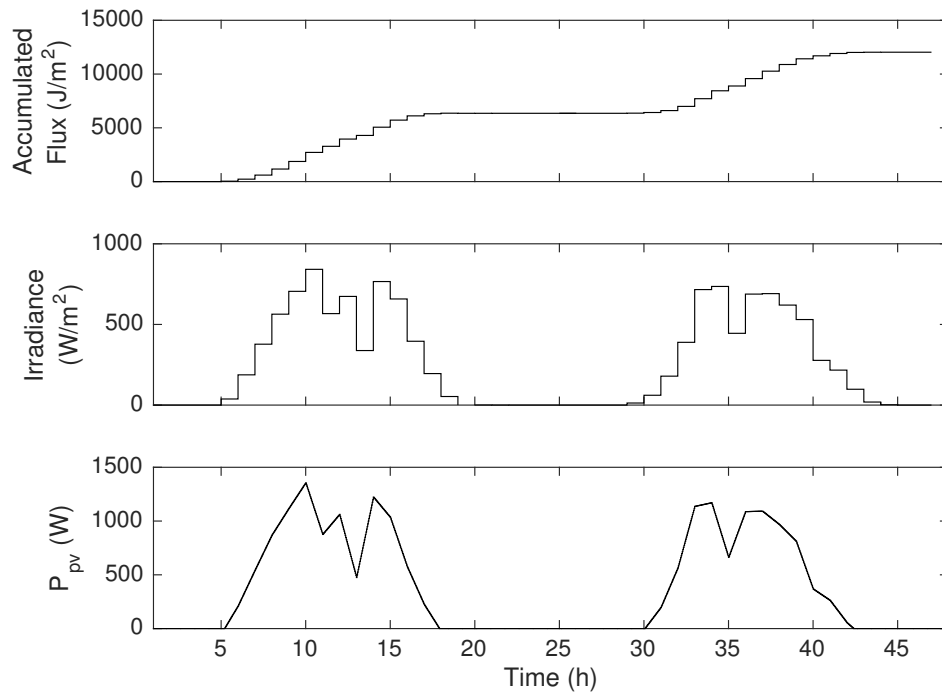


Figure 3.3: Examples of the accumulated downward incident solar flux forecast, extracted irradiance, and interpolated PV production forecast.

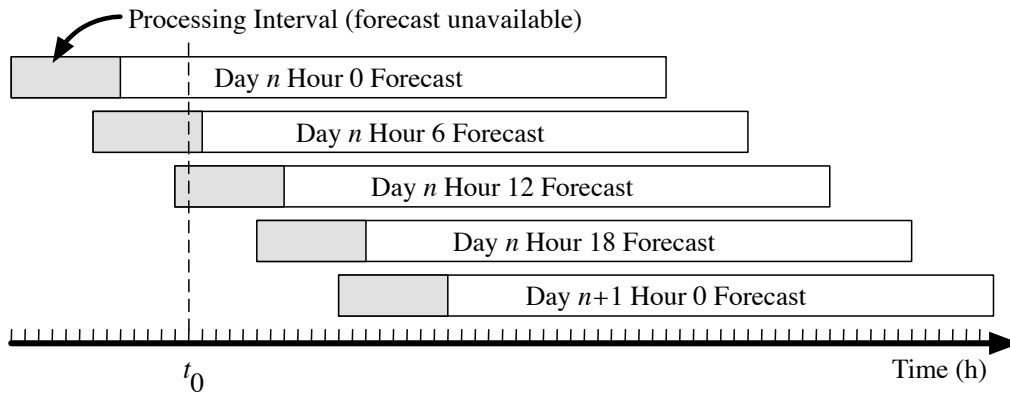


Figure 3.4: Weather forecast horizons, where the shaded areas indicate the 8 hour processing interval when the forecast is not yet publicly available. For example, at $t = t_0$ the active forecast is the Day n Hour 0 Forecast, which has a horizon of 35 hours. The active forecast will switch to the Hour 6 Forecast when it becomes available in another hour, at which point it will have a horizon of 40 hours.

3.1.3 Prediction of Energy Imbalance

The battery unit is responsible for maintaining the power balance in the system, supplying power when the load exceeds the PV supply, and charging when the available PV power exceeds the load. An outage can be predicted by determining if and when the energy available from the PV source and the battery will be unable to balance the load demand.

With the information on PV generation and load predictions, the microgrid behaviour can be calculated from the current timestep k to $k + N$, where N is the number of timesteps to the horizon, by applying the predictions as inputs to the microgrid model and calculating its state and output behaviour up to the prediction horizon. The step size T_s is chosen to be 2 minutes. The current estimate for the energy stored in the battery is provided by the battery converter running the SOC estimation function. Although new information from the PV forecasts is only available every 6 hours, the prediction algorithm is executed more frequently, in this case at 4 minute intervals, in order to incorporate the updated SOC information.

From (2.8), the predicted generation/load power imbalance at each step of the prediction can be expressed as

$$\hat{P}_{\text{batt}}[k] = \hat{P}_{\text{load}}[k] - \hat{P}_{\text{PV}}[k]. \quad (3.1)$$

Since the battery will try to supply or absorb this power imbalance, it can be used to predict the amount of energy stored at each point up to the horizon using (2.9)

$$\hat{E}_{\text{batt}}[k] = \hat{E}_{\text{batt}}[k-1] - \hat{P}_{\text{batt}}[k]T_s \quad (3.2)$$

where $\hat{E}_{\text{batt}}[k-1]$ is the prediction of the energy stored in the battery at the previous timestep $k-1$, measured in Watt-hours (Wh). Note that the capacity limit of the battery must also be accounted for. As the stored energy in the battery nears its full capacity, the battery converter will signal the PV system to curtail its output to prevent the battery from overcharging, and this

feature is reflected in the stored energy prediction implementation. Also, at the other extreme, when the stored energy prediction drops below the lower limit, the prediction continues to reflect the effect of the power imbalance in order to calculate the energy deficit as shown below.

An outage can be predicted if the stored energy level drops below its lower limit as illustrated in Fig. 3.5. The timestep k_{outage} where \hat{E}_{batt} is predicted to reach the discharge limit can be used to calculate the remaining time until the outage. The estimate of the predicted outage energy deficit, E_{deficit} , can be found by integrating the predicted battery power supplied during the outage. First, k_{recover} is identified as the timestep where \hat{E}_{batt} returns from its excursion below the lower limit, or, if it does not return, the timestep of the horizon. The outage duration is therefore

$$T_{\text{outage}} = (k_{\text{recover}} - k_{\text{outage}})T_s. \quad (3.3)$$

The outage energy deficit in Watt-hours can then be calculated as

$$E_{\text{deficit}} = \sum_{j=k_{\text{outage}}}^{k_{\text{recover}}} \hat{P}_{\text{batt}}^{\gt 0}[j]T_s. \quad (3.4)$$

where $\hat{P}_{\text{batt}}^{\gt 0}$ is the prediction of the power required to be supplied by the battery.

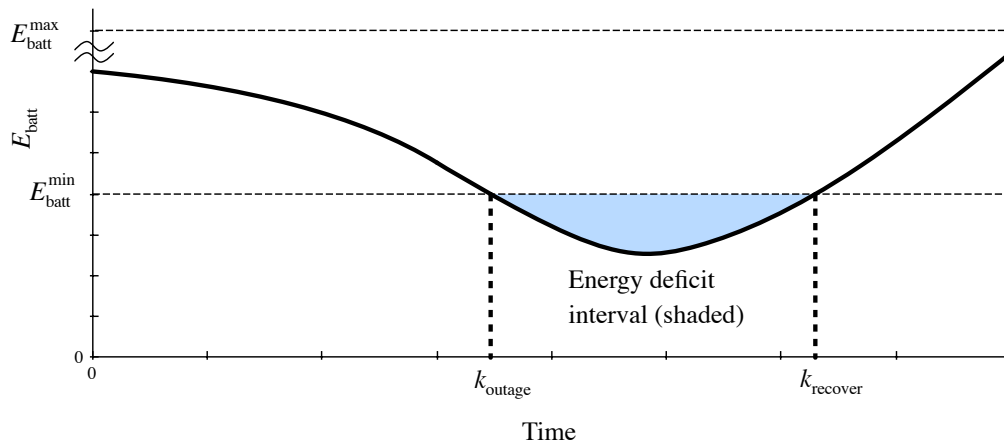


Figure 3.5: Lower stored energy limit and energy deficit region.

If the prediction results in multiple outages only the first outage is identified and characterized. Subsequent outages will be considered as the horizon advances.

3.1.4 Mitigation of Outages

Once a potential outage has been predicted, actions can be scheduled immediately to mitigate the severity of the outage by reducing its duration or delaying its occurrence. Pre-emptively shedding a less critical part of the load, for example non-critical lighting loads, at an appropriate time and for the needed duration can potentially reduce the length of the outage, or eliminate it altogether.

The required reduction in the energy consumed must be at least equal to E_{deficit} to avoid the outage. It is presumed that there is a fixed amount of load, $P_{\text{sheddable}}$ available to be shed. The load shedding must therefore occur for a period of

$$T_{\text{shedding}} = \frac{E_{\text{deficit}}}{P_{\text{sheddable}}}. \quad (3.5)$$

Once the duration of the load shedding action is determined, the next decision to be made is when to shed it. A conservative choice is to start shedding immediately, when the potential outage is first identified. However, this can result in unnecessary shedding if the situation improves. Alternately, the shedding endpoint k_{endshed} can be selected to be the timestep k_{outage} , thus delaying the shedding action until closer to the predicted outage. Note that a choice somewhere between these extremes may be optimal based on the degree of confidence in the quality of the predictions. However, for the purpose of this discussion $k_{\text{endshed}} = k_{\text{outage}}$ is the chosen approach.

The timestep of the shedding start point $k_{\text{startshed}}$ can then be calculated, based on the previously calculated shedding period, as

$$k_{\text{startshed}} = k_{\text{endshed}} - \frac{T_{\text{shedding}}}{T_s} \quad (3.6)$$

The resulting shedding action is then scheduled as shown in Fig. 3.6. As the forecasts are updated and up-to-date SOC estimates are received from the battery converter, which are based on the actual PV and load behaviour, the timing and/or duration of the predicted outage will change. Therefore, the start and end times (points A and B, respectively) of the shedding schedule will be recalculated. Once the current time reaches the scheduled shedding start time at point A, then the shedding action will begin.

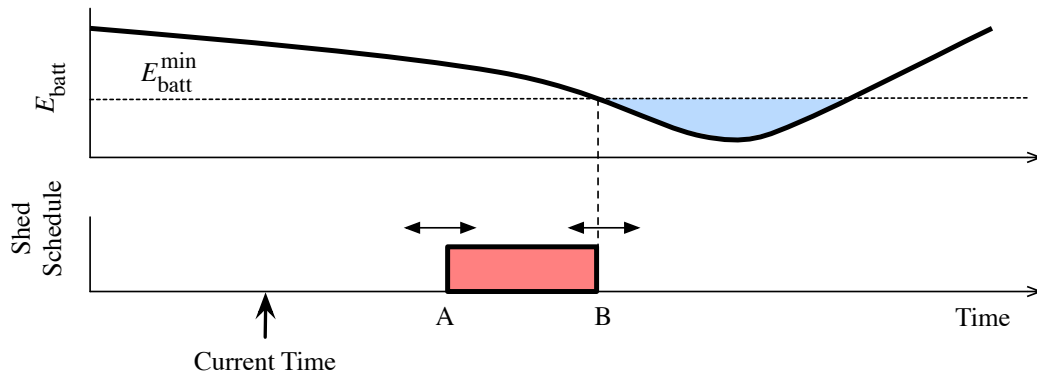


Figure 3.6: Pre-scheduling of load shedding action prior to the start of shedding.

Once shedding has started, the scheduling algorithm is adaptively adjusted as shown in Fig. 3.7, where the shed end time at point D can be adjusted according to the latest information in the prediction. This adaptive approach prevents the chattering that can otherwise occur if the shedding is completely re-scheduled.

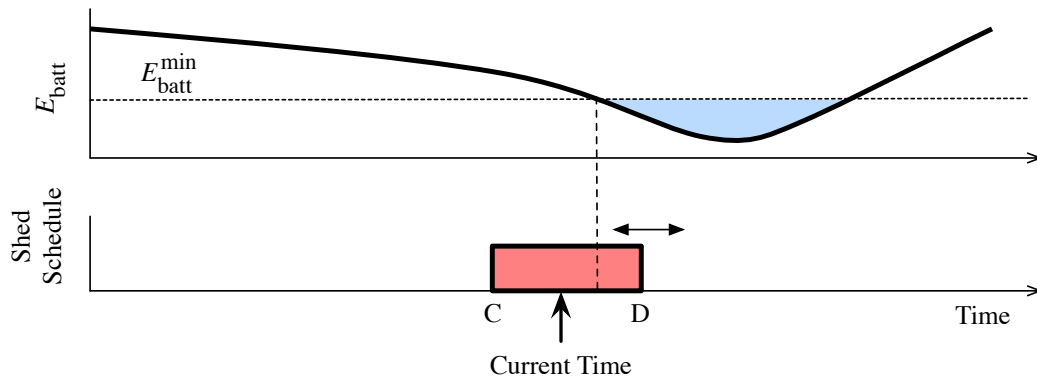


Figure 3.7: Scheduling of load shedding endpoint after shedding has begun.

Note that if an outage is predicted, P_{shedable} will be shed for at least T_s , which may result in shedding more than the minimum energy necessary to avoid the outage. On the other hand, if a large energy deficit has been predicted, it may not be possible to avoid an outage completely. In this case, the noncritical load shedding will start immediately, and the outage will be deferred for as long as possible.

The technique can be extended to cases where there are multiple controllable loads available to be shed, and the necessary communication infrastructure to reach them all. A prioritized list of these loads can be established. Once the lowest priority load shedding event has been scheduled, an attempt can be made to resolve the remaining balance of the energy deficit by scheduling the shedding of the next-lowest priority loads in a similar fashion, with the procedure continuing until the deficit is accommodated or there are no more sheddable loads available to be scheduled.

Note that if the actual PV generation is greater than predicted, then the shedding will be postponed further with each timestep (or shortened if shedding has already started), and may potentially not even be necessary. If the actual PV generation is lower than predicted, then subsequent evaluations will cause a longer shedding event to be scheduled.

3.1.5 Uncertainties in Prediction

One issue with the technique described above is that uncertainty in the stored energy estimate has not been considered. One possible solution to handling such uncertainty is to assign a safety margin to the shedding schedule, for example by shedding the load for a 10% longer period than the minimum required. However, this approach is somewhat arbitrary, and does not account for the fact that the uncertainty changes with time, with near-term forecasts being generally more accurate than the forecasts out at the horizon.

Recognizing the fact that the amount of stored energy becomes known only when the battery is at the fully charged or discharged state [87], one can use an error bound on the amount of stored energy to capture such uncertainty. The bound will increase with time, as the confidence

in the value of the estimate decreases.

At each timestep, the bound on the stored energy can be calculated as

$$E_{\text{batt}}^+[k] = E_{\text{batt}}[k] + \delta[k] \quad (3.7)$$

$$E_{\text{batt}}^-[k] = E_{\text{batt}}[k] - \delta[k] \quad (3.8)$$

where $\delta[k]$ represents the uncertainty in the amount of stored energy, with

$$\delta[k] = \delta[k - 1] + \epsilon \quad (3.9)$$

where ϵ is the per-timestep bounding parameter. This parameter is chosen empirically, and accounts for the potential sources of error in the stored energy estimate, such as inaccuracies in the battery model, and errors in the measurement of power flow in and out of the battery. In this study the bounding parameter is chosen to be 0.3% per hour to illustrate the concept. The resulting cumulative uncertainty bound will be monotonically increasing with time, reflecting the decrease in certainty about the amount of stored energy as a function of the time since the last fully charged or fully discharged state. The bounding approach is applicable to both the estimation of the actual stored energy based on measurements from the converters, and to the prediction of the future stored energy trajectory. The use of the bound is illustrated in Fig. 3.8, where the lower bound is used to determine the potential time, extent, and energy deficit of the outage.

The bound is reset when the battery terminal behaviour indicates that the battery is in the fully charged or fully discharged state, during which time $\delta[k] = 0$. Note that in practice, if the battery does not reach either state over a long period of time, the bound will continue to grow and will eventually exceed the practical limits of the battery itself. Therefore some limits must be placed on the growth of the bound, however the details of such a mechanism will be explored in future work.

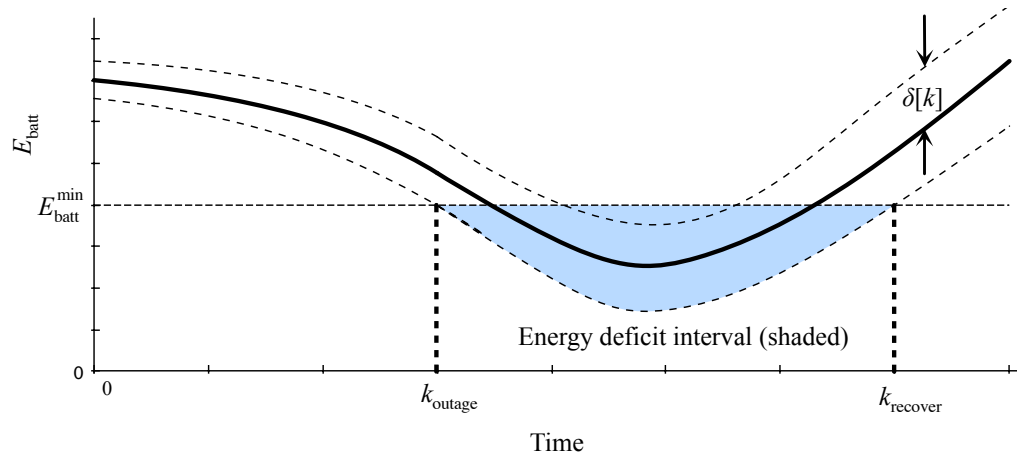


Figure 3.8: Lower stored energy limit with the uncertainty bounds.

3.2 Model Parameter Uncertainties

3.2.1 Overview

The two parameter uncertainties under investigation are the PV system rating and the battery capacity. For the PV system rating, the approach taken is to identify intervals where the prediction of the PV power is expected to be well correlated with the actual PV power. A 1-day history of the incoming data from the inverters is stored, along with the matching prediction of the PV generation based on the weather forecast. Days that are relatively cloud-free are then identified, and the peak ratio of the predicted PV power generation versus the actual measured production is determined. The resulting ratio is then used to adjust the prediction in order to improve its accuracy. For the battery capacity parameter, the measured power charging or discharging the battery system is recorded and then used as an input to the battery model to create an SOC prediction. The resulting SOC profile is then compared against the actual recorded SOC profile, and a least-squares fit is used to determine the battery capacity compensation factor.

By following this approach and applying the adjusted model parameters in the predictions, the resulting improvements in prediction accuracy can potentially improve the operational performance of the microgrid. For example, it will be demonstrated that when the technique is

used in a predictive EMS system the result is a 12% reduction in the total duration of outages. Also, by using only relatively cloud-free days to calculate the PV adjustment, the impact of forecast variability is minimized, which improves upon the previous state of the art solution.

3.2.2 Compensation Factor for Uncertainties in the PV System Rating

The key concept for determining γ_{PV} from (2.11) is to compare the actual measured PV power production against the forecast predicted production under a clear-sky condition. Note that the proposed technique uses only the measurements from the converters and the forecasts, and does not depend on any additional sensors.

On a cloud-free day, the PV production will follow the rise and set of the sun, with a peak at approximately mid-day. Under these conditions, it is sufficient to consider just the peak values in the measured and predicted datasets to calculate the compensation factor. However, this approach is complicated by the variability of the PV power production, caused mostly by changes in the cloud cover during the day. Comparing the peaks on a cloudy day is unlikely to result in an accurate compensation factor. However, if relatively cloud-free days, where the forecast PV profile is similar to the actual PV profile, are identified then this variability can be removed from the problem.

To determine whether a given day is relatively cloud free, the root-mean-squared error between P_{PV} and \hat{P}_{PV} can be used

$$\text{RMSE}_{PV} = \sqrt{\frac{1}{N-1} \sum_{i=0}^{N-1} (P_{PV}[i] - \hat{P}_{PV}[i])^2} \quad (3.10)$$

where, for an ideal day with a correct value for γ_{PV} , the resulting RMSE_{PV} would be near zero. However, given that γ_{PV} is unknown, the stored data must be normalized first, and the effects of any outages must be removed so that the comparison is valid. Therefore, the resulting solution is separated into four steps: PV dataset normalization, removal of outage periods, determination of cloud-free conditions, and calculation of the PV compensation factor. These

steps are illustrated in Fig. 3.9.

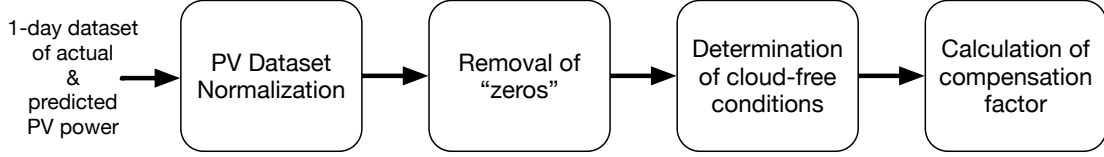


Figure 3.9: PV compensation steps

PV Dataset Normalization

First, the peaks of the actual PV measurements and the PV prediction datasets are determined using

$$P_{\text{PV-peak}} = \max_{i=0}^{N-1} P_{\text{PV}}[i] \quad (3.11)$$

$$\hat{P}_{\text{PV-peak}} = \max_{i=0}^{N-1} \hat{P}_{\text{PV}}[i] \quad (3.12)$$

where i indexes the dataset of N values stored during the previous day. These peak values are used for both normalization and later for determining the PV compensation factor.

The datasets are normalized by using

$$P_{\text{PV-nor}}[i] = 100 \frac{P_{\text{PV}}[i]}{P_{\text{PV-peak}}}, \quad i=0, \dots, N-1 \quad (3.13)$$

$$\hat{P}_{\text{PV-nor}}[i] = 100 \frac{\hat{P}_{\text{PV}}[i]}{\hat{P}_{\text{PV-peak}}}, \quad i=0, \dots, N-1 \quad (3.14)$$

where $P_{\text{PV-nor}}$ and $\hat{P}_{\text{PV-nor}}$ are the normalized datasets containing the actual PV power measurements and the forecast PV power predictions, respectively. This approach has the added benefit

of removing the artificially low error level that would otherwise occur during very cloudy days if absolute measures were used in the comparison.

Removal of Outage Periods

An additional challenge is that the actual recorded PV data will also show the effects of control actions, such as a shutdown due to an outage, but these actions will not appear in the prediction. To resolve this issue, a subset of the data that contains just the non-zero PV production periods is used for the comparison. This subset can be found using the algorithm illustrated in Fig. 3.10, where $P_{\text{PV-nz}}$ and $\hat{P}_{\text{PV-nz}}$ are the non-zero datasets of normalized PV power measurements and the forecast PV power predictions, respectively, and M is the length of the non-zero datasets.

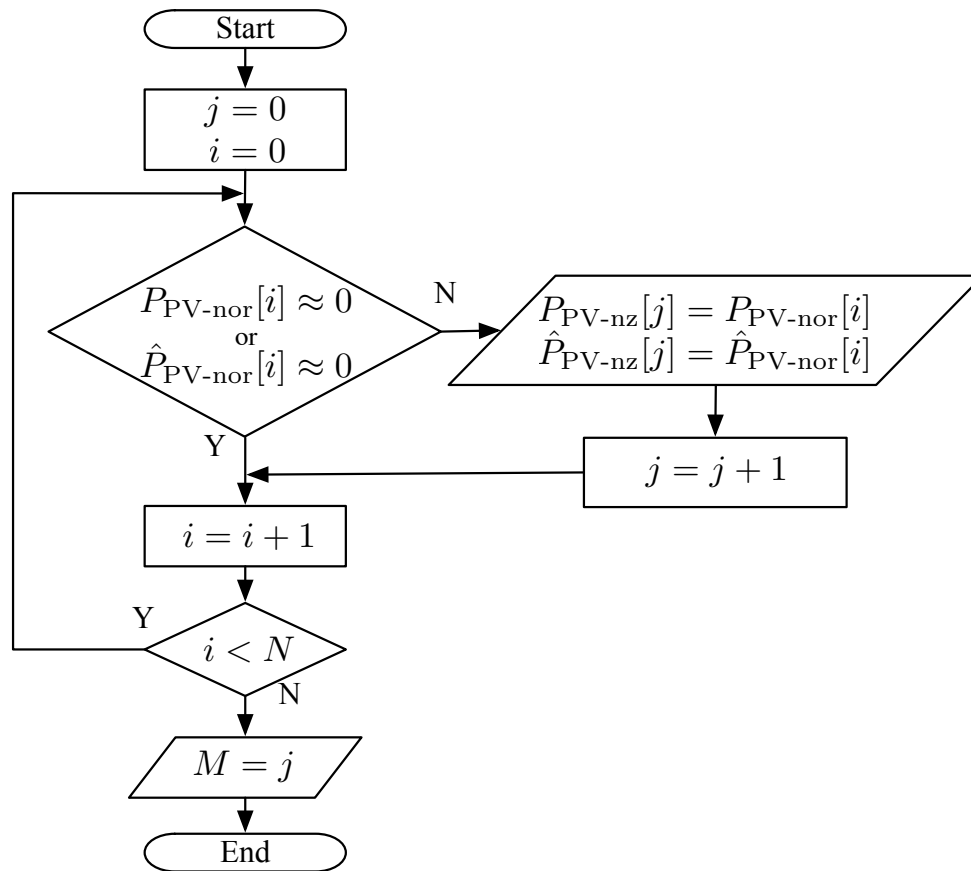


Figure 3.10: Flowchart of algorithm to remove near-zero datapoints.

Determination of Cloud-free Conditions

The root-mean-squared error can now be found using (3.10), after substituting $P_{\text{PV-nz}}$ for P_{PV} , $\hat{P}_{\text{PV-nz}}$ for \hat{P}_{PV} , and m for n

$$\text{RMSE}_{\text{PV-nz}} = \sqrt{\frac{1}{M-1} \sum_{i=0}^{M-1} (P_{\text{PV-nz}}[i] - \hat{P}_{\text{PV-nz}}[i])^2} \quad (3.15)$$

If the calculated $\text{RMSE}_{\text{PV-nz}}$ is less than a threshold L then the agreement is deemed to be good, suggesting that the day is relatively cloud-free. The threshold value L is chosen experimentally, and in this case it was found that a limit of 10% effectively discriminated between sunny and cloudy days, approximately corresponding with the metrological criteria separating a “sunny” forecast from a “mostly sunny” one.

Calculation of the PV Compensation Factor

Given that the day in question has been determined to be relatively cloud-free, the PV compensating factor can now be calculated using

$$\gamma_{\text{PV}} = \frac{P_{\text{PV-peak}}}{\hat{P}_{\text{PV-peak}}} \quad (3.16)$$

This factor is then applied to subsequent predictions in order to improve their accuracy, as will be demonstrated in Section 5.2.1.

3.2.3 Compensation Factor for Uncertainties in the Battery Capacity

The battery capacity compensation factor γ_{batt} from (2.12) is found by comparing the SOC profile calculated using the battery model from the recorded P_{batt} values, against the actual recorded SOC values. First, substitute for \hat{E}_{batt} in (2.9) using (2.3) to obtain the battery model

in terms of the predicted state-of-charge ($\widehat{\text{SOC}}$).

$$\widehat{\text{SOC}}[i] = \widehat{\text{SOC}}[i-1] - \frac{100\%}{E_{\text{batt}}^{\text{max}}} (\hat{P}_{\text{batt}}[i] - \epsilon_{\text{batt}}) T_s \eta_{\text{batt}} \quad (3.17)$$

The calculated $\widehat{\text{SOC}}$ profile can then be found by iterating over the recorded P_{batt} values, starting with the initial value $\widehat{\text{SOC}}[0] = \text{SOC}[0]$ reported by the battery unit at the start of the period.

Second, the two datasets are differenced to create a linear algebraic problem that can be solved using least-squares.

$$\Delta\text{SOC}[i] = \text{SOC}[i+1] - \text{SOC}[i], \quad i=0, \dots, N-1 \quad (3.18)$$

$$\Delta\widehat{\text{SOC}}[i] = \widehat{\text{SOC}}[i+1] - \widehat{\text{SOC}}[i], \quad i=0, \dots, N-1 \quad (3.19)$$

A least-squares fit is then calculated to determine the battery capacity compensation factor

$$\gamma_{\text{batt}} = \text{slope of the linear least squares fit of } \Delta\text{SOC} \text{ and } \Delta\widehat{\text{SOC}} \quad (3.20)$$

which is applied to future predictions.

3.3 Summary

The predictive EMS described in this chapter uses weather forecasts to predict the behaviour of the microgrid up to the horizon. When an upcoming outage is predicted, the EMS attempts to avert or reduce the duration of the outage by shedding a less critical load pre-emptively. In order to account for uncertainties in the SOC, a bound is applied to the SOC estimate, and the lower limit of this bound is used in the outage prediction strategy.

A solution to the problem of model parameter uncertainties in the PV system rating and the

battery capacity specification is also presented. The PV compensation factor is determined by detecting relatively cloud-free days where the variability of clouds are not a factor, and then calculating the peak ratio of the measured versus the predicted PV production on these days. This factor is then used to adjust the future PV predictions. The SOC compensation factor is found by applying the recorded P_{batt} data for the most recent one-day period to the microgrid model, and then comparing the resulting SOC prediction against the actual recorded SOC data for the same day. The compensation factor is determined from the solution to the least-squares fit of the two datasets, and is then used to adjust the battery capacity parameter for future predictions.

Chapter 4

Experimental Setup

The energy management system has been implemented in software and validated against an experimental microgrid constructed by the author and his colleagues in the laboratory. This configurable PV/battery microgrid has been used for previous studies on reactive power sharing and adaptive droop techniques involving both hybrid and independent configurations. It has been equipped with a communication network to facilitate data collection and analysis, and this capability is also used to enable the EMS strategy under investigation here.

In addition, an accelerated software simulation of the microgrid has been developed to allow for debugging and testing of the proposed EMS strategy without requiring operation of the microgrid hardware. The implementation of the EMS, and the hardware and software of the experimental microgrid, are presented in this chapter. The the system hardware and firmware elements are presented first, followed by the details of the software implementation.

4.1 Apparatus

4.1.1 Overview of the Experimental Microgrid

The main components of the experimental setup are shown in Fig. 4.1, along with a photograph of the apparatus in Fig. 4.2. The setup is equipped with a microgrid bus that interconnects the ac

sources and loads. The PV converters shown include the PV dc-dc converter and its associated 3-phase inverter. The power source for the PV dc-dc converter is the Chroma PV simulator. The battery converters are a bidirectional dc-dc converter and its associated inverter, which are connected to a lead-acid battery bank. The programmable NHR 3-phase load emulates the critical and sheddable loads in the system. All the controllers are interconnected with the computer running the EMS software over an Ethernet network. Details on these components are provided in the sections that follow.

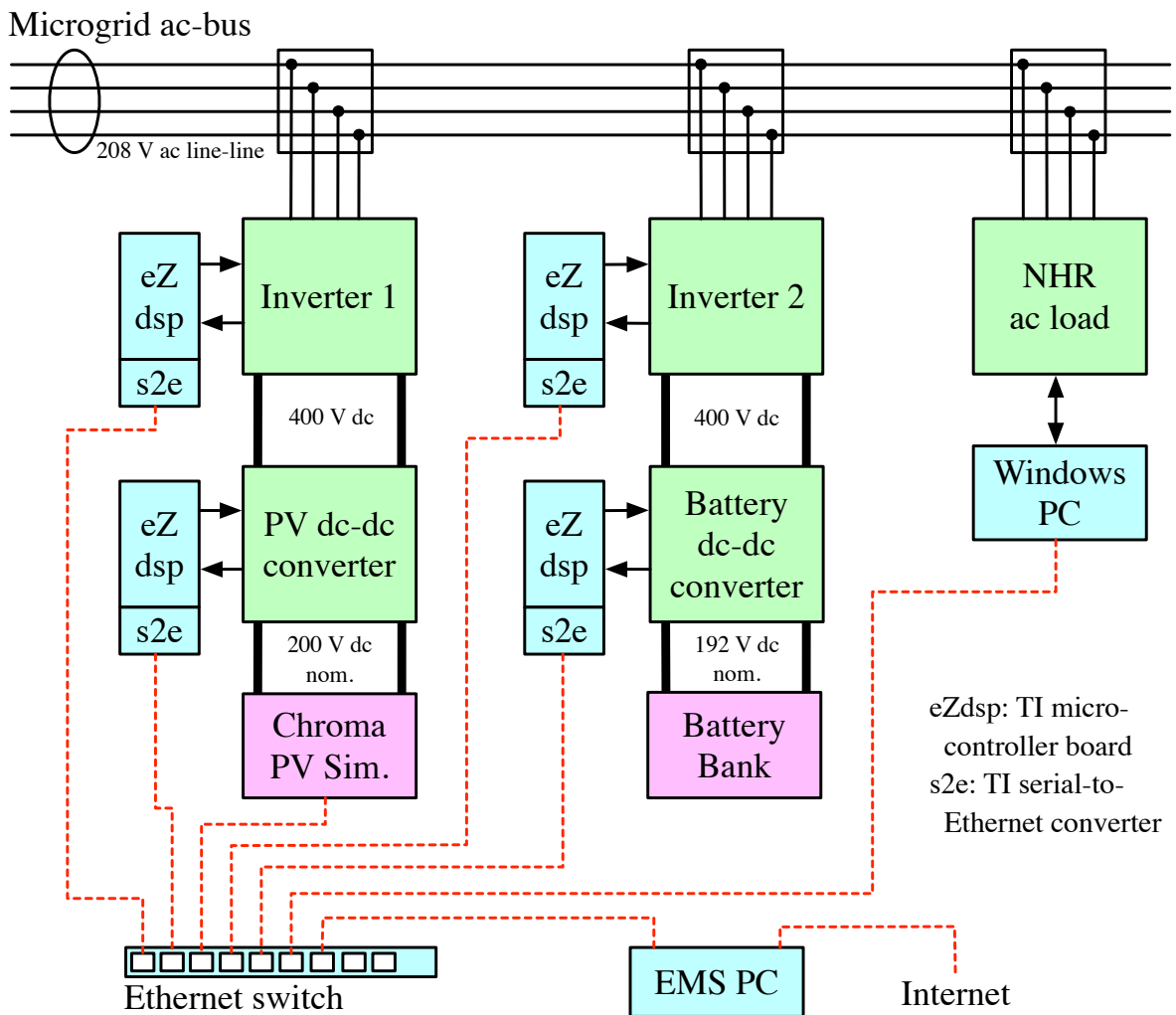


Figure 4.1: Experimental microgrid overview

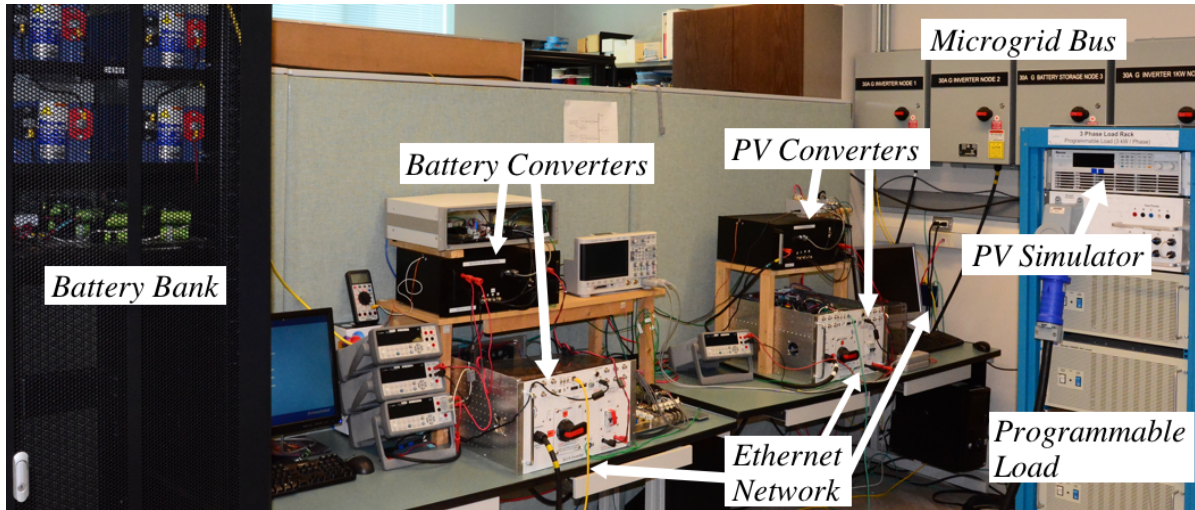


Figure 4.2: Experimental microgrid

4.1.2 Specifications

The key specifications of the system are presented in Table 4.1.

Table 4.1: System Parameters

Description	Parameter	Value
PV System Rating	P_{PV}^{\max}	1400 W
Battery System Rating	P_{batt}^{\max}	1000 W
Battery Capacity (nominal)	E_{batt}^{\max}	7000 Wh
EMS Update Period	T_u	4 minutes
Prediction Step Size	T_s	2 minutes
Acceleration Multiplier	K_a	120 times
Sheddable Load	$P_{sheddable}$	75 W
Battery SOC Lower Limit	SOC_{\min}	30 %

Note that the system can be configured to operate in an accelerated mode, where the execution time of the test scenarios has been accelerated by 120 times. This means that 2 minutes of real time are executed in 1 second. This allows the chosen multi-day scenarios to be tested in approximately an hour, rather than requiring multi-day runs of the experimental system.

4.1.3 Power Electronic Converters

The dc-dc converters and the 3-phase inverters share several common elements, including the microcontroller boards and the sensor circuitry. These common elements are described first, including some details on the chosen firmware architecture, followed by descriptions of the PV dc-dc converter, the battery dc-dc converter, and the inverter implementations.

Controller Implementation

Each of the converter controllers is implemented using a Spectrum Digital eZdsp board containing a Texas Instruments TMS320F28335 32-bit floating-point microcontroller running at 150 MHz. The microcontroller board is shown in Fig. 4.3. These microcontrollers are targeted at the real-time control market, and include sophisticated analog to digital converter (ADC), multi-phase pulse-width modulation (PWM), and serial communication (SCI) subsystems to support complex power electronic control algorithms.

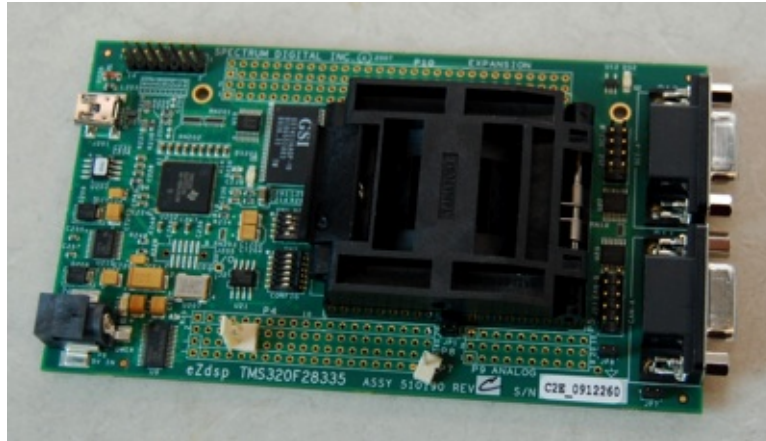


Figure 4.3: TMS320F28335 microcontroller board.

The microcontrollers are programmed using the Simulink Embedded Coder / Code Composer Studio toolchain. This approach allows the controller structure to be easily defined and revised using Simulink blocks, and then uses the code generation capability of Simulink to automatically create the corresponding C code. The main hardware elements of the microcontroller are accessed using platform-specific interface blocks, which enable access to the

hardware features in a user-friendly form. For example, blocks are provided to access the ADCs, the PWM subsystem, and the SCI port.

Once the C program for the controller is generated, the TI Code Composer Studio application is used to compile the program into binary executable code. This code is then downloaded into the flash memory on-board the microcontroller, and runs once the microcontroller is reset.

By default, the code generated from the Simulink model will run in a main line loop at a sample rate determined by the shortest time constant in the model. However, this approach can result in significant jittering or even the loss of synchronization between the hardware and the executed code. To resolve this, the structure of the model has been split in such a way that the relatively slow external functions (processing of switch inputs, indicator lights, serial communication) are run in the main line, and the critical real-time functions are moved into an interrupt routine. Smooth control behaviour has been obtained by configuring the PWM subsystem to initiate an ADC cycle each time the PWM counter is reset to zero. The completion of the ADC cycle, which scans multiple analog input channels, then triggers the interrupt that runs the controller code. The C-code generated by the Simulink Embedded Coder toolchain is relatively well structured, and reflects the naming of the elements from the Simulink model, so the code can be manually checked (and modified) if needed to ensure the desired results are obtained. Note also that a triangle shaped pattern is chosen for the PWM counter configuration, which keeps the ADC conversions away from the noisy switching transients, at least for the dc-dc cases.

Care must be taken in the design of the controller to ensure that the controller model can be run within the available cycle time prior to the arrival of the next interrupt. Otherwise, if the controller model takes too long to execute, the next interrupt may be missed, resulting in a controller that executes at half of the expected speed. This is further complicated if the controller contains potential multiple paths of execution (for example, logic that enables and disables internal functions or loops), since this can result in variable execution times which can be difficult to detect and debug. In particular, lookup functions were found to be problematic,

since the default models used iterative interpolation algorithms that caused widely varying time delays. The use of an output signal toggled at each model execution step, combined with an oscilloscope that can be triggered by a configurable pulse width range, have been used to detect overflowing interrupt cases, and the controller models are adjusted accordingly to eliminate them.

Sensor Signal Conditioning

In all the converters, measurements of current and voltage are taken internally using LEM Hall-effect sensors, and the resulting signals are scaled, level-shifted (if needed for bipolar signals such as the battery current and the ac measurements), and filtered to match the 0 to 3.0 Volt range of the ADC inputs. A typical example of a single channel showing the sensor and the signal conditioning circuitry for a unipolar case is shown in Fig. 4.4(a), and the level shifter circuit is shown in Fig. 4.4(b). These signals are sampled by the ADC, and are utilized by the low-level controllers. Selected signals are also down-sampled and periodically sent over the Ethernet link to the central EMS.

Internal Protection

While the laboratory facility is relatively low power (sub-10 kW), the converters operate at voltages (150 V to 410 V) and currents (up to 10 A peak) which are high enough to pose a safety concern. The controllers use an averaged current-mode control strategy, and can therefore limit the range of the internal current reference signals to avoid exceeding the specifications of the power electronic devices. However, during development the interactions between the converters in the system did occasionally lead to over-voltage conditions that required emergency shutdown of the converter so that the devices would not be damaged. This over-voltage shutdown has been achieved by combining the voltage sensor ADC measurements with the trip-zone mechanism of the microcontroller PWM subsystem, allowing a near-immediate controlled shutdown and de-energizing of the converter. In particular, for the battery dc-dc con-

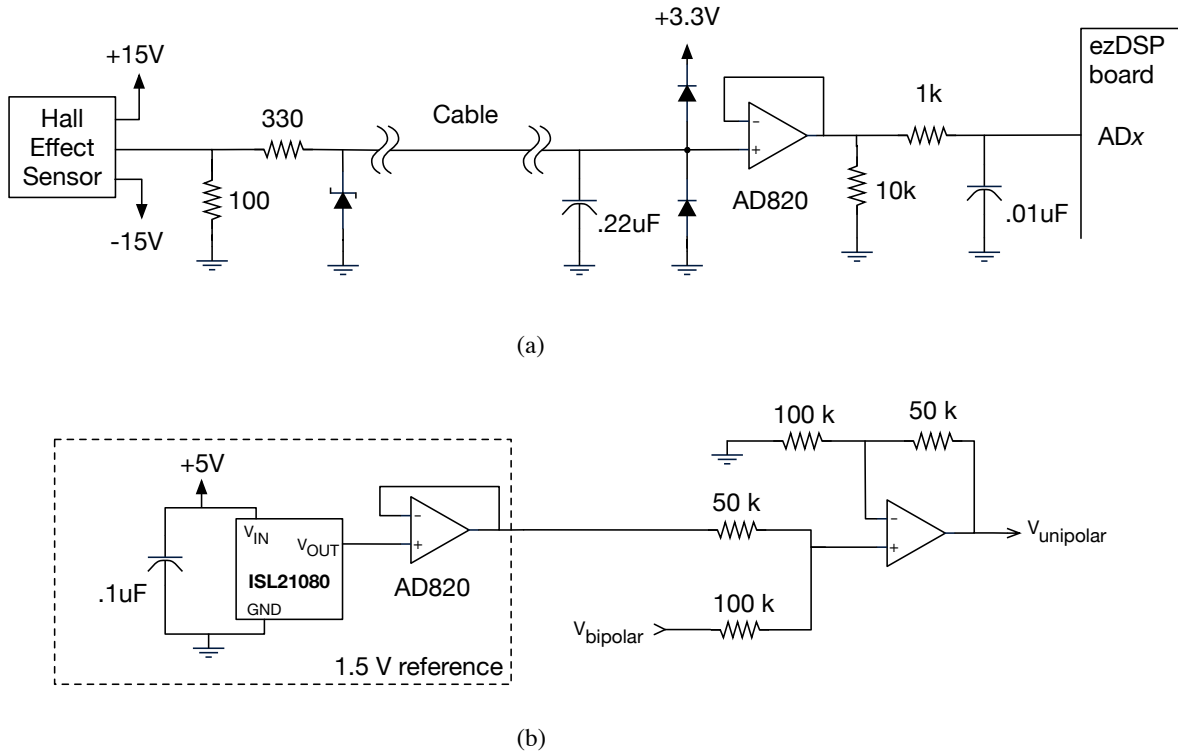


Figure 4.4: Current and voltage sensor signal conditioning circuitry: (a) typical unipolar interface circuit; (b) level shifter for bipolar signals.

verters and the inverters, the trip zone mechanism ensures that all power electronic switches are opened and locked in a safe state. The power-circuit terminal contactors are also opened to isolate the converter, and the dc filter capacitor bleeder resistors dissipate any remaining charge and de-energize the converter fully. In this case the trip zone mechanism is triggered by a designated digital input pin. This input is looped back to a digital output that is triggered by a comparator, which evaluates whether the measured voltage exceeds its limit.

PV dc-dc Converter

The PV dc-dc converter is a boost topology configuration built using a discrete MOSFET, as shown in Fig. 4.5. The apparatus includes the necessary gate driver and an RCD snubber (not shown). A picture of the PV dc-dc converter is shown in Fig. 4.6. The converter uses averaged current-mode control, and includes a perturb-and-observe maximum power point tracker to

maximize PV power production when possible. The pulse-width modulation (PWM) switching frequency is 40 kHz.

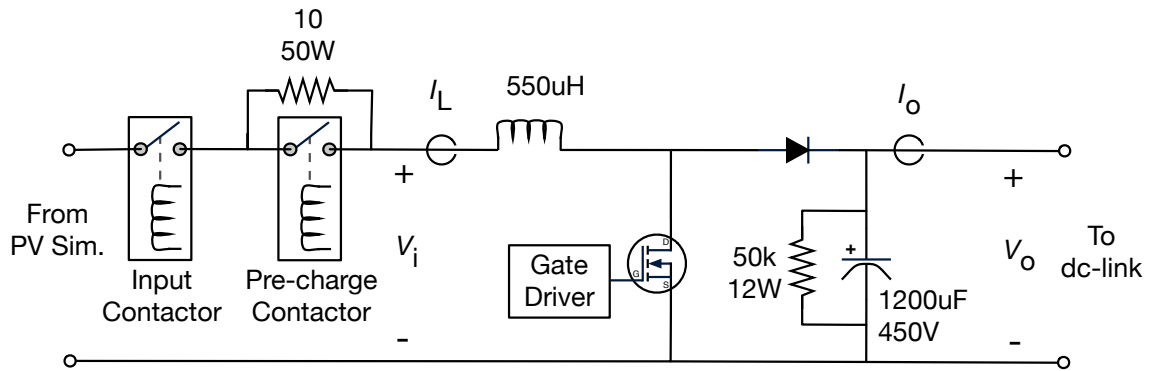


Figure 4.5: Simplified schematic of the PV dc-dc converter.

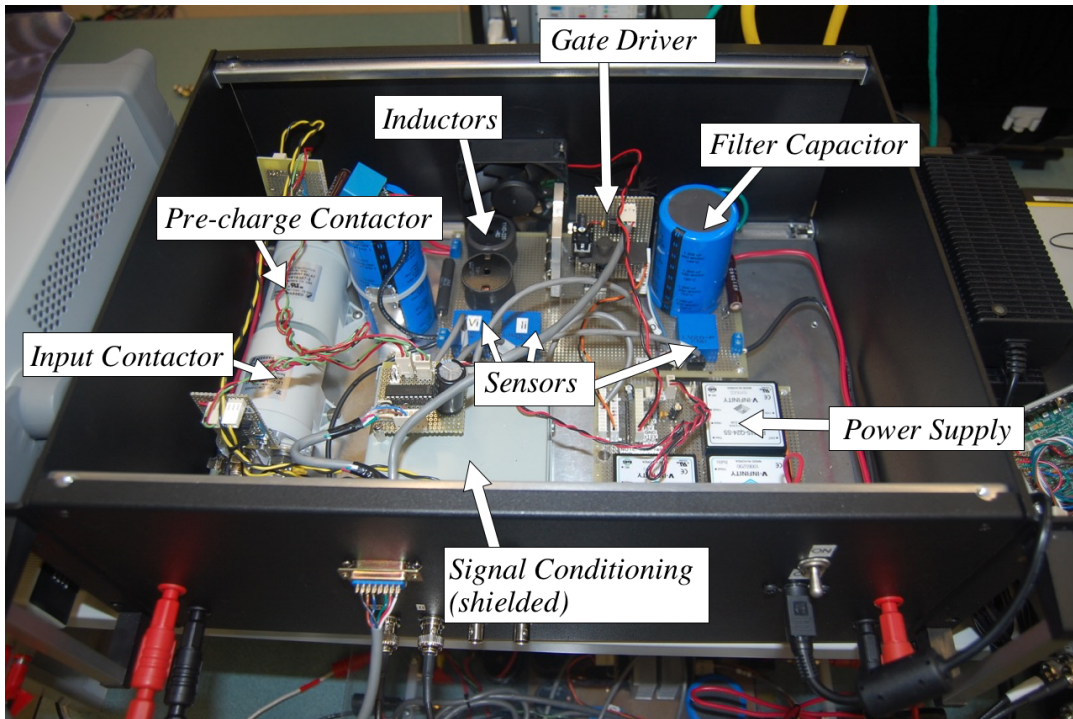


Figure 4.6: PV dc-dc converter.

Battery dc-dc Converter

The battery dc-dc converter is a synchronous-boost topology as shown in Fig. 4.7, and is built with discrete MOSFETS and isolated drivers.

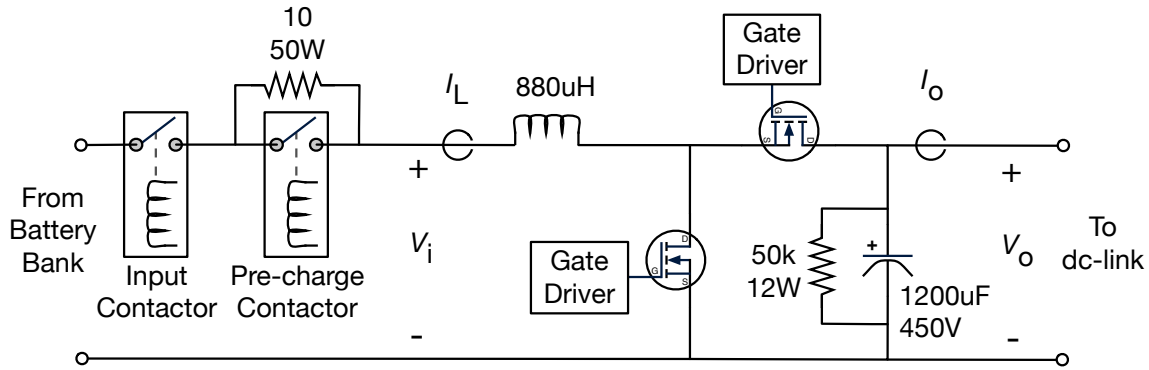


Figure 4.7: Simplified schematic of the battery dc-dc converter.

The primary function of this converter is to maintain the desired fixed dc-link voltage at the output, and to manage charging and discharging of the battery. A series-resistor pre-charge circuit is also included to limit the inrush current and allow controlled charging of the filter capacitor from the battery during system startup. The converter uses averaged current-mode control with a PWM frequency of 40 kHz to regulate its output at 400V dc, and charges or discharges the battery as needed to maintain the output voltage. The battery dc-dc converter controller also contains the SOC estimation function, which uses the Coulomb-counting technique to provide the SOC values used by the EMS. More details on the real-time control of the battery converter are presented in [29]. The constructed battery dc-dc converter is shown in Fig. 4.8, prior to being packaged in its enclosure. Note that this converter topology is particularly sensitive to the dead-time setting within the PWM subsystem, and requires careful snubber design and thermal management to operate reliably.

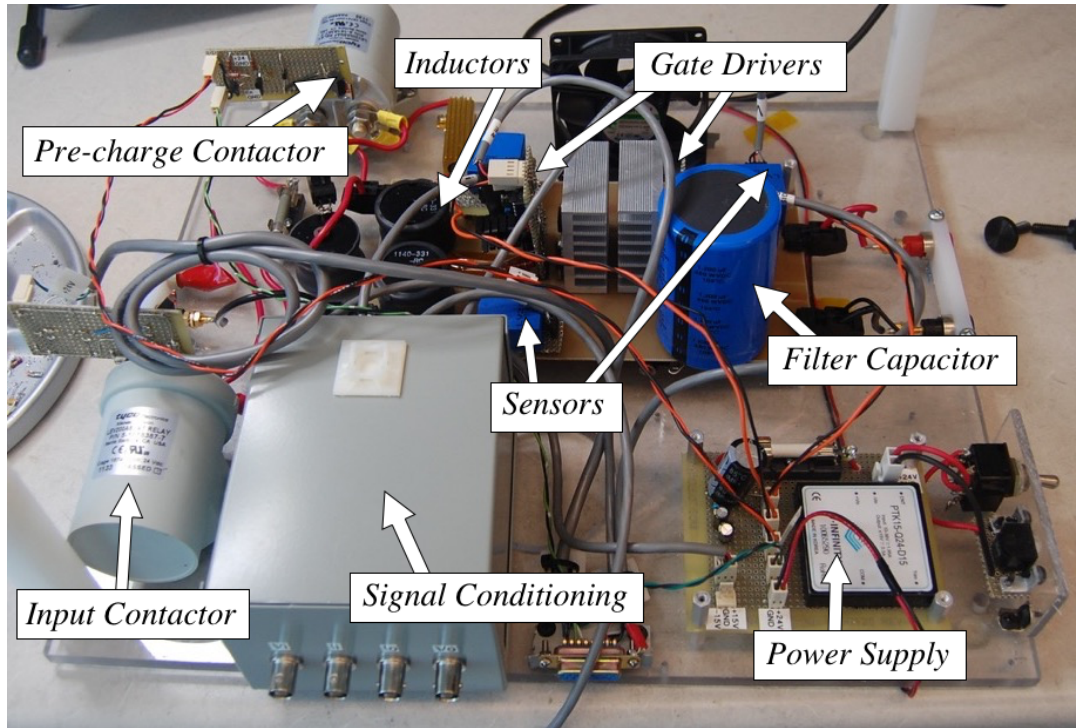


Figure 4.8: Battery dc-dc converter, prior to packaging.

Inverters for PV and Battery

The inverters are 2-level 3-phase voltage-sourced converters as shown in Fig. 4.9, rated at 3 kW each. A partially assembled inverter is shown in Fig. 4.10. The heart of the inverter is a Powerex PS22A78-E six-switch IGBT module. The switched waveform is passed through an LC filter, a software-controllable connection contactor, an interface inductor and a delta-wye isolation transformer. The inverter is connected to the microgrid through a manually operated fused disconnect. The current and voltage sensors identified in Fig. 4.9 are used for feedback control, internal power measurements for the EMS, and waveform synchronization prior to closing the interface contactor. The internal control scheme is based on dq-frame current-mode control, and the PWM switching frequency is 10 kHz. These inverters are controlled using a multi-segment adaptive droop approach based on [28], and include the necessary synchronization mechanism to allow the PV inverter to connect in to the microgrid and share power once the initial voltage and frequency are established by the battery inverter.

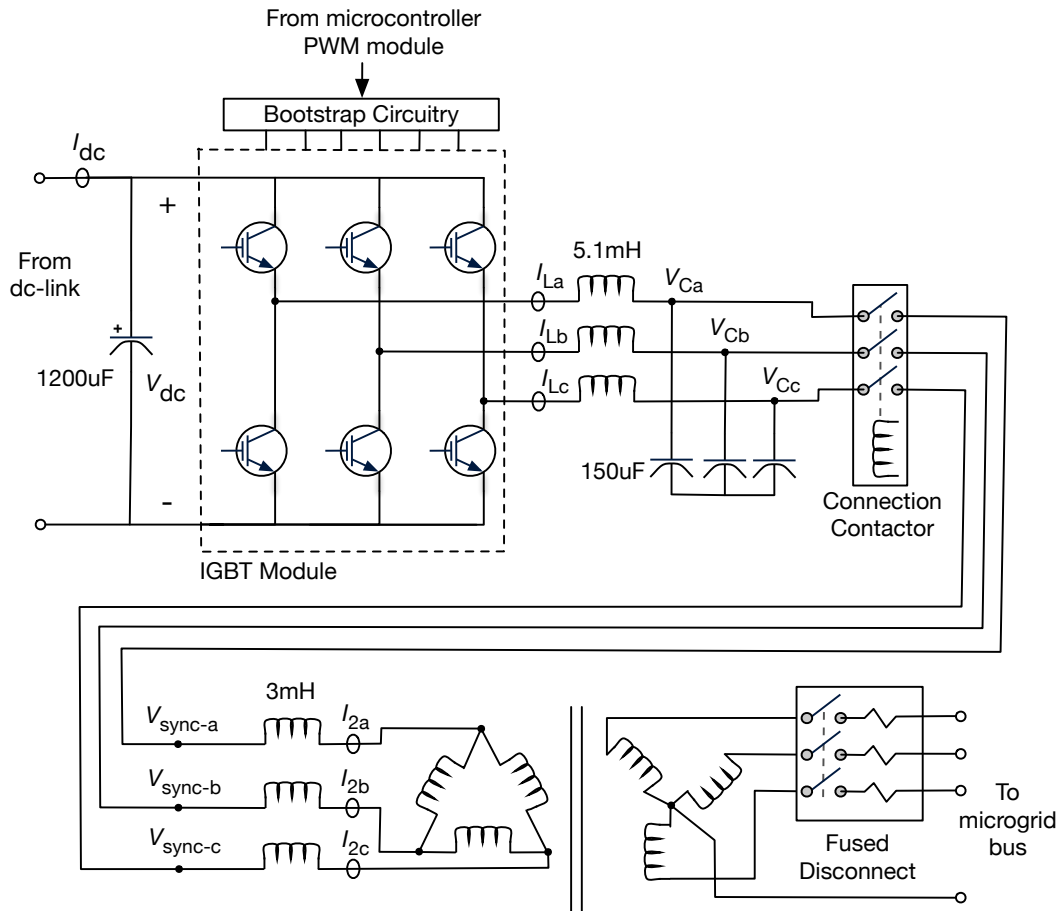


Figure 4.9: Schematic of the 3-phase inverter.

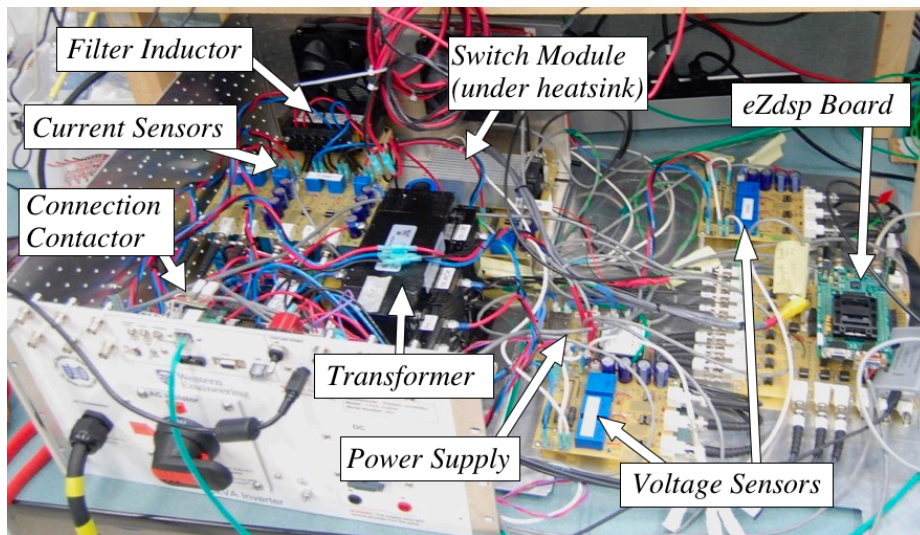


Figure 4.10: 3-phase 3 kVA Inverter, disassembled with the controller chassis on the right.

4.1.4 Supporting Apparatus

PV Array Simulator

The PV array is emulated by a 5 kW Chroma 62050H Solar Array Simulator, which is operated in the PV setpoint mode. In this mode, the active I-V characteristic curve is specified by sending sets of $(V_{mp}, I_{mp}, V_{oc}, I_{sc})$ parameters to the solar simulator over the Ethernet network. This device is used to play back previously recorded PV profiles at an accelerated rate. In this work, the PV array is operated with a nominal working voltage of 200 V and a current setpoint ranging from 0 to 7 A.

Electronic Loads

The load is emulated by a programmable NHR 3-phase balanced load operated in the constant power mode with a unity power factor. The NHR load is managed by an intermediate Windows XP computer running custom software described in Section 4.2.3.

Microgrid Bus

The inverters and load are interconnected via the 3-phase 4-wire ac bus. Each node of the bus is fused and instrumented, and includes a safety disconnect and emergency stop contactor. In addition, several nodes are equipped with power quality analyzers that can capture detailed traces of events for offline analysis.

Battery Bank

The battery bank consists of 16 series-connected East Penn 8AU1 12 V 32 Ah AGM lead-acid batteries. The nominal terminal voltage is 192 V, and ranges in practice from 189 V to 230 V, depending on the SOC and charge/discharge current level. In the experiments, the battery capacity is intentionally limited in the dc-dc converter firmware to emulate the behaviour of a smaller scaled battery in order to examine the features of the proposed system. The lead-

acid battery chemistry was chosen because it provides a robust and economical solution for laboratory work, however the developed techniques are equally applicable to other battery chemistries.

EMS Platform

The EMS software is run on a Dell Optiplex computer, under the Ubuntu Server 12.04.5 LTS operating system using the default Python 2.7 interpreter, along with the corresponding required Python support libraries. The computer has two Ethernet connections: one is connected to the Internet, for accessing the Environment Canada weather forecasts, and the other to the internal microgrid communication network that connects to the power electronic converters, loads, and instrumentation.

Communications Infrastructure

The devices in the microgrid are interconnected using a 10/100 Base-T Ethernet network and Netgear switches. The eZdsp boards are connected to the Ethernet network using Texas Instruments serial-to-Ethernet adapters, shown in Fig. 4.11. These adapters buffer bidirectional datastreams that are represented within the Simulink model as periodically sampled signals, and therefore provide a mechanism for transferring data from the controllers to the outside world. The datastreams are exposed through a raw TCP/IP socket interface that starts streaming as soon as a connection is made to the adapter. However, the presence of a buffer means that a received datapoint may not be the most current one, which can lead to the datasets from the different converters being out of synchronization. The EMS software is therefore designed to flush the buffer so that the time accuracy of the data can be established and that the EMS is always acting on the most up to date information.

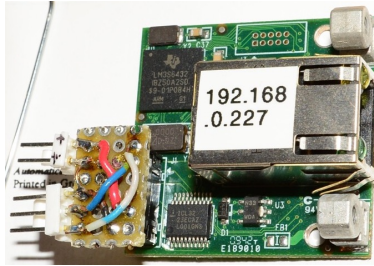


Figure 4.11: Serial-to-Ethernet adapter.

4.2 Software Architecture

The high-level operation of the microgrid is managed and supported by a set of software applications described in this section. They include the EMS software itself, a microgrid emulator used to simulate the hardware protocols, a PV and load sequencer that provides stimuli to the system, an application to interface to the NHR load, and a set of visualization tools.

4.2.1 EMS Software

Predictive energy management inherently involves communication with multiple devices over communication networks. Since each of these devices operates with its own independent clock, the communication is asynchronous. The lower layers of the network protocols ensure that the messages are successfully sent and received, but the EMS application must still be structured to deal with these incoming messages effectively. Multitasking and multithreading are both potential solutions to this challenge, however these techniques can add considerable complexity to the programming task. Implementation using low-level multithreading constructs requires careful design, and can easily fall victim to synchronization issues. Another alternative is to make use of an event-driven framework, which can be thought of as an abstraction of the classical interrupt-driven mechanism used within micro-controller hardware.

Event-driven frameworks are often used in situations that must accommodate many asynchronous inputs, the classic example of which is the Microsoft Windows graphical user interface. This characteristic makes the approach a good foundation for a microgrid EMS, which

has to handle inputs from multiple devices and make time-sensitive decisions. Such frameworks are structured around a single-threaded event loop, which essentially waits for events to occur and dispatches handlers as needed to process the events. Actions that require long execution times are handled using callback mechanisms, which stops them from blocking the main event loop. When these actions are completed the callback is triggered, which is acted on like another event.

The event driven framework selected for this application is the open-source Twisted networking engine [88]. The main conceptual focus of this framework is on defining protocols that are used for the different device communication tasks, which in this case involves communication with the power electronic converters and loads. Periodic tasks such as forecast processing and prediction can be defined as timer driven events that are managed by the event loop.

The energy management system software is implemented in the Python language, and uses the SciPy [89] library for mathematical functions and the *PyTables* library [90] to store the collected data and interim results. The EMS software architecture is shown in Fig. 4.12, and is described in detail below. An online graphical user interface has been implemented to provide visualization of the running simulation or experiment, and a TCP command channel is provided to allow for online interaction with the EMS.

Device Protocol Handlers

Incoming information from the power electronic converters is gathered by asynchronous event handlers for each device, as shown in Fig. 4.12. The execution of these handlers is managed by the event processor, which triggers each custom protocol handler when data arrives at the corresponding network socket. The framework provides supporting network services, such as buffering, connection timeouts/restoration, and message parsing. A rolling 1-day history of each datapoint is retained internally, and the full dataset is stored in a file for later analysis.

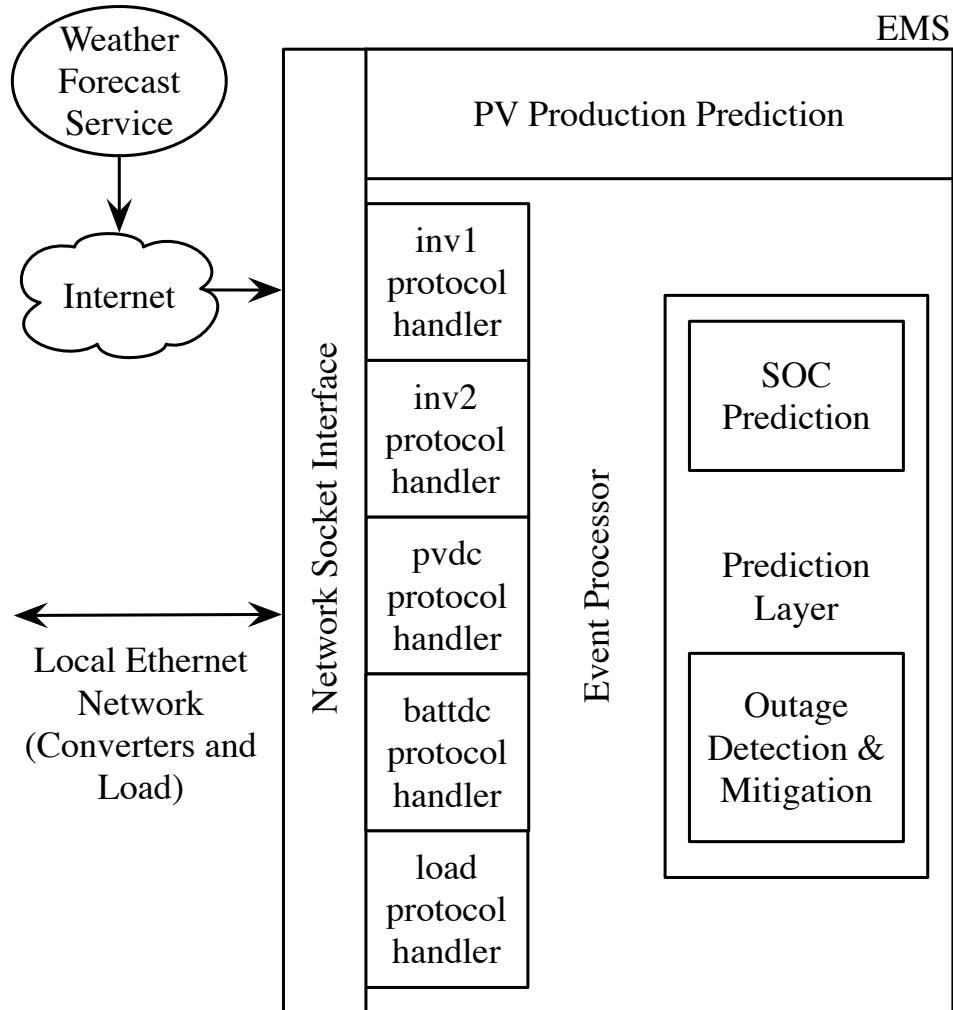


Figure 4.12: Architecture of the EMS.

Outage Detection and Pre-emptive Load Shedding

The predictive strategy described in Section 3.1 is executed by a periodic timed event. The resulting SOC predictions are used to plan the load shedding actions, which are then executed by sending messages to the Load Sequencer software to shed a portion of the load. Interim results from the algorithm are also stored for later analysis.

4.2.2 Model Parameter Uncertainties Compensation Features

The parameter compensation technique described in Section 3.2 is implemented as a part of the prediction mechanism within the EMS. On a once-daily basis, the previously stored values and forecast predictions are used to calculate the corresponding compensation factors, and, when the technique is enabled, these factors are used to adjust the future predictions. One challenge encountered with the developed EMS architecture is that extended runs of the simulation were time consuming due to the protocol overhead, which limited the execution speed of the simulation. To solve this issue, an accelerated version of the EMS simulator was developed. This required replacing the network protocol layers with direct function calls, allowing the simulation to operate at the full single-threaded speed of the host processor.

4.2.3 Supporting Software Applications

Microgrid Emulator

To facilitate testing and debugging without requiring the full operation of the microgrid, a software application was created by the author to emulate the microgrid at a network level. The program emulates the network interfaces of the PV simulator, the NHR AC Load, and the four power electronic converters. Internally the program executes a simplified model of the microgrid that takes the PV and load profiles as inputs, and then calculates the corresponding battery power, SOC, and resultant output data streams from the converters. The microgrid emulator accounts for microgrid losses, PV curtailment, and shutdown behaviour. It does not, however, attempt to calculate any internal measurements beyond those required for the EMS, so values such as the dc-link voltages and internal currents, which can be found in the real converter data streams, are set to fixed placeholder values in the emulator data streams.

PV and Load Sequencer

The key external stimuli for the systems under investigation are the PV power and the load demand profiles. In both the real and simulated systems, these values are stored in a flat file, and are presented in sequence, at one second intervals, to the PV simulator and the NHR Load Controller software (or their simulated versions) by the sequencer application.

NHR Load Controller

The manufacturer-supplied application for the NHR loads does not provide the networking features required to execute the proposed experimental scenarios. Therefore, a custom application was written in Visual Basic running under Windows XP that used the NHR driver DLL to perform the low-level RS-232 communication with the load, and provided manual, sequenced, and network automated control of the device. The key feature required for the experiments was the ability to receive load setpoint values over the Ethernet network, and therefore emulated any desired load profile. The user interface for this application is shown in Fig. 4.13.

Visualization Tools

Three different types of tools were developed to support visualization of the data from the EMS. The first set of programs generated the EMS results plots in this thesis from the HDF5 datafiles using either the Python Matplotlib library, or within MATLAB. The second, a wx-Python application, produced a live updated animation of the EMS strategy in action, and was used in both experimental and simulation scenarios to gain insight into the system operation in real-time. Finally, a visualization utility was created using the Bokeh library to generate publication-quality plots of the intermediate daily prediction results in real-time.

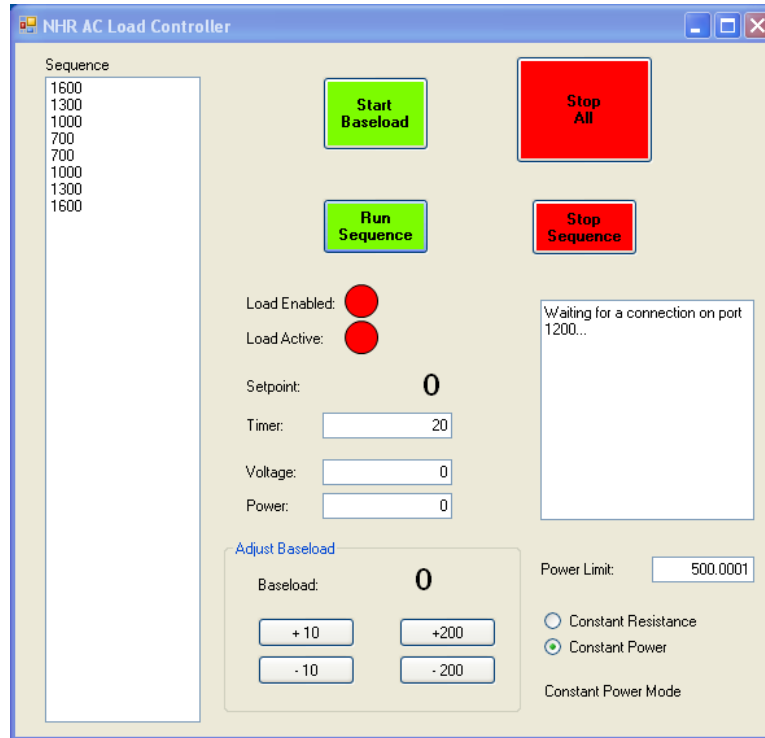


Figure 4.13: Developed NHR load controller software user interface.

4.3 Summary

The key elements of the hardware and software implementations of the system under investigation have been presented. The custom-built PV and battery dc-dc converters and their corresponding 3-phase inverters are connected to the ac-bus to form the experimental microgrid, and the PV simulator and programmable load are used to execute the operational scenarios. A software emulator for these devices has also been developed to facilitate offline testing. The energy management system itself is programmed in Python using the Twisted framework, and is executed on a Linux platform. An accelerated simulation version of the software has also been developed to facilitate the long-running operational scenarios needed to evaluate the parameter compensation techniques.

Chapter 5

Validation and Discussion

First, the scenarios used to validate the proposed techniques are presented. Then the results showing the operation of the developed predictive EMS are presented, followed by the results that demonstrate the effectiveness of the model parameter uncertainties compensation techniques.

5.1 Validation Scenarios

5.1.1 Predictive Energy Management

The purpose of the simulations and experiments is to demonstrate the operation of the developed predictive energy management strategy, and to show how this strategy can result in the elimination or the reduction in duration of outages affecting the critical loads in the microgrid. Furthermore, the use of the bounding technique to accommodate uncertainty in the SOC estimate is also explored.

Irradiance and Load Profiles

In order to accurately represent the behaviour of the PV array, a set of data from rooftop irradiance and temperature sensors was recorded. This dataset was then filtered, subsampled,

and rate-limited to create a photovoltaic generation profile that can be used to represent the PV resource in the simulated microgrid. A subset of four days is selected to demonstrate the behaviour of the energy management strategy under both sunny and cloudy conditions. An arbitrary real power load profile based on a typical aggregated residential dataset is also chosen. The selected generation and load profiles are shown in Fig. 5.1, with a mostly-sunny first day followed by two variable-cloudy days, and ending with the morning of a sunny day. The load profile shows characteristic morning and evening peaks, and does not include any phase imbalance or reactive loads (i.e. $X \ll R$). The sheddable portion of the load in this scenario is chosen to be 75 W. This value is meant to represent, for example, a portion of a lighting load, and its magnitude is approximately 18 % of the peak load in the chosen profile. An outage occurs if the battery SOC drops below 30%.

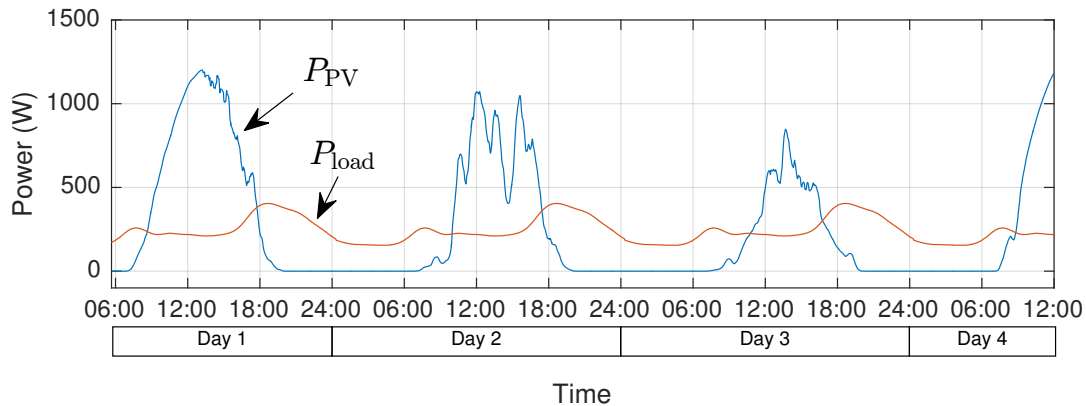


Figure 5.1: Chosen four day PV generation and load profiles.

The corresponding set of Environment Canada HRDPS weather forecasts for the same period has also been collected and is made available in a file to the EMS.

Simulation and Experimental Scenarios

The EMS strategy described in Chapter 3 is validated using the microgrid emulator software, and then tested on the laboratory-scale experimental microgrid. In each case, a test scenario is run first with the outage mitigation mechanism disabled. Then, the scenario is repeated with the predictive EMS strategy enabled, but without using the bounding mechanism. Finally, the

scenario is re-run with the bounded EMS feature fully enabled. The key metrics in each case are the number and duration of outages.

5.1.2 Model Parameter Uncertainties Compensation

The simulations conducted in this section will demonstrate the effect that uncertainties in the PV system rating and battery capacity parameters can have on the operation of the predictive EMS. The developed parameter compensation technique will then be applied to evaluate its effectiveness in dealing with these uncertainties, and restoring the correct operation of the microgrid.

Simulation Scenarios

An extended PV dataset collected from the rooftop irradiance sensor is used to supply the simulation with PV production data so that the effects of the technique can be clearly demonstrated. Note that while the need for the technique was inspired by observations taken during the experimental work, the technique itself is only explored in simulation. The extended 42-day PV profile is shown in Fig. 5.2, and exhibits a variety of irradiance conditions. The daily load profile is the same as the one used in the energy management scenarios. The corresponding 42-day set of Environment Canada weather forecasts has also been collected and is made available to the EMS. Note that the four-day profile used for the EMS validation is a subset of this 42-day dataset.

The two model parameters under investigation are deliberately incorrectly specified in the prediction model. The PV system rating is overrated by a 14%, and the battery capacity is overrated by 12%.

PV System Rating

The RMSE between the predicted PV power production and the actual production is compared, both on a daily basis over the 42 day period, and for an illustrative day. This is done in order

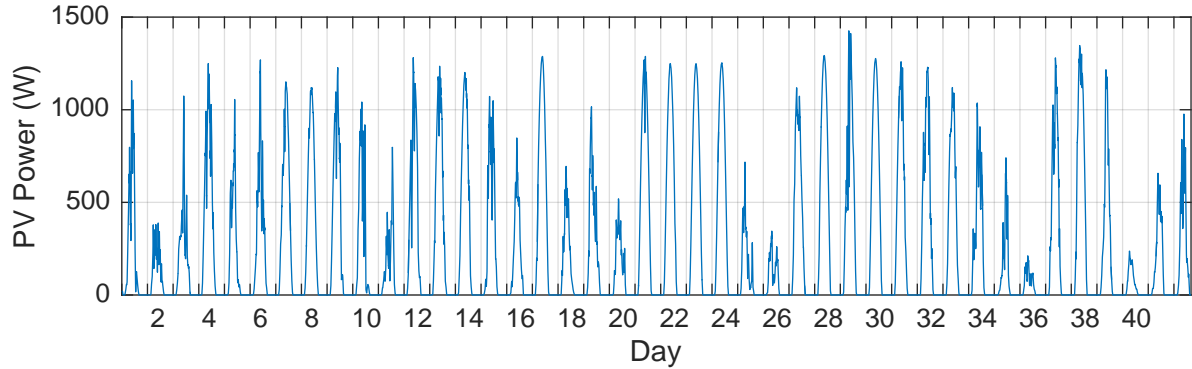


Figure 5.2: Chosen 42 day PV generation profile.

to demonstrate the effectiveness of the PV system rating parameter compensation technique in improving the accuracy of the prediction.

Battery Capacity

The RMSE between the predicted SOC and the actual SOC is compared, both on a daily basis over the 42 day period, and for an illustrative day, in order to demonstrate the effectiveness of the battery capacity parameter compensation technique.

Determining the Effect on Microgrid Outages

Three scenarios will be simulated to demonstrate the effectiveness of the model parameter uncertainties compensation technique when it is applied within the EMS. The predictive EMS described in Section 3.1.4 (not the bounded EMS) is used in the evaluation. The key performance indicators of interest are the number and duration of any outages. In the first scenario, the correct parameters are used in the prediction algorithm to provide a baseline set of results. In the second scenario, the incorrect parameters are used to illustrate the effect of the parameter uncertainties. In the third scenario, with the incorrect parameter settings, the parameter compensation technique is enabled.

5.2 Predictive Energy Management

To demonstrate the operation of the predictive EMS, the microgrid is operated using the previously discussed 42-day profile for the three scenarios: predictive EMS disabled, predictive EMS enabled, and bounded EMS feature enabled. The results for the simulated scenarios are presented first, followed by the results for the experimental microgrid.

5.2.1 Analysis of Simulation Results

Predictive EMS Disabled

The result of a run of the simulated microgrid with the selected profiles is shown in Fig. 5.3, with the EMS operating to collect the data only, but with the predictive mechanisms disabled.

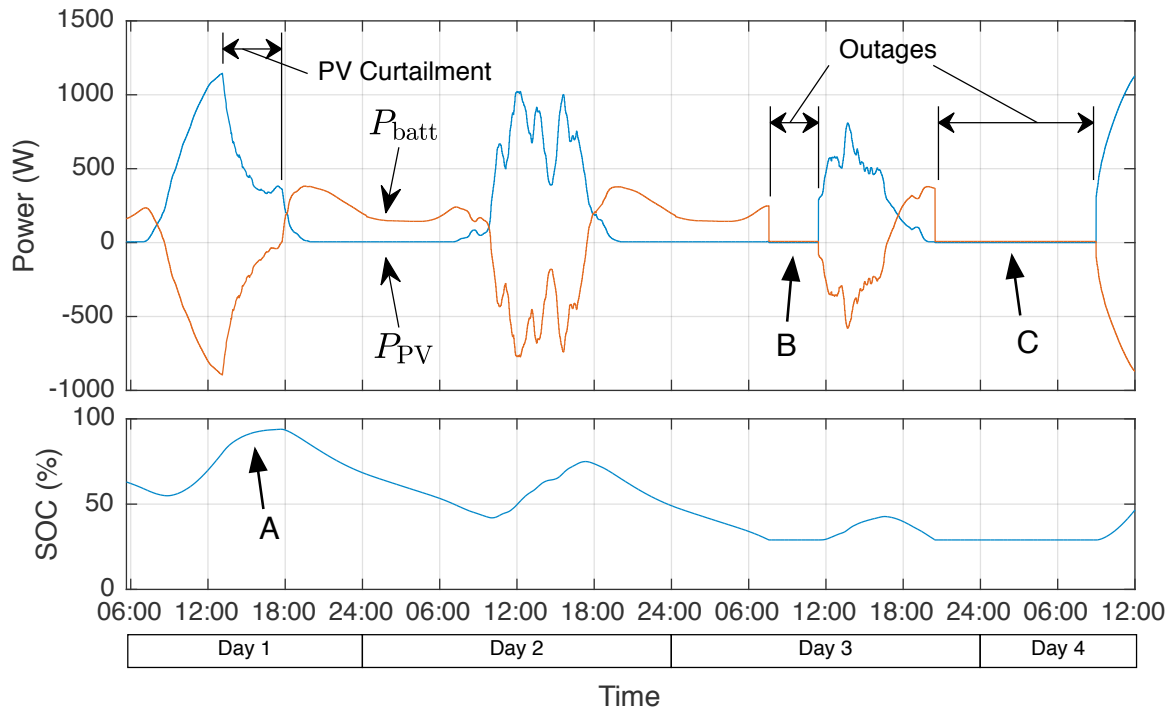


Figure 5.3: Simulated results with the predictive EMS disabled.

In this case, the available PV power is adequate to fully charge the battery on the first day.

After the battery is fully charged, the PV power is curtailed to maintain the generation/load balance (see A in Fig. 5.3). On the following day, there is not enough PV power available to charge the battery adequately, so there is a brief outage (marked B in Fig. 5.3) in the early morning of Day 3 where the microgrid is shut down and the load is disconnected. The microgrid restarts and the load is re-connected once the PV production is large enough to support the load, but there is very little excess energy available to charge the battery. This low level of PV power production leads to a long outage (marked C) during the following night.

Predictive EMS Enabled

When the same scenario is run with the predictive EMS enabled, the EMS strategy is able to detect potential upcoming outages and characterize their energy deficits. It then schedules a pre-emptive load shedding actions as shown in Fig. 5.4, where the distinct 75 W steps in the P_{batt} plot indicate where the load shedding begins. This result demonstrates that the first outage has been averted, and that the duration of the second outage (marked A) has been shortened. In this test scenario, the developed algorithm leads to three shedding events with a total duration of approximately 43 hours, which results in a reduction of the total outage length by a factor of 87%.

An intermediate prediction taken on Day 2 at 15:30 illustrates the shedding scheduling process in Fig. 5.4. The predicted powers \hat{P}_{load} and \hat{P}_{PV} are used to calculate the predicted SOC (marked B on Fig. 5.4), which indicates an upcoming outage. The planned shedding schedule shows the action planned (see C on Fig. 5.4), but not yet initiated, to avoid the outage. Note that as new information becomes available, the predictions are updated, both with new SOC estimates and with new PV production forecasts, which will result in a change to the predicted SOC (marked B) as the prediction start time advances to the right. This will then lead to adjustments in the planned shedding schedule that incorporates this new information.

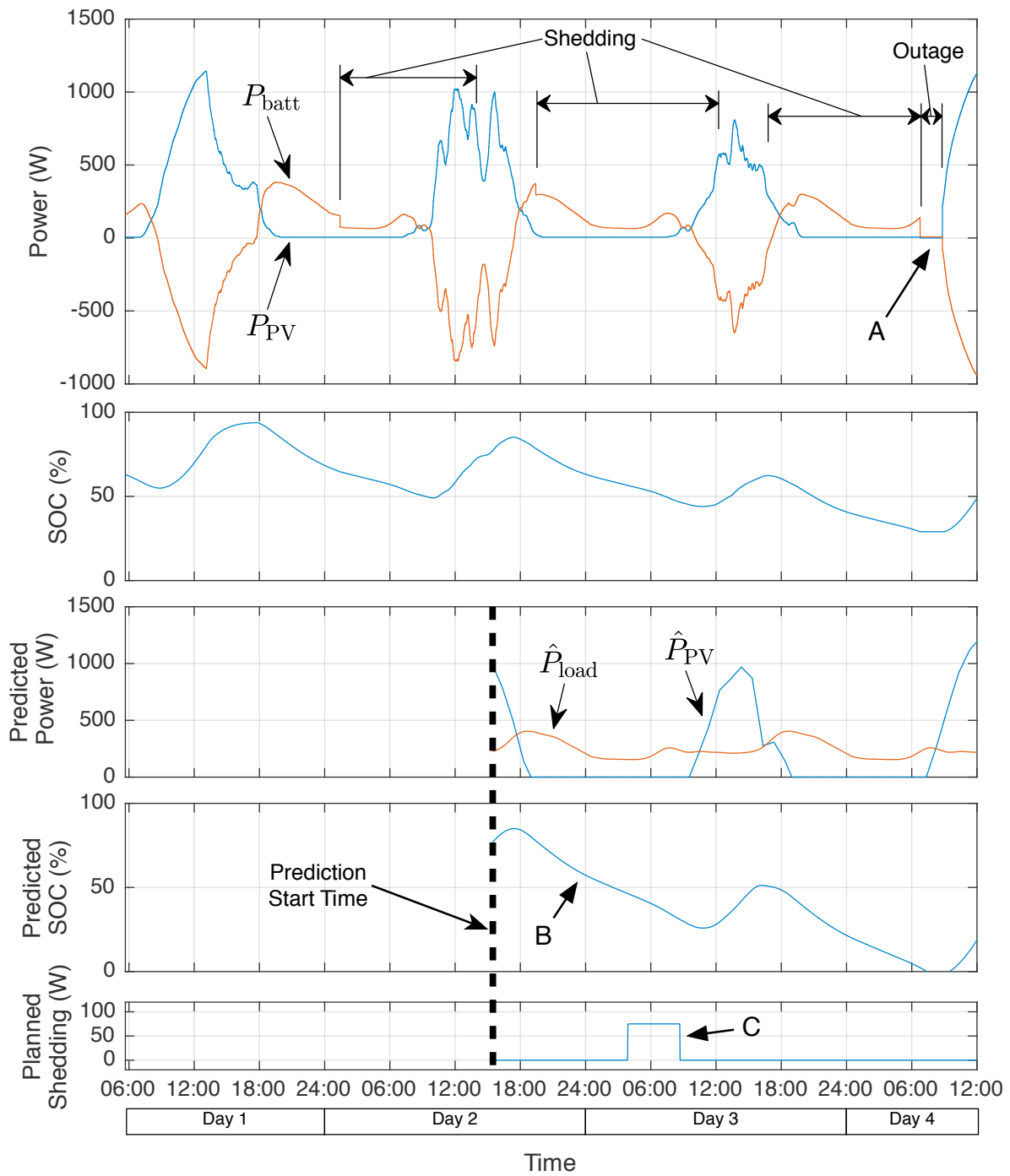


Figure 5.4: Simulated results with the predictive EMS enabled, including an intermediate prediction taken on Day 2 at 15:30.

Bounded EMS Feature Enabled

When the bounded EMS functionality is enabled, the EMS detects the upcoming outages based on the lower SOC bound, and ultimately schedules two load shedding events with a total duration of approximately 50.5 hours as shown in Fig. 5.5. The results demonstrate that in this case both outages have been averted. One feature to note is that at approximately 01:00 on Day 3, the system briefly stops shedding (marked A in Fig. 5.5). At this point in time the previously detected outage has been averted, shedding has stopped, and no upcoming outage is predicted. However, a new PV forecast arrives a few minutes later, and this new forecast reflects a reduction in the expected PV production from the previous prediction. The prediction based on this new information indicate a large upcoming outage, which leads to the scheduling of a shedding event that starts immediately.

An example intermediate prediction on Day 2 at 15:00 is shown in Fig. 5.5, and illustrates a shedding event (marked B) that is scheduled. The bounds are clearly visible in this example, and the lower bound leads to an earlier detection of the upcoming outage and a more conservative measure of the energy deficit. At the time of the prediction, shedding has already started, so only the shedding endpoint is being adjusted.

5.2.2 Analysis of Experimental Results

Predictive EMS Disabled

A baseline experiment is run first, and the results are shown in Fig. 5.6, where the prediction and shedding features are disabled. This result shows the PV curtailment mechanism activating when the SOC nears its upper limit (see A in Fig. 5.6), thus reducing the incoming PV power so that the battery bank does not get overcharged. The result also shows the two outages that occurred when the low-irradiance days did not provide enough power to re-charge the battery bank, and the timing and durations of these outages show good agreement with the simulation results. Note that due to limitations in the design of the experimental apparatus, specifically

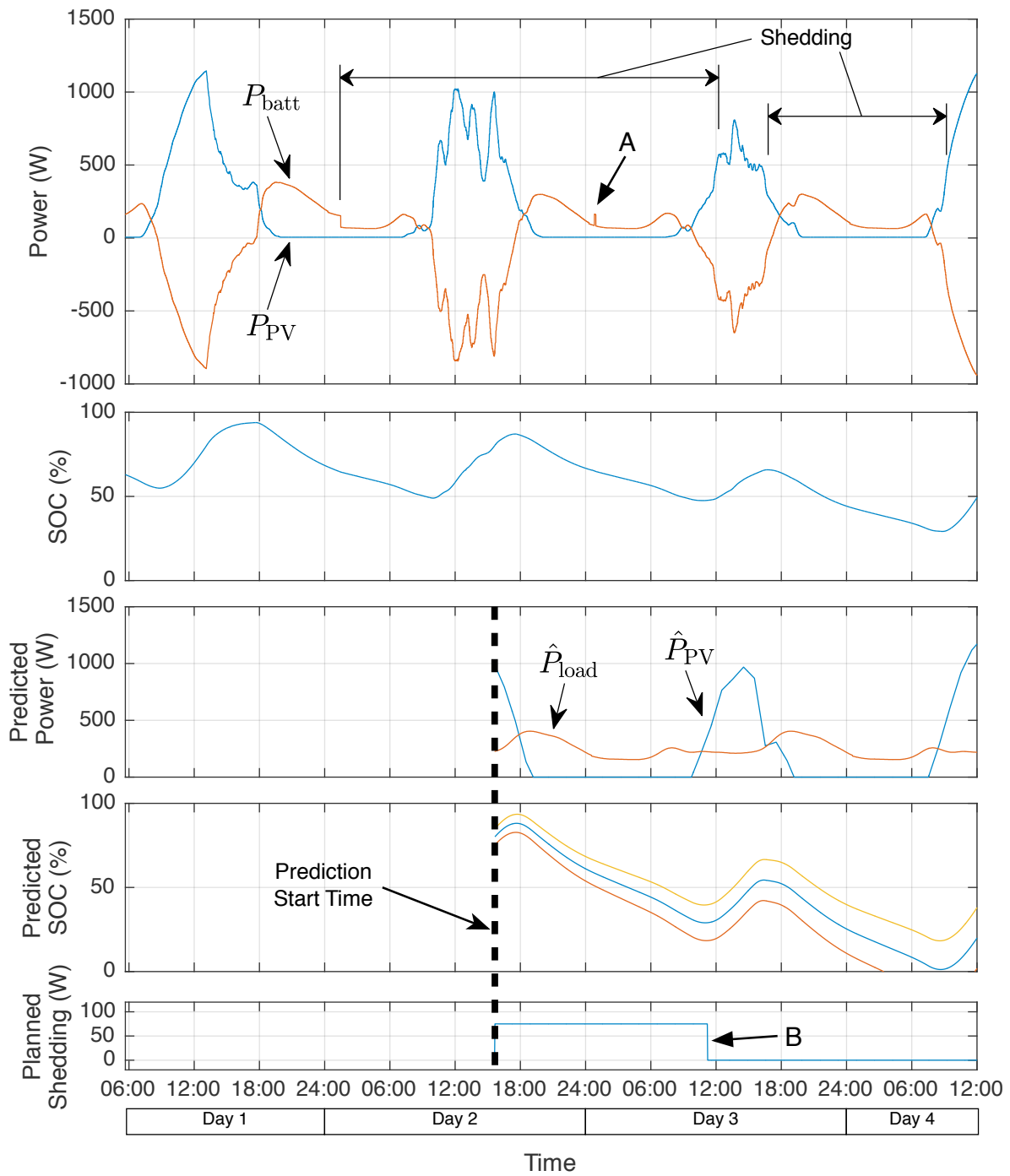


Figure 5.5: Simulated results with the bounded EMS feature enabled.

the lack of an auto-start mechanism, the inverters remain connected and operating during the outage, where the load is set to zero. Therefore, the experimental results show some charging action during PV startup (marked B in Fig. 5.6), and show some decline in the SOC during the outage, which is caused by the need for the battery to continue supplying the system losses during the outage. This behaviour would not be present in a fully shut-down system.

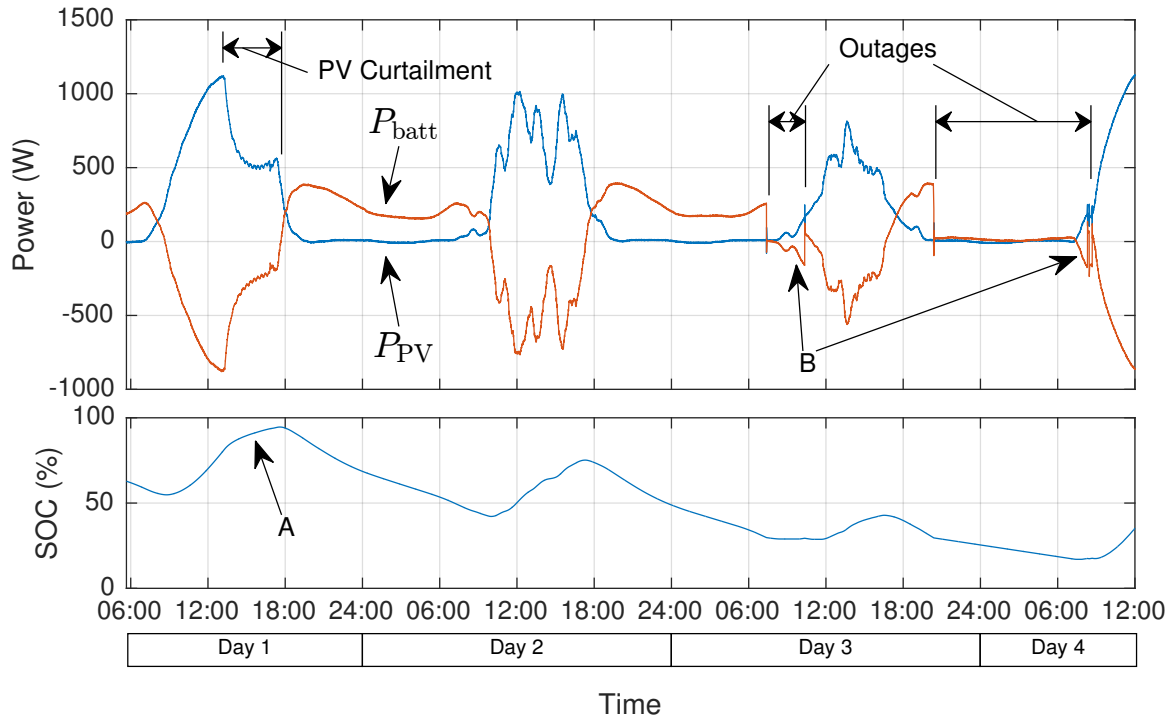


Figure 5.6: Experimental results with the predictive EMS disabled.

Predictive EMS Enabled

The experimental results from the laboratory microgrid with the predictive EMS enabled are shown in Fig. 5.7. The first outage is eliminated completely, and the duration of the second outage is reduced significantly, demonstrating good agreement with the simulation results. Note the thicker traces for the power plots, which reflect small amounts of measurement noise present in the real data that is not seen in the simulation.

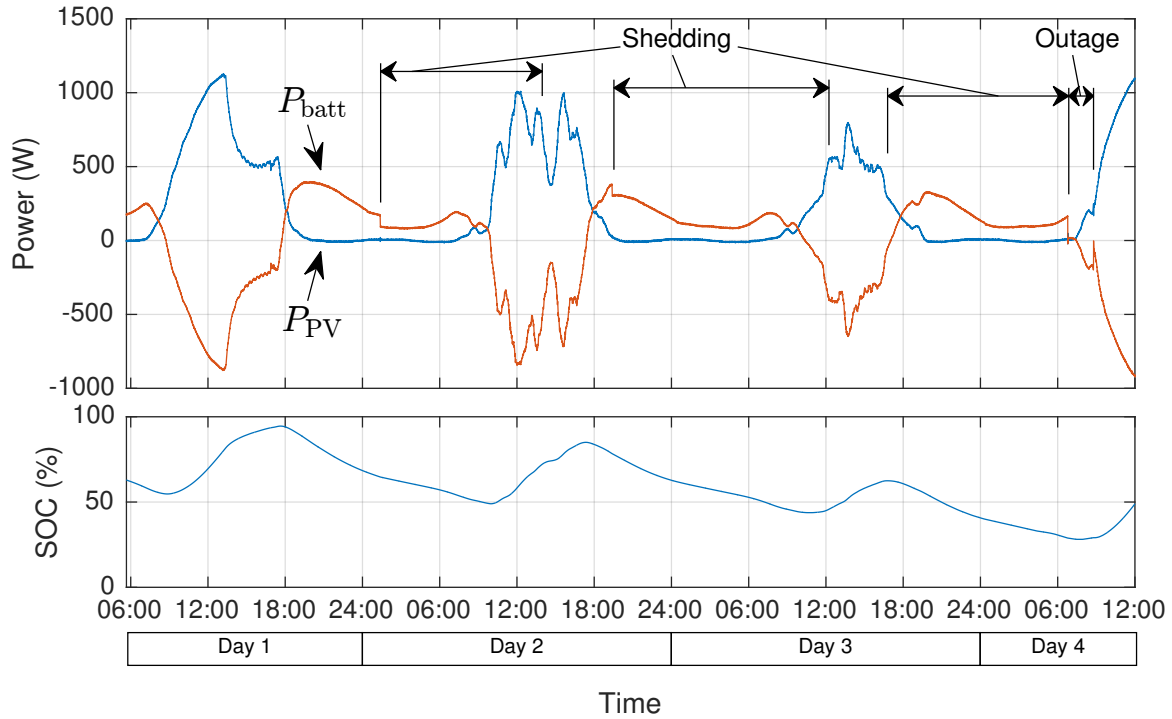


Figure 5.7: Experimental results with the predictive EMS enabled.

Bounded EMS Feature Enabled

The experimental results with the bounded EMS prediction and shedding features fully enabled are shown in Fig. 5.8.

As previously shown in the simulation, the bounded approach results in an additional shedding duration of approximately 7.5 hours, leading to the elimination of both outages. Note that, while not illustrated in this result scenario, once the battery becomes fully charged again the bound will reset to zero, reflecting the known SOC once that condition is reached.

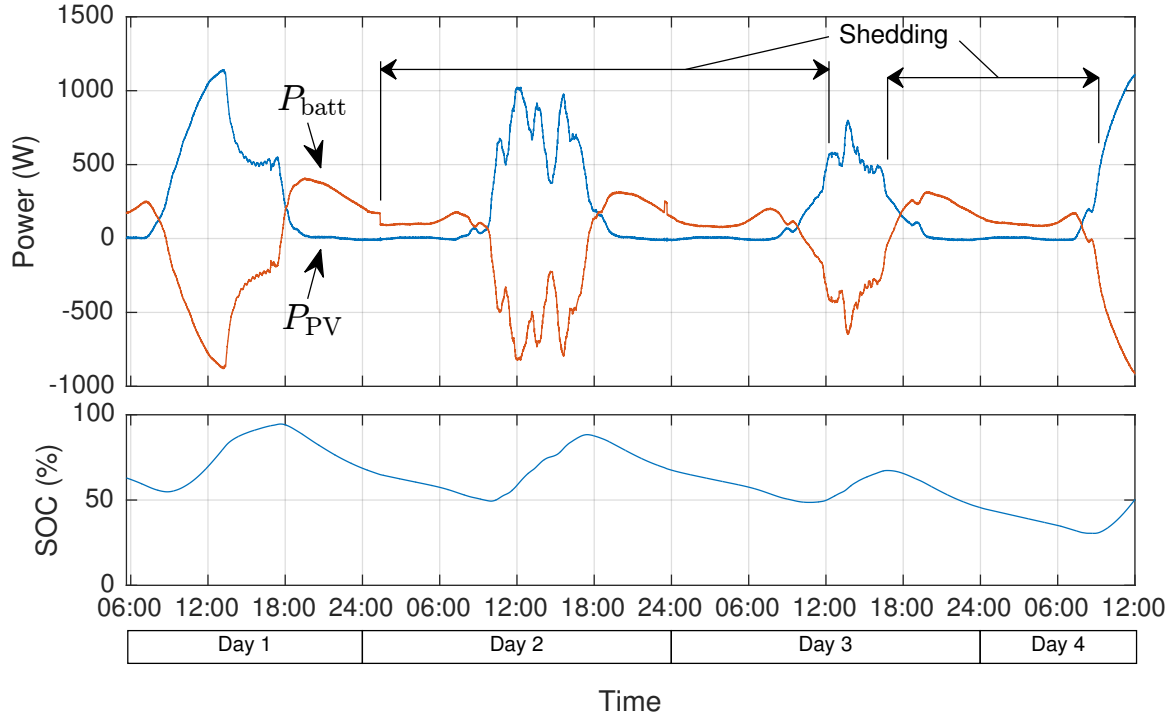


Figure 5.8: Experimental results with the bounded EMS feature enabled.

5.3 Model Parameter Uncertainties Compensation

The performance of the PV system rating and battery capacity parameter compensation techniques are presented first, followed by a demonstration of the effectiveness of such compensations on the overall outage performance of the microgrid using a predictive EMS.

5.3.1 Improvement in the Accuracy of PV Production Predictions

The effect of the uncertainty compensation of the prediction of the PV production is illustrated in Fig. 5.9 over a period of one day. The original, uncompensated forecast PV prediction is denoted $\hat{P}_{PV,0}$. It can be seen that the compensated prediction matches the actual PV production much more accurately than the original uncompensated prediction, with a reduction in the root-mean-squared prediction error of 58% for this particular day. This represents a significant improvement in the accuracy of the PV prediction, which will ultimately improve the effectiveness of the EMS.

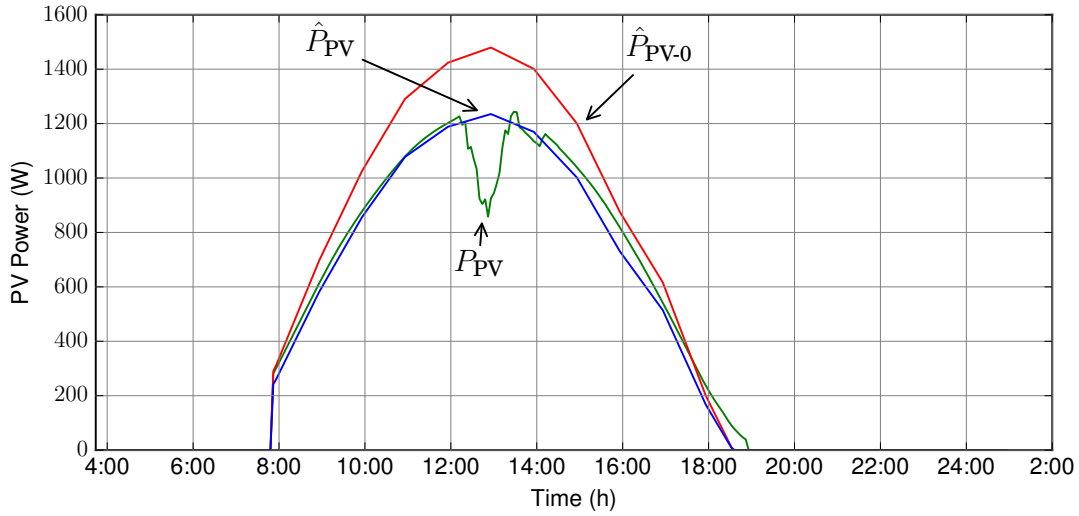


Figure 5.9: The original forecast PV prediction, the compensated forecast PV prediction, and the measured PV power for Day 21.

To evaluate the effectiveness of the approach over time, the difference between the actual and predicted PV production based on the weather forecast is determined on a daily basis. The root-mean-squared error (RMSE) measured in W between these datasets is then calculated for each day in the dataset. The resulting RMSE values are shown in Fig. 5.10.

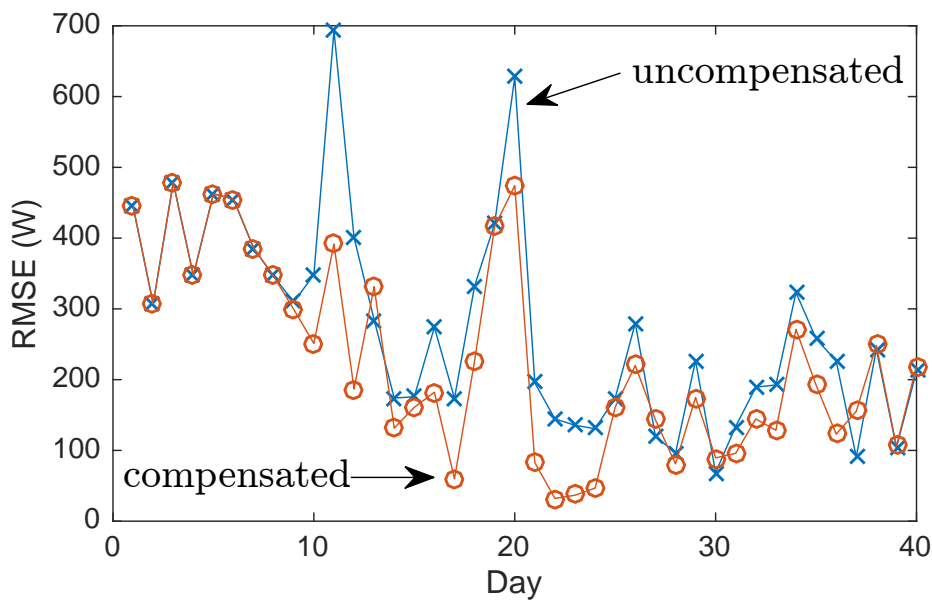


Figure 5.10: Daily PV actual vs. forecast RMSE, with and without uncertainty compensation.

Note that for the initial nine days no compensation was carried out, since those days were mostly cloudy. None of them can be used to set the reference for determining the compensation factors. On the tenth day, a near full-sun irradiance day has been detected and subsequently used as a reference for the PV compensation factor calculation. On the eleventh day this resulted in a noticeable improvement in the RMSE between the actual and predicted values, improving the error by 300 W. By using this compensation factor, the accuracy of the PV production prediction has been improved significantly. In fact, an improvement in terms of the RMSE statistic is obtained for 80% of the remaining days. Over the 42 days the average daily improvement in RMSE shown by this technique is 17%, which represents a considerable improvement in the PV power production prediction accuracy.

5.3.2 Improvement in the Accuracy of SOC Predictions

To evaluate the effectiveness of the battery capacity parameter uncertainty compensation technique, the predicted SOC with and without compensation over a period of one day are shown in Fig. 5.11. The uncompensated prediction is labeled as \widehat{SOC}_0 . It can be seen that the compensation has almost completely eliminated the error in the prediction.

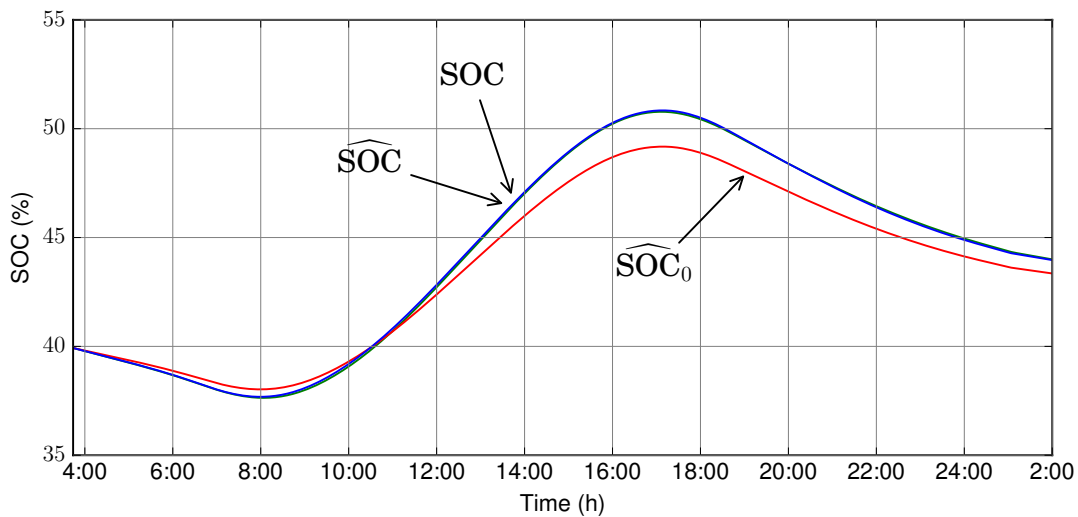


Figure 5.11: The predicted SOC with and without compensation for a period of one day.

The daily RMSE values for the SOC predictions with and without compensation are also presented in Fig. 5.12. It can be seen that the compensation can indeed improve the performance of the SOC predictions, which will result in an improvement in the outage performance of the microgrid, as will be shown in the next section.

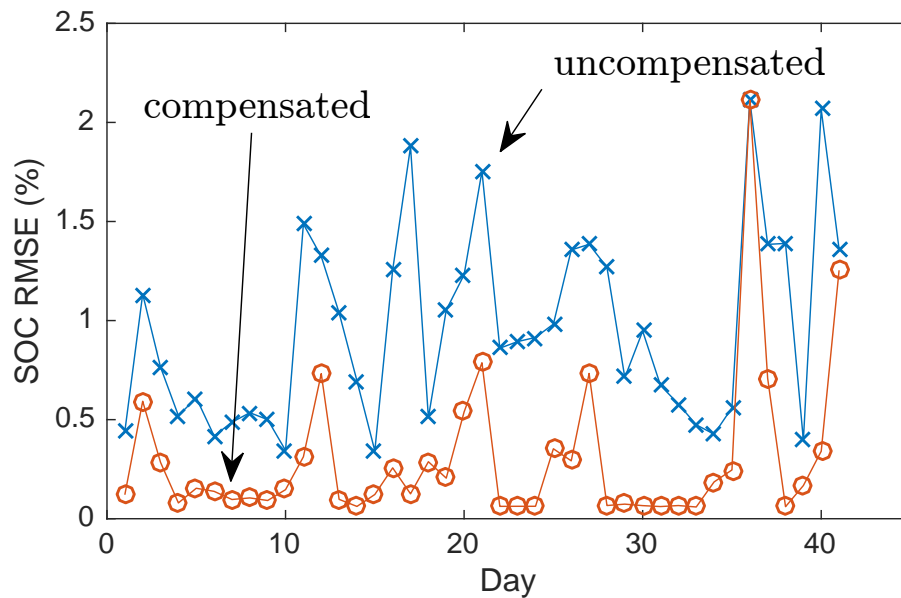


Figure 5.12: The RMSE between the actual and predicted SOC with and without compensation.

5.3.3 Effect of Model Parameter Uncertainties Compensation on Outage Durations

The ultimate objective of the developed compensation technique is to obtain more accurate predictions of PV production and the SOC so that the predictive EMS can make more informed decisions to minimize both the number and the duration of any outages. To demonstrate the effectiveness of the compensation scheme, three case studies have been performed for the same duration of 42 days, but with various levels of parameter uncertainties and degrees of compensation.

The results, when the correct prediction model parameters are used, are shown in Fig. 5.13.

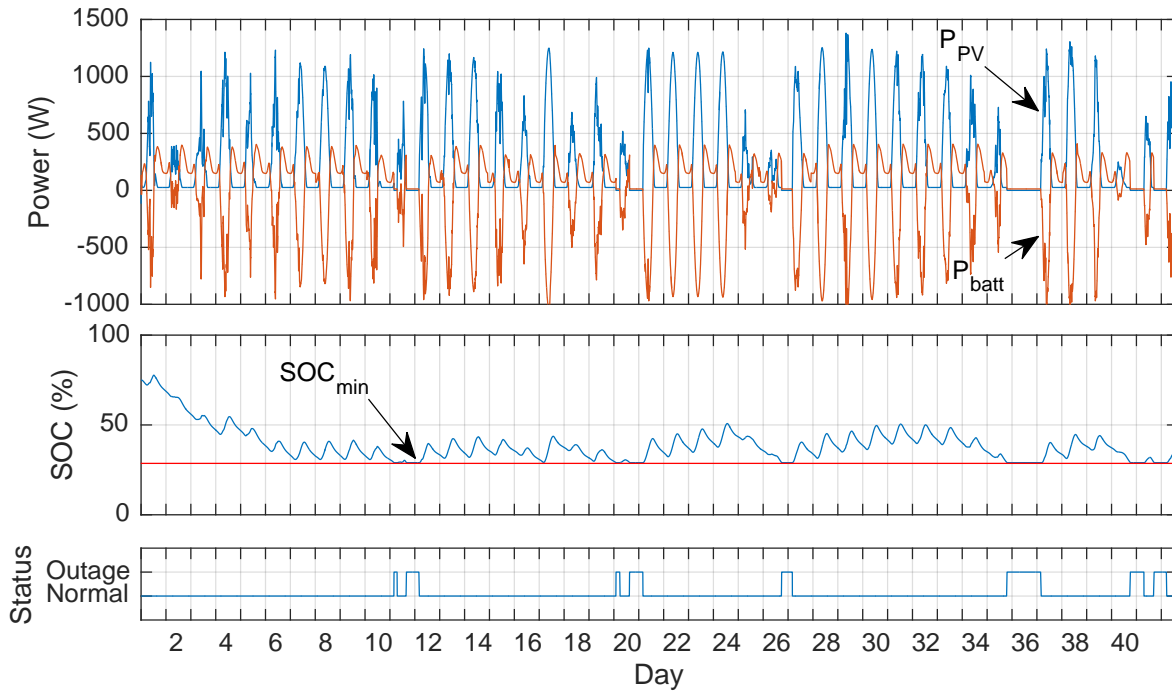


Figure 5.13: The behavior of the microgrid with the exact model parameters. (Scenario 1)

There are 8 outages totalling 101 hours. This represents the best possible outcome for this algorithm under these conditions. As a comparison, in the same system operating environment, if no predictive EMS is used, there would have been 21 outages totaling 208 hours.

In the second scenario, it is assumed that there are some uncertainties in the model parameters. The PV system rating is overrated by a factor of 14%, and the battery capacity is overrated by a factor of 12%. The corresponding results are shown in Fig. 5.14. There are 11 outages registered with a total duration of 117 hours.

Under the same level of initial parameter uncertainties as in the above case, the third scenario employs the uncertainty compensation scheme developed in Section 3.2. The results are shown in Fig. 5.15. As can be seen, the microgrid has experienced 8 outages in total, of collectively 103 hours in duration. This is a 12% reduction in the overall outage duration. The results have demonstrated that the developed technique can almost completely recover the performance to near the same level as when the correct parameters are used in the model.

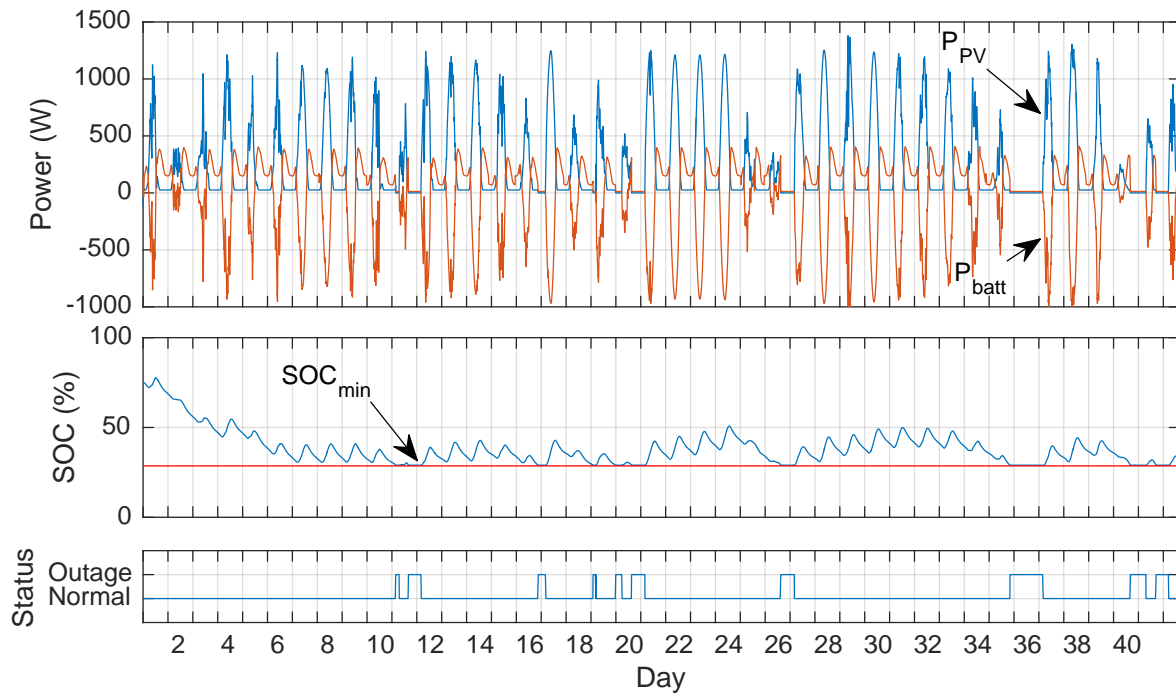


Figure 5.14: The behavior of the microgrid with incorrect model parameters. (Scenario 2)

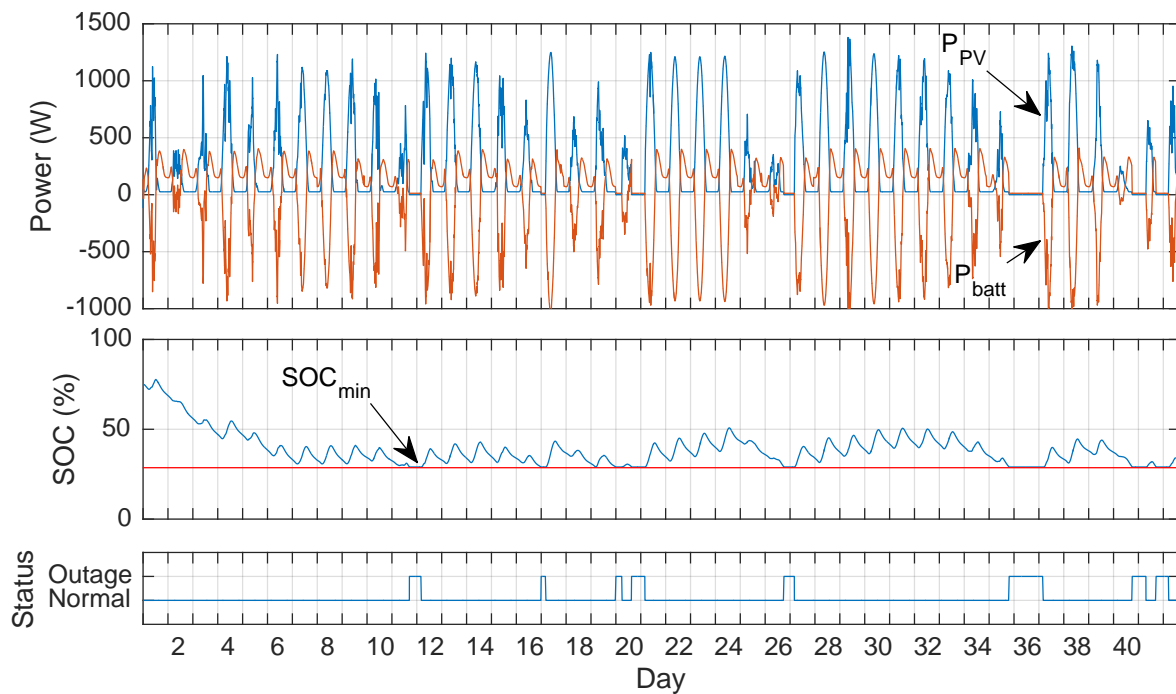


Figure 5.15: The behavior of the microgrid with the developed uncertainty compensation scheme enabled. (Scenario 3)

The results of the above studies are summarized in Table 5.1.

Table 5.1: Performance Improvement using Parameter Uncertainties Compensation

Scenario	Outages	Total Outage Time
EMS with Exact Parameters	8	101 hours
EMS with Incorrect Parameters	11	117 hours
EMS with Corrected Parameters	8	103 hours
No EMS (worst case)	21	208 hours

5.4 Summary

In this chapter, the techniques developed in this research work have been validated using both simulation and experimental studies. The simulation and experimental scenarios used to validate the predictive energy management system and the model parameter uncertainty compensation techniques were presented. For the EMS, a four-day scenario is run for a baseline case, an EMS-enabled case, and a bounded EMS-enabled case. The parameter compensation techniques are evaluated using a 42-day set of profiles, and the effectiveness of the technique is shown through error measurements and through evaluating its effect on the outage performance of the EMS.

The predictive EMS is shown to be able to reduce the duration of microgrid outages, and in some cases eliminate them entirely, by scheduling pre-emptive load shedding actions based on the predicted battery storage behaviour. The model parameter uncertainty compensation technique has been shown to be able to compensate for uncertainties introduced into the PV system rating and battery capacity parameters, and is able to recover the outage performance to near the level seen when the correct parameters are used in the prediction schemes.

Chapter 6

Conclusions and Future Work

6.1 Summary

6.1.1 Predictive Energy Management System

A predictive energy management system for an islanded PV-powered microgrid with battery storage has been developed in this work. The EMS uses forecasts of PV production and the expected load to predict the future state of charge and determine when outages may occur. A pre-emptive load shedding mechanism is proposed that can minimize or avert the outage. The approach is enhanced with a bounding approach to accommodate potential errors in the SOC estimate. An implementation of the proposed scheme using an event-driven framework has been carried out. Both simulation and experimental studies have been conducted to validate the performance of the proposed scheme in a laboratory-scale microgrid. The results demonstrate, for the chosen test scenario, a reduction in the outage duration of 87% to 100% is achievable. The technique can be extended to larger microgrids containing multiple storage and generation units. The approach requires only modest computational resources, making it cost effective to implement the EMS in an embedded system.

6.1.2 Compensation of Model Parameter Uncertainties

A method for tuning incorrect model parameters in a predictive microgrid energy management system has also been developed. The technique uses measurements provided by the power electronic converters, along with weather forecast data, to improve the accuracy of the predictions, which are then used to plan outage mitigation actions using the predictive EMS. No additional information is required in order to apply the technique, and it is computationally efficient to execute within the EMS. The technique was implemented within a predictive EMS and tested using previously recorded data. The results show that additional outages caused by incorrect model parameters can be almost completely mitigated by using the proposed tuning technique, resulting in a 12% improvement in performance over the uncompensated case.

6.2 Conclusions

The predictive EMS developed in this work has been shown to be effective at improving the performance of an islanded photovoltaic microgrid by either eliminating or reducing the duration of critical load outages. The enhancement provided by the bounding technique helps to account for uncertainties in the stored energy estimate. Finally, the proposed compensation techniques can be used to improve the quality of the predictions in the presence of model parameter uncertainties, and therefore improve the overall system performance, without requiring additional instrumentation beyond that required for the EMS.

The EMS software framework used in this research can be expanded upon and implemented in real world islanded photovoltaic microgrids and isolated power systems, and the developed EMS techniques can be used to improve the performance of such systems. Broader trends, including the continuing reduction in the cost of PV arrays and batteries, and the increasing availability of network-connected “smart” power devices that enable load management, make such energy management approaches more and more feasible in practice. This can ultimately contribute to an efficient and environmentally sound path to electrification in the developing

world, and to reductions in fossil fuel consumption in isolated communities.

6.3 Future Work

There are several possible extensions to this work that can be investigated with respect to the handling of uncertainties. While a simple constant bounding parameter was presented here, a useful enhancement would be to develop a time-varying bounding parameter that incorporates additional information, such as the time history of the SOC, to refine the bound.

Another direction of investigation is to consider the information contained in the overlapping solar irradiance forecasts. In the current technique, older forecasts are simply replaced by the most recent one. However, previous forecasts, where they overlap with the new one, can reflect the change in volatility of the solar resource over time, and therefore suggest the level of uncertainty for a given prediction.

More complex load configurations also represent an important area of research. For example, the presence of multiple shiftable loads, such as refrigeration or air conditioning systems, presents another set of factors that could be incorporated into the EMS strategy.

The compensation factors discussed in this work have been calculated based on analysis of a single day dataset. Given that the parameters under discussion are unlikely to change drastically (except under a failure mode), another enhancement to consider would be averaging and outlier removal to take advantage of the time history of the compensation factors. In addition, these values could also be used to detect sudden changes in parameter values which might indicate a fault, and subsequently trigger alerting and/or reconfiguration actions to mitigate the issue.

Finally, all the techniques explored herein are deterministic in nature, which provides simplicity in analysis and implementation. However, the solar resource and the loads exhibit stochastic behaviour, which may be characterized using random processes. Therefore, the analysis and development of stochastic techniques to approach the problem also represents a

direction that could lead to many possible research contributions. Such techniques could be developed and tested within the hardware and software architecture presented here.

In conclusion, the research reported in this thesis has resulted in a flexible energy management system framework, a predictive EMS that can reduce critical load outage durations by using pre-emptive shedding of less critical loads, and a parameter compensation approach that can improve the quality of energy management decisions. This work can ultimately be developed further and deployed in real world islanded microgrid settings to improve the performance of such systems.

Bibliography

- [1] “World Energy Outlook 2016,” International Energy Agency, Tech. Rep., 2016.
- [2] A. H. Hubble and T. S. Ustun, “Scaling renewable energy based microgrids in underserved communities: Latin America, South Asia, and Sub-Saharan Africa,” in *2016 IEEE PES PowerAfrica Conference*, 2016, pp. 134–138.
- [3] G. Venkataramanan and C. Marnay, “A larger role for microgrids,” *Power and Energy Magazine, IEEE*, vol. 6, no. 3, pp. 78–82, May-June 2008.
- [4] S. Bacha, D. Picault, B. Burger, I. Etxeberria-Otadui, and J. Martins, “Photovoltaics in microgrids: An overview of grid integration and energy management aspects,” *IEEE Ind. Electron. Mag.*, vol. 9, no. 1, pp. 33–46, March 2015.
- [5] R. H. Lasseter, “Smart distribution: Coupled microgrids,” *Proc. IEEE*, vol. 99, no. 6, pp. 1074–1082, June 2011.
- [6] P. R. Walsh and J. Wu, “Building Sustainable First Nation Communities: Alternative Energy Systems in Ontario’s Northern Remote Communities,” *IAEE Energy Forum*, vol. First Quarter, 2014.
- [7] M. Arriaga, C. A. Cañizares, and M. Kazerani, “Renewable Energy Alternatives for Remote Communities in Northern Ontario, Canada,” *IEEE Trans. Sustain. Energy*, vol. 4, no. 3, pp. 661–670, July 2013.
- [8] M. Arriaga, C. A. Cañizares, and M. Kazerani, “Northern Lights: Access to Electricity in Canada’s Northern and Remote Communities,” *IEEE Power Energy Mag.*, vol. 12, no. 4, pp. 50–59, 2014.
- [9] A. Hajimiragha and M. R. D. Zadeh, “Practical aspects of storage modeling in the framework of microgrid real-time optimal control,” in *IET Conference on Renewable Power Generation*, 2011, pp. 1–6.
- [10] R. H. Lasseter, “Control of distributed resources,” in *Bulk Power System and Controls IV Conf.*, Santorini, Greece, 1998.
- [11] R. H. Lasseter, “Microgrids [distributed power generation],” in *Proceedings of the IEEE PES winter meeting*, vol. 1, 2001, pp. 146–149.

- [12] N. Hatziargyriou, H. Asano, R. Iravani, and C. Marnay, "Microgrids," *Power and Energy Magazine, IEEE*, vol. 5, no. 4, pp. 78–94, July-Aug. 2007.
- [13] B. Kroposki, R. Lasseter, T. Ise, S. Morozumi, S. Papatlianassiou, and N. Hatziargyriou, "Making microgrids work," *Power and Energy Magazine, IEEE*, vol. 6, no. 3, pp. 40–53, May-June 2008.
- [14] C. Marnay, S. Chatzivasileiadis, C. Abbey, R. Iravani, G. Joos, P. Lombardi, P. Macarella, and J. von Appen, "Microgrid evolution roadmap," in *Intl. Symposium on Smart Elect. Dist. Sys. and Tech. (EDST15)*, 2015.
- [15] R. Lasseter, A. Akhil, C. Marnay, J. Stephens, J. Dagle, R. Guttromson, A. S. Meliopoulos, R. Yinger, and J. Eto, "Integration of distributed energy resources: The CERTS Microgrid Concept," Lawrence Berkeley National Laboratory, White Paper LBNL-50829, April 2002.
- [16] F. Katiraei, R. Iravani, N. Hatziargyriou, and A. Dimeas, "Microgrids management," *IEEE Power and Energy Magazine*, vol. 6, no. 3, pp. 54–65, May-June 2008.
- [17] J. M. Guerrero, J. C. Vasquez, J. Matas, L. G. de Vicuña, and M. Castilla, "Hierarchical control of droop-controlled ac and dc microgrids – a general approach towards standardization," *IEEE Trans. Ind. Electron.*, vol. 58, no. 1, pp. 158–172, Jan. 2011.
- [18] A. Bidram and A. Davoudi, "Hierarchical structure of microgrids control system," *IEEE Trans. Smart Grid*, vol. 3, no. 4, pp. 1963–1976, December 2012.
- [19] J. M. Guerrero, M. Chandorkar, T.-L. Lee, and P. C. Loh, "Advanced control architectures for intelligent microgrids — Part I: Decentralized and hierarchical control," *IEEE Trans. Ind. Electron.*, vol. 60, no. 4, pp. 1254–1262, April 2013.
- [20] J. M. Guerrero, P. C. Loh, T.-L. Lee, and M. Chandorkar, "Advanced control architectures for intelligent microgrids — Part II: Power quality, energy storage, and AC/DC microgrids," *IEEE Trans. Ind. Electron.*, vol. 60, no. 4, pp. 1263–1270, April 2013.
- [21] J. Rocabert, A. Luna, F. Blaabjerg, and P. Rodríguez, "Control of power converters in ac microgrids," *IEEE Trans. Power Electron.*, vol. 27, no. 11, pp. 4734–4749, Nov. 2012.
- [22] P. Kundur, *Power System Stability and Control*. McGraw-Hill, 1994.
- [23] J. G. de Matos, F. S. F. e Silva, and L. A. de S. Ribeiro, "Power control in ac isolated microgrids with renewable energy sources and energy storage systems," *IEEE Trans. Ind. Electron.*, vol. 62, no. 6, pp. 3490–3498, June 2015.
- [24] J. A. P. Lopes, C. L. Moreira, and A. G. Madureira, "Defining control strategies for microgrids islanded operation," *IEEE Trans. Power Syst.*, vol. 21, no. 2, pp. 916–924, May 2006.
- [25] F. Katiraei and M. R. Iravani, "Power management strategies for a microgrid with multiple distributed generation units," *IEEE Trans. Power Syst.*, vol. 21, no. 4, pp. 1821–1831, November 2006.

- [26] M. Delghavi and A. Yazdani, "A unified control strategy for electronically interfaced distributed energy resources," *IEEE Trans. Power Del.*, vol. 27, no. 2, pp. 803–812, April 2012.
- [27] D. Wu, F. Tang, T. Dragicevic, J. C. Vasquez, and J. M. Guerrero, "A control architecture to coordinate renewable energy sources and energy storage systems in islanded microgrids," *IEEE Trans. Smart Grid*, vol. 6, no. 3, pp. 1156–1166, May 2015.
- [28] H. Mahmood, D. Michaelson, and J. Jiang, "Strategies for independent deployment and autonomous control of pv and battery units in islanded microgrids," *IEEE J. Emerg. Sel. Topics Power Electron.*, vol. 3, no. 3, pp. 742–755, Sept. 2015.
- [29] H. Mahmood, D. Michaelson, and J. Jiang, "Control strategy for a standalone PV/battery hybrid system," in *38th Annual Conference of the IEEE Industrial Electronics Society (IECON'12)*, October 2012, pp. 3412–3418.
- [30] H. Mahmood, D. Michaelson, and J. Jiang, "A power management strategy for pv/battery hybrid systems in islanded microgrids," *IEEE J. Emerg. Sel. Topics Power Electron.*, vol. 2, no. 4, pp. 870–882, Dec. 2014.
- [31] H. Mahmood, D. Michaelson, and J. Jiang, "Decentralized power management of a pv /battery hybrid unit in a droop-controlled islanded microgrid," *IEEE Trans. Power Electron.*, vol. 30, no. 12, pp. 7215–7229, 2015.
- [32] Q.-C. Zhong, "Power-electronics-enabled autonomous power systems: Architecture and technical routes," *IEEE Trans. Ind. Electron.*, vol. 64, no. 7, pp. 5907–5918, July 2017.
- [33] J. He and Y. W. Li, "An enhanced microgrid load demand sharing strategy," *IEEE Trans. Power Electron.*, vol. 27, no. 9, pp. 3984–3995, September 2012.
- [34] J. He, Y. W. Li, J. M. Guerrero, J. C. Vasquez, and F. Blaabjerg, "An islanded microgrid reactive power sharing scheme enhanced by programmed virtual impedances," in *Proc. IEEE International Symposium on Power Electronics for Distributed Generation Systems*, 2012, pp. 229–235.
- [35] H. Mahmood, D. Michaelson, and J. Jiang, "Accurate reactive power sharing in an islanded microgrid using adaptive virtual impedances," *IEEE Trans. Power Electron.*, vol. 30, no. 3, pp. 1605–1617, 2015.
- [36] H. Mahmood, D. Michaelson, and J. Jiang, "Reactive power sharing in islanded microgrids using adaptive voltage droop control," *IEEE Trans. Smart Grid*, vol. 6, no. 6, pp. 3052–3060, 2015.
- [37] A. G. Tsikalakis and N. D. Hatziargyriou, "Centralized control for optimizing microgrids operation," *IEEE Trans. Energy Convers.*, vol. 23, no. 1, pp. 241–248, Mar. 2008.
- [38] D. Olivares, A. Mehrizi-Sani, A. Etemadi, C. Canizares, R. Iravani, M. Kazerani, A. Hajimiragha, O. Gomis-Bellmunt, M. Saeedifard, R. Palma-Behnke, G. Jimenez-Estevez, and N. Hatziargyriou, "Trends in microgrid control," *IEEE Trans. Smart Grid*, vol. 5, no. 4, pp. 1905–1919, Jul. 2014.

- [39] E. Barklund, N. Pogaku, M. Prodanovic, C. Hernandex-Aramburo, and T. C. Green, "Energy management in autonomous microgrid using stability-constrained droop control of inverters," *IEEE Trans. Power Electron.*, vol. 23, no. 5, pp. 2346–2352, Sep. 2008.
- [40] T. Logenthiran and D. Srinivasan, "Short term generation scheduling of a microgrid," in *Proceedings of TENCON 2009*, 2009.
- [41] R. Palma-Behnke, C. Benavides, F. Lanas, B. Severino, L. Reyes, J. Llanos, and D. Sáez, "A microgrid energy management system based on the rolling horizon strategy," *IEEE Trans. Smart Grid*, vol. 4, no. 2, pp. 996–1006, 2013.
- [42] S. Pelland, J. Remund, J. Kleissl, T. Oozeki, and K. D. Brabandere, "Photovoltaic and solar forecasting: State of the art," International Energy Agency: Photovoltaic Power Systems Programme, Tech. Rep. IEA-PVPS T14-01: 2013, 2013.
- [43] M. G. Villalva, J. R. Gazoli, and E. R. Filho, "Comprehensive approach to modeling and simulation of photovoltaic arrays," *IEEE Trans. Power Electron.*, vol. 24, no. 5, pp. 1198–1208, May 2009.
- [44] Y. A. Mahmoud, W. Xiao, and H. H. Zeineldin, "A parameterization approach for enhancing pv model accuracy," *IEEE Trans. Ind. Electron.*, vol. 60, no. 12, pp. 5708–5716, December 2013.
- [45] H. Beltran, E. Pérez, N. Aparicio, and P. Rodriguez, "Daily solar energy estimation for minimizing energy storage requirements in pv power plants," *IEEE Trans. Sustain. Energy*, vol. 4, no. 2, pp. 474–481, April 2013.
- [46] S. Subbayya, J. Jetcheva, and W.-P. Chen, "Model selection criteria for short-term microgrid-scale electricity load forecasts," in *Innovative Smart Grid Technologies (ISGT), 2013 IEEE PES*, February 2013.
- [47] L. Hernandez, C. Baladron, J. M. Aguiar, B. Carro, A. J. Sanchez-Esguevillas, J. Lloret, and J. Massana, "A survey on electric power demand forecasting: Future trends in smart grids, microgrids, and smart buildings," *Commun. Surveys Tuts.*, vol. 16, no. 3, pp. 1460–1495, 2014.
- [48] Z. C. Sun, T. H. Chen, K. L. Lian, C. C. Kuo, I. T. Cheng, Y. R. Chang, and Y. H. Ho, "Study on load forecasting of an actual micro-grid system in Taiwan," in *2013 IEEE International Symposium on Industrial Electronics*, May 2013, pp. 1–7.
- [49] N. Amjady, F. Keynia, and H. Zareipour, "Short-term load forecast of microgrids by a new bilevel prediction strategy," *IEEE Trans. Smart Grid*, vol. 1, no. 3, pp. 286–294, Dec. 2010.
- [50] J. Llanos, D. Sáez, R. Palma-Behnke, A. Núñez, and G. Jiménez-Estévez, "Load profile generator and load forecasting for a renewable based microgrid using self organizing maps and neural networks," in *Neural Networks (IJCNN), The 2012 International Joint Conference on*, 2012.

- [51] C. Chen, S. Duan, T. Cai, B. Liu, and G. Hu, "Smart energy management system for optimal microgrid economic operation," *IET Renew. Power Gener.*, vol. 5, no. 3, pp. 258–267, 2011.
- [52] A. Parisio and L. Glielmo, "Stochastic model predictive control for economic/environmental operation management of microgrids," in *Control Conference (ECC), 2013 European*, July 2013, pp. 2014–2019.
- [53] H. Kanchev, D. Lu, F. Colas, V. Lazarov, and B. Francois, "Energy management and operational planning of a microgrid with a pv-based active generator for smart grid applications," *IEEE Trans. Ind. Electron.*, vol. 58, no. 10, pp. 4583–4592, Oct. 2011.
- [54] F. Garcia-Torres and C. Bordons, "Optimal economical schedule of hydrogen-based microgrids with hybrid storage using model predictive control," *IEEE Trans. Ind. Electron.*, vol. 62, no. 8, pp. 5195–5207, Aug. 2015.
- [55] A. Parisio, E. Rikos, and L. Glielmo, "A model predictive control approach to microgrid operation optimization," *IEEE Trans. Control Syst. Technol.*, vol. 22, no. 5, pp. 1813–1827, 2014.
- [56] M. Ross, R. Hidalgo, C. Abbey, and G. Joós, "Energy storage system scheduling for an isolated microgrid," *IET Renew. Power Gener.*, vol. 5, no. 2, pp. 117–123, 2011.
- [57] L. Valverde, F. Rosa, and C. Bordons, "Design, planning and management of a hydrogen-based microgrid," *IEEE Trans. Ind. Informat.*, vol. 9, no. 3, pp. 1398–1404, August 2013.
- [58] A. Parisio and L. Glielmo, "A mixed integer linear formulation for microgrid economic scheduling," in *IEEE International Conference on Smart Grid Communications (Smart-GridComm)*, 2011, pp. 505–510.
- [59] W. Shi, N. Li, C.-C. Chu, and R. Gadh, "Real-time energy management in microgrids," *IEEE Trans. Smart Grid*, vol. 8, no. 1, pp. 228–238, Jan. 2015.
- [60] D. E. Olivares, C. A. Canizares, and M. Kazerani, "A centralized energy management system for isolated microgrids," *IEEE Trans. Smart Grid*, December 2013.
- [61] A. Parisio and L. Glielmo, "Energy efficient microgrid management using model predictive control," in *IEEE Conference on Decision and Control and European Control Conference (CDC-ECC)*, 2011, pp. 5449 – 5454.
- [62] A. Parisio and L. Glielmo, "Multi-objective optimization for environmental/economic microgrid scheduling," in *Cyber Technology in Automation, Control, and Intelligent Systems (CYBER), 2012 IEEE International Conference on*, May 2012, pp. 17–22.
- [63] T. Samad, E. Koch, and P. Stluka, "Automated demand response for smart buildings and microgrids: The state of the practice and research challenges," *Proc. IEEE*, vol. 104, no. 4, pp. 726–744, April 2016.

- [64] T. Strasser, F. Andr en, J. Kathan, C. Cecati, C. Buccella, P. Siano, P. Leit o, G. Zhabelova, V. Vyatkin, P. Vrba, and V. Mařík, "A review of architectures and concepts for intelligence in future electric energy systems," *IEEE Trans. Ind. Electron.*, vol. 62, no. 4, pp. 2424–2438, Apr. 2015.
- [65] P. Palensky and D. Dietrich, "Demand side management: Demand response, intelligent energy systems, and smart loads," *IEEE Trans. Ind. Informat.*, vol. 7, no. 3, pp. 381–388, Aug. 2011.
- [66] R. Faranda, A. Pievatolo, and E. Tironi, "Load shedding: A new proposal," *IEEE Trans. Power Syst.*, vol. 22, no. 4, pp. 2086–2093, Nov 2007.
- [67] J. Kennedy, P. Ciufu, and A. Agalgaonkar, "Intelligent load management in microgrids," in *IEEE Power and Energy Soc. General Meeting*, 2012.
- [68] I. J. Balaguer, Q. Lei, S. Yang, U. Supatti, and F. Z. Peng, "Control for grid-connected and intentional islanding operations of distributed power generation," *IEEE Trans. Ind. Electron.*, vol. 58, no. 1, pp. 147–157, Jan. 2011.
- [69] G. Graditi, M. L. Di Silvestre, R. Gallea, and E. R. Sanseverino, "Heuristic-based shiftable loads optimal management in smart micro-grids," *IEEE Trans. Ind. Informat.*, vol. 11, no. 1, pp. 271–280, February 2015.
- [70] C. A. Hans, V. Nenchev, J. Raisch, and C. Reincke-Collon, "Minimax model predictive operation control for microgrids," in *IFAC World Congress*, 2014.
- [71] Y. Zhang, R. Wang, T. Zhang, Y. Liu, and B. Guo, "Model predictive control-based operation management for a residential microgrid with considering forecast uncertainties and demand response strategies," *IET Gener. Transm. Distrib.*, vol. 10, no. 10, pp. 2367–2378, 2016.
- [72] A. Gholami, T. Shekari, F. Aminifar, and M. Shahidehpour, "Microgrid scheduling with uncertainty: The quest for resilience," *IEEE Trans. Smart Grid*, vol. 7, no. 6, pp. 2849–2858, Nov. 2016.
- [73] D. E. Olivares, J. D. Lara, C. A. Cañizares, and M. Kazerani, "Stochastic-predictive energy management system for isolated microgrids," *IEEE Trans. Smart Grid*, vol. 6, no. 6, pp. 2681–2693, Nov. 2015.
- [74] W. Su, J. Wang, and J. Roh, "Stochastic energy scheduling in microgrids with intermittent renewable energy resources," *Smart Grid, IEEE Transactions on*, vol. PP, no. 99, pp. 1–9, 2013.
- [75] H. Farzin, M. Fotuhi-Firuzabad, and M. Moeini-Aghaie, "A stochastic multi-objective framework for optimal scheduling of energy storage systems in microgrids," *IEEE Trans. Smart Grid*, vol. 8, no. 1, pp. 117–127, Jan. 2017.

- [76] C. Chen, S. Duan, T. Cai, B. Liu, and G. Hu, "Optimal allocation and economic analysis of energy storage system in microgrids," *IEEE Trans. Power Electron.*, vol. 26, no. 10, pp. 2762–2773, October 2011.
- [77] M. Chen and G. A. Rincón-Mora, "Accurate electrical battery model capable of predicting runtime and i-v performance," *IEEE Trans. Energy Convers.*, vol. 21, no. 2, pp. 504–511, Jun. 2006.
- [78] S. Piller, M. Perrin, and A. Jossen, "Methods for state-of-charge determination and their applications," *Journal of Power Sources*, vol. 96, no. 1, pp. 113–120, 2001.
- [79] K. S. Ng, C.-S. Moo, Y.-P. Chen, and Y.-C. Hsieh, "Enhanced coulomb counting method for estimating state-of-charge and state-of-health of lithium-ion batteries," *Applied Energy*, vol. 86, no. 9, pp. 1506–1511, 2009.
- [80] V. Agarwal, K. Uthaichana, R. A. DeCarlo, and L. H. Tsoukalas, "Development and validation of a battery model useful for discharging and charging power control and lifetime estimation," *IEEE Trans. Energy Convers.*, vol. 25, no. 3, pp. 821–835, Sep. 2010.
- [81] B. Riar, J. Lee, A. Tosi, S. Duncan, M. Osborne, and D. Howey, "Energy management of a microgrid: Compensating for the difference between the real and predicted output power of photovoltaics," in *2016 IEEE 7th International Symposium on Power Electronics for Distributed Generation Systems (PEDG)*, June 2016.
- [82] D. Michaelson, H. Mahmood, and J. Jiang, "A predictive energy management strategy with pre-emptive load shedding for an islanded pv-battery microgrid," in *39th Annual Conference of the IEEE Industrial Electronics Society (IECON'13)*, November 2013, pp. 1501–1506.
- [83] D. Michaelson, H. Mahmood, and J. Jiang, "A predictive energy management system using pre-emptive load shedding for islanded photovoltaic microgrids," *IEEE Trans. Ind. Electron.*, vol. 64, no. 7, pp. 5440–5448, July 2017.
- [84] S. M. Hakimi and S. M. Moghaddas-Tafreshi, "Optimal planning of a smart microgrid including demand response and intermittent renewable energy resources," *IEEE Trans. Smart Grid*, vol. 5, no. 6, pp. 2889–2900, Nov. 2014.
- [85] A. Luque and S. Hegedus, *Handbook of Photovoltaic Science and Engineering*, 2nd ed. Wiley, 2011, ch. 22.
- [86] J. A. Milbrandt, S. Belair, M. Faucher, M. Vallee, M. L. Carrera, and A. Glazer, "The pan-Canadian high resolution (2.5 km) deterministic prediction system," *Weather and Forecasting*, vol. 31, no. 6, pp. 1791–1816, Nov. 2016.
- [87] A. Affanni, A. Bellini, G. Franceschini, P. Guglielmi, and C. Tassoni, "Battery choice and management for new-generation electric vehicles," *IEEE Trans. Ind. Electron.*, vol. 52, no. 5, pp. 1343–1349, Oct. 2005.

- [88] J. McKellar and A. Fettig, *Twisted Network Programming Essentials*, 2nd ed. O'Reilly, 2013.
- [89] T. E. Oliphant, "Python for scientific computing," *IEEE Comput. Sci. Eng.*, vol. 9, no. 3, pp. 10–20, May-June 2007.
- [90] F. Alted and M. Fernandez-Alonso, "PyTables: Processing and analyzing extremely large amounts of data in Python," in *PyCon Convention*, Washington, D.C., April 2003.

©2017 IEEE. Reprinted, with permission, from D. Michaelson, H. Mahmood, J. Jiang, "A Predictive Energy Management System using Pre-emptive Load Shedding for Islanded Photovoltaic Microgrids," *IEEE Trans. Ind. Electron.*, vol. 64, no. 7, pp. 5440–5448, July 2017.

Appendix A

Supporting Tools

A.1 Rooftop Data Acquisition

In order to characterize the solar insolation, an apparatus to collect irradiance and temperature data was constructed and used to collect a dataset in the fall of 2015. The apparatus consisted of a Bruhl and Kjier pyranometer, a TM01 temperature sensor, an Arduino Uno embedded platform with a real-time clock and SD card shield, and the necessary interfacing circuitry and power supply, as shown in Fig. A.1. This apparatus was installed on the solar array located on the roof of the Claudette McKay-Lassonde Pavillion at Western University.

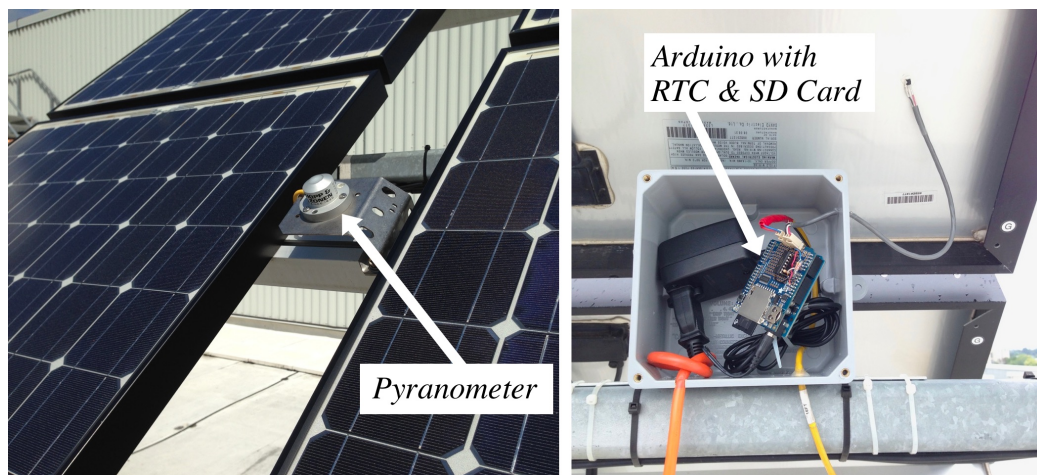


Figure A.1: Rooftop data acquisition apparatus.

The software running on the Arduino platform recorded timestamped samples at 1-second intervals and stored them into a text file on an SD card. Note that this sampling rate is much greater than what is required for energy management purposes, however the higher fidelity recording gives a better sense of the actual solar variation, and can be post-processed as needed for multiple applications. This data was manually retrieved every week and post-processed using MATLAB. The datasets were averaged and sub-sampled to provide a representation suitable for the energy management algorithm. They were also rate-limited to meet the slew rate limitations of the Chroma solar simulator system when running the accelerated experiments.

A.2 High-speed Ring Buffer

One fundamental challenge when testing low-level control algorithms on microcontrollers is the difficulty in accessing the internal variables as the discretized control algorithms are executed. In this case the controllers operate at frequencies between 10 kHz and 40 kHz, so any of the communication techniques available on the target are unable to transfer the internal variables at full rate to the host computer. One technique is to use a pulse-width modulated digital-to-analog converter to view the signal, but since this signal is by definition low-pass filtered it can miss short events of importance. It also suffers from the inability to provide an absolute output and a lack of resolution (typically 8-12 bits), which is a challenge when dealing with 32-bit floating-point values.

The other approach is to sample the internal signal and send it out as a digital bitstream via a serial port. This approach provides full resolution, but still suffers from the lack of real-time fidelity, with typically hundreds of interim steps between each sampled datapoint.

To solve these challenges it was noted that the controllers under development were of the high-speed, low-memory-use type, where a large part of the available RAM was left unused on the microcontroller. Therefore, there was room available in the memory to store a considerable amount of data. A ring-buffer was built to store variables of interest during each cycle, as

shown in Fig. A.2.

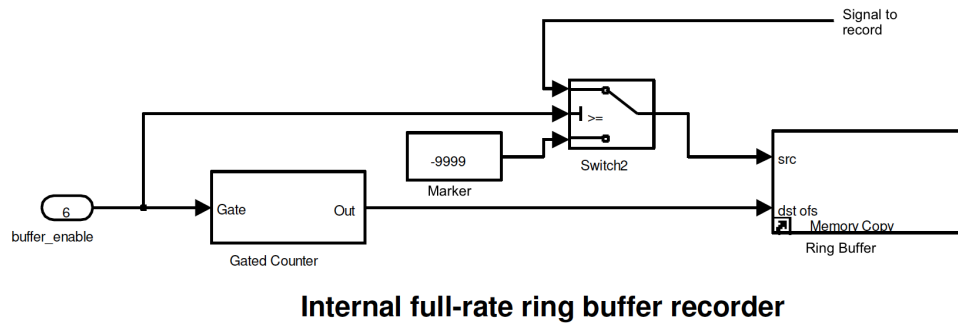


Figure A.2: High-speed ring buffer.

The ring-buffer is either free running, in which case it holds the most recent several seconds of data, or it can be triggered by some internal event. This event can be generated using an internal measurement of interest, for example a voltage that exceeds a chosen limit. The ring buffer logic places a marker the buffer so that the starting point can be found later during post-processing. A manual front panel switch is used to trigger the dumping of the buffer to the serial port, where it can be picked up by an external application and stored on the EMS computer. An example of a full-rate current waveform recorded using the ring-buffer is shown in Fig. A.3. The tool proved to be indispensable in finding and correcting issues during the testing of both the inverters and the dc-dc converters.

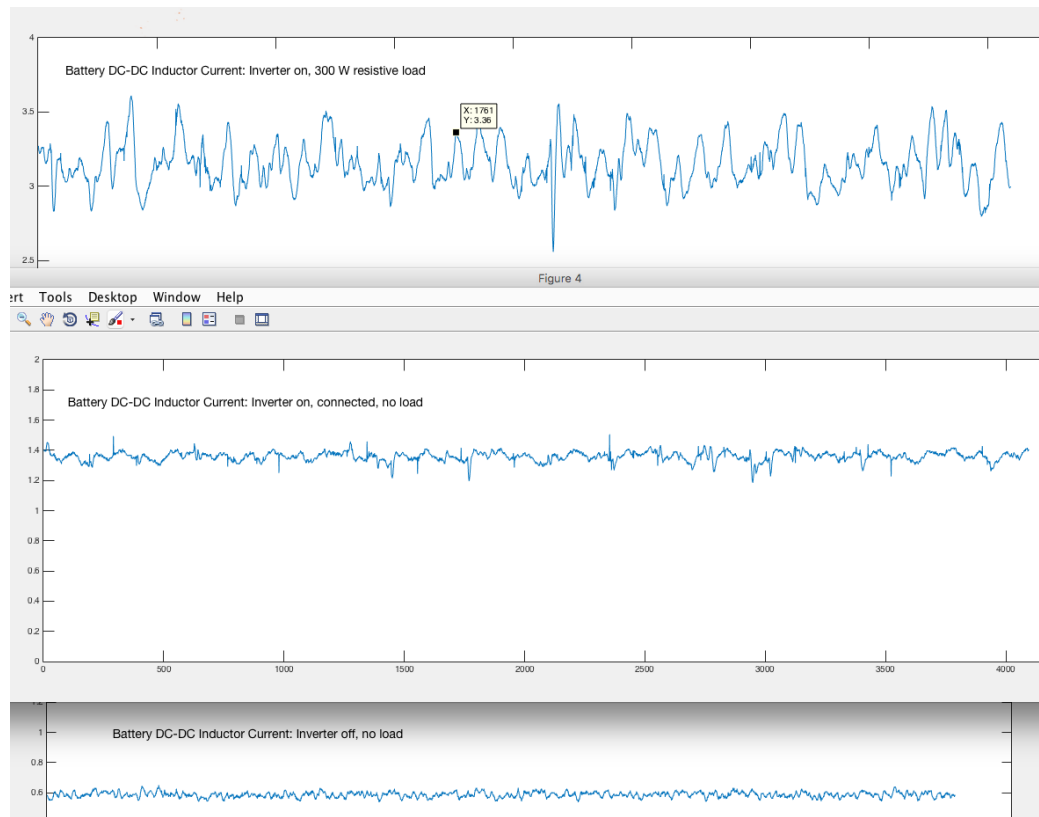


Figure A.3: Example of data recorded by the high-speed ring buffer.

Appendix B

Copyright Release



The screenshot shows the Copyright Clearance Center RightsLink interface. On the left is the IEEE logo with the text "Requesting permission to reuse content from an IEEE publication". In the center, the following information is displayed:

Title: A Predictive Energy Management System Using Pre-Emptive Load Shedding for Islanded Photovoltaic Microgrids
Author: Dennis Michaelson
Publication: Industrial Electronics, IEEE Transactions on
Publisher: IEEE
Date: July 2017
Copyright © 2017, IEEE

On the right, there are navigation buttons for "Home", "Create Account", "Help", and an email icon. Below these is a "LOGIN" button and a text box that reads: "If you're a copyright.com user, you can login to RightsLink using your copyright.com credentials. Already a RightsLink user or want to learn more?"

Thesis / Dissertation Reuse

The IEEE does not require individuals working on a thesis to obtain a formal reuse license, however, you may print out this statement to be used as a permission grant:

Requirements to be followed when using any portion (e.g., figure, graph, table, or textual material) of an IEEE copyrighted paper in a thesis:

- 1) In the case of textual material (e.g., using short quotes or referring to the work within these papers) users must give full credit to the original source (author, paper, publication) followed by the IEEE copyright line ♦ 2011 IEEE.
- 2) In the case of illustrations or tabular material, we require that the copyright line ♦ [Year of original publication] IEEE appear prominently with each reprinted figure and/or table.
- 3) If a substantial portion of the original paper is to be used, and if you are not the senior author, also obtain the senior author's approval.

Requirements to be followed when using an entire IEEE copyrighted paper in a thesis:

- 1) The following IEEE copyright/ credit notice should be placed prominently in the references: ♦ [year of original publication] IEEE. Reprinted, with permission, from [author names, paper title, IEEE publication title, and month/year of publication]
- 2) Only the accepted version of an IEEE copyrighted paper can be used when posting the paper or your thesis on-line.
- 3) In placing the thesis on the author's university website, please display the following message in a prominent place on the website: In reference to IEEE copyrighted material which is used with permission in this thesis, the IEEE does not endorse any of [university/educational entity's name goes here]'s products or services. Internal or personal use of this material is permitted. If interested in reprinting/republishing IEEE copyrighted material for advertising or promotional purposes or for creating new collective works for resale or redistribution, please go to http://www.ieee.org/publications_standards/publications/rights/rights_link.html to learn how to obtain a License from RightsLink.

If applicable, University Microfilms and/or ProQuest Library, or the Archives of Canada may supply single copies of the dissertation.

Curriculum Vitae

Name: Dennis Michaelson

Post-Secondary Education and Degrees: The University of Western Ontario
London, Ontario, Canada
2017 Ph.D. (Electrical & Computer Engineering)

Simon Fraser University
Burnaby, British Columbia, Canada
1993 B.A.Sc. (Automation Engineering)

Selected Work Experience: Director/Vice President of Engineering
EK3 Technologies Inc., London, Ontario, Canada
2001 – 2009

Selected Honours and Awards: IEEE London PES Chapter Outstanding Engineer Award
2012
NSERC PGS B & Canadian Space Agency Supplement
1997-1998

Selected Publications:

Journals

D. Michaelson, H. Mahmood, J. Jiang, “A Predictive Energy Management System using Pre-emptive Load Shedding for Islanded Photovoltaic Microgrids,” IEEE Trans. Industrial Electronics, vol. 64, no. 7, pp. 5440–5448, 2017.

Hisham Mahmood, D. Michaelson, J. Jiang, “Decentralized Power Management of a PV/Battery Hybrid Unit in a Droop-Controlled Islanded Microgrid,” IEEE Trans. Power Electronics, vol. 30, no. 12, pp. 7215–7229, 2015.

Hisham Mahmood, D. Michaelson, J. Jiang, "Reactive Power Sharing in Islanded Microgrids Using Adaptive Voltage Droop Control," IEEE Trans. Smart Grid, vol. 6, no. 6, pp. 3052–3060, 2015.

Hisham Mahmood, D. Michaelson, J. Jiang, "Strategies for Independent Deployment and Autonomous Control of PV and Battery Units in Islanded Microgrids," IEEE J. Emerging and Selected Topics in Power Electronics, vol. 3, no. 3, pp. 742–755, 2015.

Hisham Mahmood, D. Michaelson, J. Jiang, "Accurate reactive power sharing in an islanded microgrid using adaptive virtual impedances," IEEE Trans. Power Electronics, vol. 30, no. 3, pp. 1605–1617, 2015.

Hisham Mahmood, D. Michaelson, J. Jiang, "A power management strategy for PV/battery hybrid systems in islanded microgrids," IEEE J. Emerging and Selected Topics in Power Electronics, vol. 2, no. 4, pp. 870–882, 2014.

Conferences

D. Michaelson, H. Mahmood, J. Jiang, "A predictive energy management strategy with preemptive load shedding for an islanded PV-battery microgrid," in Proc. of IECON2013 - the 39th Ann. Conf. of the IEEE Industrial Electronics Soc., pp. 1501-1506, 10-13 Nov. 2013.

Hisham Mahmood, D. Michaelson, J. Jiang, "Control strategy for a standalone PV/battery hybrid system," in Proc. of IECON2012 - the 38th Ann. Conf. of the IEEE Industrial Electronics Soc., pp. 3412–3418, Oct. 2012.

Patents

D. Michaelson, J. Hishon, US patent 8001418 "Fault detection and correction for single and multiple media players connected to electronics displays, and related devices, methods and systems," issued August 16, 2011.

K. Stuart, D. Michaelson, E. Elliott, US patent 7519703 "Media content display system with presence and damage sensors," issued April 14, 2009.